Design of Biofunctional Liposomes for Delivery of Bioactive Molecules

Design of Biofunctional Liposomes for Delivery of Bioactive Molecules

Eiji Yuba

February 2010

Doctoral Thesis at Osaka Prefecture University

Contents

Chapter 1

General Introduction

1. 1. Drug Delivery System~a Promising Technology for Advanced Medical Treatments

Since the early 19th century, progress of organic chemistry led pharmaceutical industry to rise. P. Ehrlich and J. Langley suggested the concept of drug and its receptor (‘magic bullet’) in the end of 19th and early 20th century, respectively, which developed medicinal chemistry. A. Fleming first found penicillin in 1928. Since 1940s, many antibiotics have been developed, resulting in real start of drug discovery.

In 1953, Watson and Crick demonstrated the molecular structure of deoxyribonucleic acid (DNA) as ‘double helix structure’ [1]. This discovery led the rapid developments of biochemistry and molecular biology. In 1970, recombinant DNA techniques were established. And then, biotechnology-based medicine has been produced for many intractable diseases. In early 1960’s, some diseases were clarified to be induced by the pathogenetic mechanisms, and genetic factors were shown to contribute to the etiology of diseases. The fundamental understandings of diseases based on genetics generated gene therapy. Gene therapy is a therapeutic method in which can be treated by expressing the curative genes or suppressing specific genes.

Recent progress in biotechnology has revealed the function of embryonic stem cell (ES cell), which has abilities to differentiate into any types of cells constructing bodies [2]. This discovery enhanced opportunities for regeneration of missing tissue or organs. However, there are ethical difficulties regarding the use of human embryos, as well as the problem of tissue rejection following transplantation in patients. In 2006, S. Yamanaka et al. suggested the notion that could overcome all these problems, the induction of pluripotent cells from completely differentiated fibroblasts, which were called the induced pluripotent stem (iPS) cells [3, 4]. To date, many researchers have studied the functions, efficient preparation

methods and applications of iPS cells [5-9].

In addition to stem cell-based regenerative medicine, functional cell-based cell therapy has risen. Cell therapy is the treatment in which functional cells from patient's tissue or blood induce curative effects. Especially, dendritic cells (DCs), which play a crucial role in the control of immune responses and activations, have attracted much attention for their application to cancer immunotherapy or vaccination [10, 11]. DCs recognize, acquire, process and present antigens (substance materials of diseases) to native and resting T cells for induction of an antigen-specific immune response. Because DCs presenting tumor-associated antigens (TAAs) can activate TAA-specific immune response, many researchers have attempted to use TAA-presenting DCs as a vaccine for cancer immunotherapy.

As described above, recent remarkable progress in drug discovery, medicinal chemistry and molecular biology to led a new class of medicine or approach to therapy such as biotechnology-based medicine, gene therapy, stem cell-based regenerative medicine and cell therapy. To achieve these therapies, it is required to transfer bioactive molecules to specific sites in body or specific cells or specific organelle in cells. Drug delivery system (DDS) has risen to fulfill these requirements (Fig. 1-1.). DDS carrier containing drugs has to

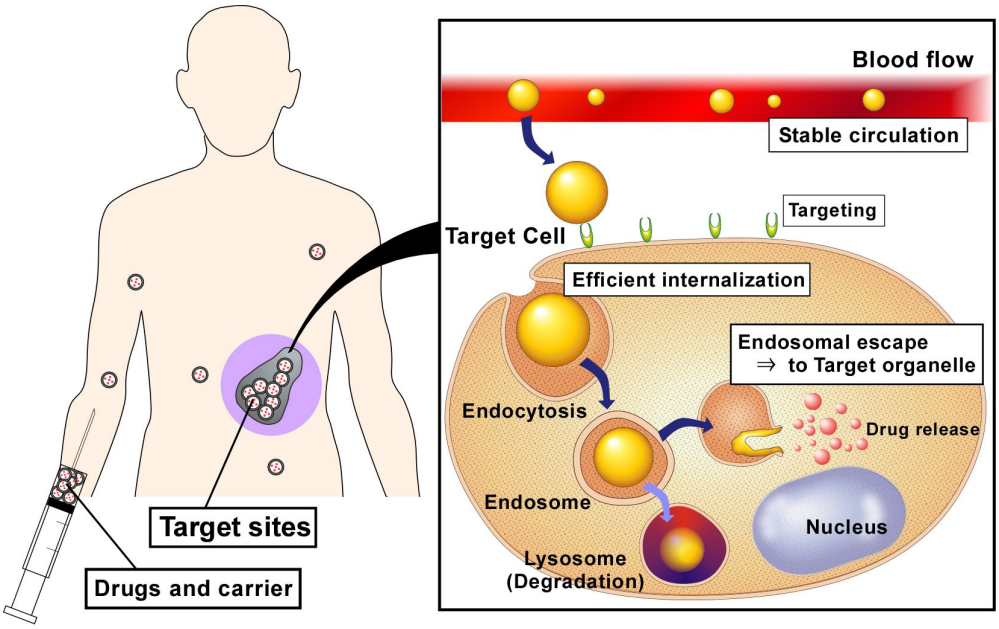

Fig. 1-1. The concept of Drug Delivery system (DDS).

overcome following processes, (i) stable circulation in blood flow, (ii) reaching to target cell (targeting), (iii) efficient internalization and (iv) delivery to target organelle.

In gene therapy, curative DNA must enter the specific cells and then their nucleus, and be expressed in the cells efficiently. Because DNA can't permeate cellular membrane spontaneously, a carrier that delivers DNA into nucleus of specific cells is necessary. Besides, ribonucleic acid interference (RNAi), which suppresses the gene expression by binding specific messenger RNA (mRNA) and preventing them from producing a protein, requires an efficient vehicle of small interfering RNAs (siRNAs) that can transfer siRNA to target cell's cytosol [12]. To reprogram the differentiated cells to iPS cells, an efficient gene carrier is desired which can induce gene expression for a proper time period [13]. In addition, it is important for cancer immunotherapy to induce the cellular immunity. To induce the cellular immunity, the delivery of antigens (such as proteins) to cytosol of DCs is essential [10, 11].

Thus, drug discovery and technology has grown the more advanced, carrier systems which can deliver bioactive molecules to specific cells or specific organelle have become the more important. To date, numerous studies have been reported to establish the efficient drug delivery system using various materials such as biopolymers, synthetic polymers, peptides, lipids, virus, virus-derived proteins and bacteria [14-31]. Above all, lipid-based carrier system is promising due to their biocompatibility, drug-loading ability and capability for functionalization.

1. 2. Liposomes and Their Functionalization

In 1964, A. D. Bangham found that lipid suspension formed bilayer vesicles, so called "liposomes" [32, 33]. Liposomes have two regions, inner water phase and lipid membrane. Therefore liposome can encapsulate both water-soluble drugs and hydrophobic drugs. Although since the early studies of liposomes they have been used as a model of biological membrane, after finding of their potentials as a drug carrier, many researches have studied

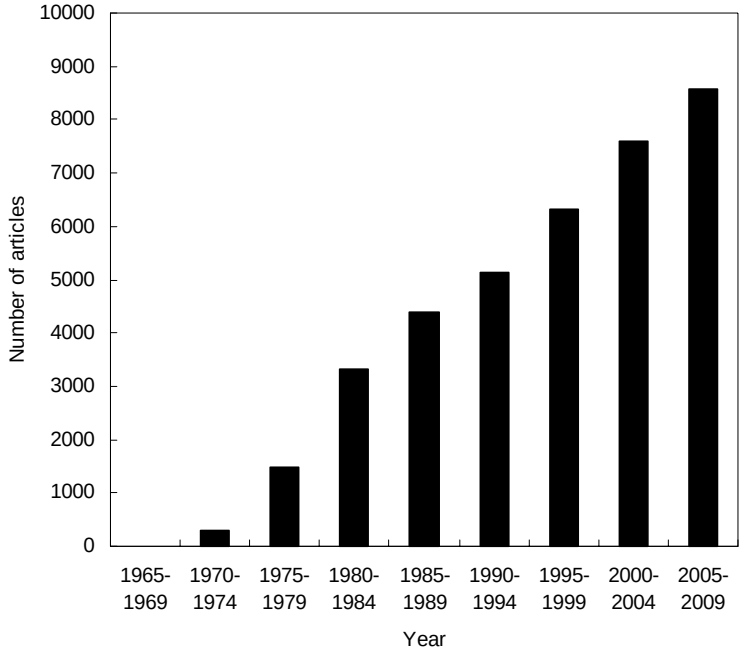

Fig 1-2. The number of articles concerning liposome searched by PubMed.

about potentials of liposomes as DDS. Fig 1-2 shows the temporal transition of the number of articles about liposome. The number of articles on liposomes has increased steadily, indicating that liposome technology is of great importance in a wide range of fields.

Liposome studies as a drug carrier have progressed markedly since appearance of the concept about ‘long-circulating liposomes’. Allen and Chonn constructed such liposomes by using a glycolipid having sialic acids because erythrocytes containing many sialic acids on their surface could circulate in blood flow by escaping from recognition of reticuloendothelial system (RES) [34]. Importantly, the concept of escape from RES has become a standard as long-circulating liposomes. In 1990, L. Huang et al. prepared poly(ethylene glycol) (PEG)-modified liposomes as a new type of long-circulating liposomes [35]. PEG forms a steric barrier against RES due to its high hydration ability. Since the appearance of PEG-modified liposomes, the utility of liposome as a DDS carrier has been showed and liposome studies have become more active. In fact, many liposome-based drug formulations have been commercialized to date, which contain anticancer drugs, antibacterial reagents, photosentitizers and so on.

In addition to long-circulating liposomes, many “functional” liposomes have so far been developed. For example, by conjugating antibodies or specific ligands to liposome surface, targeted liposomes could be constructed, which could bind to specific sites or cells bearing corresponding receptors [36-39]. By using lipid phase-transition or conjugation of thermo-sensitive materials, thermo-responsive liposomes have been developed [40, 41]. Because thermo-responsive liposomes can release the contents in response to mild heating, by local heating limited at disease sites, drugs are released only at local sites and selective drug effects are obtained. Another type of important functional liposomes is “pH-sensitive liposomes” [42, 43]. The circumstance of body is normally kept to be at neutral pH. On the other hands, inflammatory sites or tumor neighborhood are known to be at weakly acidic pH. Inside of endosome and lysosome, which are cellular compartments involved in the internalization and degradation of exogenous materials, is also weakly acidic environments [44]. In response to such pH-differences, pH-sensitive liposomes are destabilized and release drugs. Besides, various functional liposomes responsive to various external stimulations have been developed such as magnetic filed-sensitive “magnetoliposomes” [45], ultrasound-responsive micro bubble-containing “bubble liposomes” [46] and “photo-responsive liposomes” [47].

1. 3. Design of Functional Liposomes Based on Chemistry for Drug Delivery System

It is important to give functions to liposomes for their application to DDS. To date, many types of functional liposomes have been designed. One approach to establish the functional liposome is to use the property change of lipid itself under external stimulations. For example, Yatvin et al. prepared thermo-responsive liposomes containing dipalmitoyl phosphatidylcholine (DPPC), which has phase-transition temperature at 42 °C [40]. DPPC-containing liposomes showed content release around DPPC’s phase-transition temperature. H. Ellens et al. prepared pH-sensitive liposomes consisting of

non-bilayer-forming lipid, such as dioleoyl phosphatidylethanolamine (DOPE) and carboxyl group-containing amphiphilies, such as cholesteryl hemisuccinate (CHEMS) [43]. At neutral pH, deprotonated carboxyl groups promote the hydration of liposome surface and generate the electrostatic repulsion between liposomes, resulting in formation of stable liposomes. However, at acidic pH, liposomes are destabilized due to protonation of carboxyl groups.

Instead of using lipid's properties, the conjugation of functional materials to stable liposomes is an attractive approach to prepare the functional liposomes. As a pioneering work, H. Ringsdorf et al. prepared a variety of polymer-introduced liposomes and J. Sunamoto et al. constructed polysaccharide-modified liposomes [48, 49]. Because Ringsdorf and Sunamoto developed many methods for introducing polymers or functional molecules to liposomes, their works are basis of following studies about constructing functional liposomes.

K. Kono prepared thermo-sensitive liposomes by complexation of typical thermo-responsive polymer, poly(*N*-isopropylacrylamide) (PNIPAM), with stable liposomes and achieved efficient drug release above polymer's lower critical solution temperature (LCST), where polymer changes character from hydrophilic to hydrophobic [41]. In addition, PNIPAM-based copolymers containing various amounts of acrylamide units showed a variety of LCST which depends on their compositions. These polymers induced drug release from liposomes above their LCST. D.A. Tirrell et al. constructed pH-sensitive liposomes by conjugation of poly(carboxylic acid) with liposomes [50-52]. At neutral pH, deprotonated carboxyl groups don't interact to liposome membrane. However, at acidic pH, protonated carboxyl groups destabilize liposome membrane rapidly. Because hydrophobic interaction plays an important role in the interaction of polymers with lipid membrane, more hydrophobic polymers were synthesized and incorporated to liposomes. These hydrophobic polymers exhibited stronger membrane-disrupting ability [53]. K. Kono et al. also developed pH-sensitive polymers, a series of carboxylated poly(glycidol) derivatives for pH-sensitization of liposomes [54, 55]. These polymers have a backbone structure similar to

that of PEG and carboxyl groups on the side chains, which control interaction of the polymer backbone with lipid membranes in a pH-dependent manner. These polymer-modified liposomes are stable at neutral pH, but they exhibit considerable destabilization under mildly acidic conditions and deliver contents into cytosol by membrane fusion with endosome/lysosome membranes.

S.H. Park et al. reported the complex between Au nanoparticles (Au NPs) and liposomes [56]. Au NPs strongly absorb light in the visible region of the spectrum, due to the surface plasmon resonance (SPR), and convert the absorbed light to heat. Hence, Au NPs are considered to be useful for photothermal therapy as well as for imaging in the biomedical field. Because Au NPs are prone to aggregate, stabilization of Au NPs is important. Similarly, magnetite-incorporated "magnetoliposomes" were also developed for application to diagnosis and photothermal therapy [45].

Thus the complexation of functional materials with liposomes has benefits from the following viewpoints:**(i) original liposomes before complexation are stable**, and **(ii) obtained functional liposome's properties are tunable by changing properties of conjugated materials.** Hence, by using functional materials with high performance, excellent functional liposomes can be achieved.

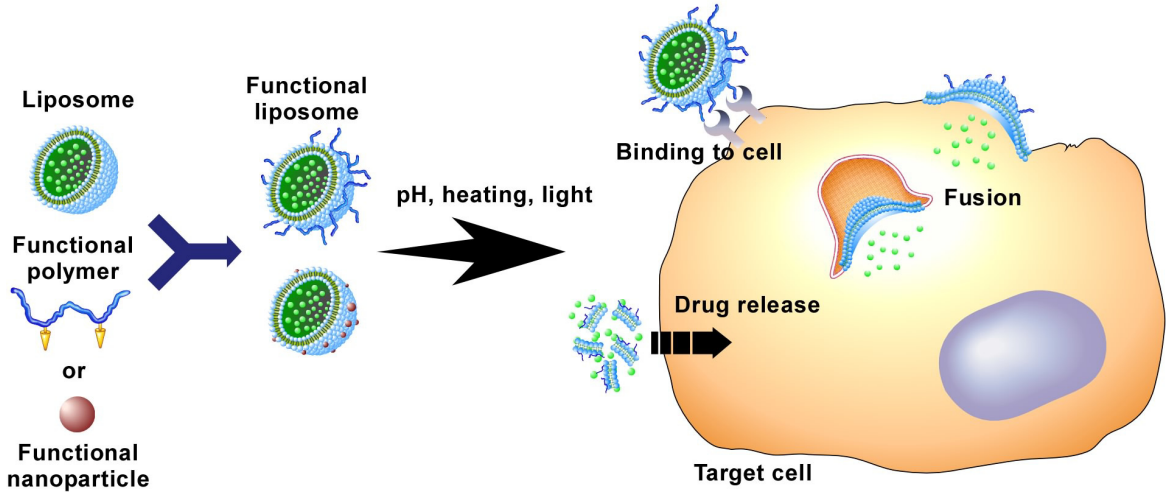

Fig. 1-3. Design of functional liposome by the conjugation of functional materials with liposome.

1. 4. Objectives and Outline of This Thesis

As mentioned above, it has been required to construct efficient functional liposomes, which can deliver bioactive molecules to specific sites, specific cells and specific cellular compartments efficiently for the establishment of advanced medical technology. The conjugation of functional materials to liposomes is a smart approach for producing functional liposome, which can overcome extra- or intracellular barriers against efficient delivery of bioactive molecules. In this study, highly potent pH-sensitive or photo-sensitive functional liposomes were developed by the conjugation of functional materials to liposomes.

This doctoral thesis consists of 8 chapters. The outline of each chapter is summarized as follows:

Chapter 1

This chapter describes the background, the objectives and the contents of this thesis.

Chapter 2

This chapter describes the correlation between cytoplasmic delivery of antigenic protein to DCs and the ability to induce cellular immunity. pH-Sensitive polymer-modified liposomes were used as a vehicle to deliver antigenic proteins. The effects of polymer structure were investigated on various aspects of polymer-modified liposomes including membrane fusion activity, cellular association, cytoplasmic delivery and the induction of cellular immune response.

Chapter 3

This chapter describes the improvement of pH-sensitive polymer and the preparation of these polymer-modified liposomes having pH-sensitive membrane fusion properties, which would ensure more efficient cytoplasmic delivery of bioactive molecules such as proteins by inducing efficient membrane fusion with acidic endosome. Hyperbranched poly(glycidol) (HPG) derivatives with carboxylated side chains and different degrees of polymerization (DPs) by reacting HPG having different DPs with 3-methylglutaric anhydride, which are

designated MGlu-HPG, were synthesized, and investigated a correlation between their backbone structures and their abilities to render stable liposomes pH-sensitive. These polymers were modified with antigenic protein-loaded liposomes, and estimated their potentials as a cytplasmic delivery vehicle for antigenic proteins.

Chapter 4

This chapter describes the gene delivery to DCs by using complexes comprised of pH-sensitive polymer-modified liposome and DNA-cationic lipid complex (lipoplexes). The effects of ligands conjugated to the polymer and polymer structure were investigated in the cellular association and transfection activity by these complexes. The importance of efficient endosomal escape of DNA on transfection was discussed. Furthermore, it was also evaluated whether transfection by these complexes induced the up-regulation of cellular immunity-associated molecules on DCs.

Chapter 5

This chapter describes the preparation of liposomes bearing pH-sensitive poly(ampholytes) for the controlled drug release. pH-Sensitive copolymers comprised of (2-dimethylamino)ethyl methacylate (DEAEMA) units and acylic acid (AA) units at various ratios were synthesized and used to modify the liposome surface. The charge states of these polymers were estimated by a titration. pH-Dependent release behaviors of fluorescent dye-loaded liposomes modified with these polymers were also investigated. The correlation between the charged states of polymers and the ability to induce drug release was discussed.

Chapter 6

This chapter describes the preparation of novel pH-sensitive lipid-based intracellular drug delivery system. Poly(amidoamine)-dendron-bearing lipid (DL) were used as an amphiphilic moleclule. The mixture of DL and poly(ethylene glycol) (PEG)-bearing lipid was dispersed in phosphate-buffered saline. The pH-sensitivity of DL/PEG dispersion was evaluated by differential scanning calorimetry, optical density analysis, dynaminc light

sccaterring and transmission electron microscopy. Using unique pH-responsive structural transition of DL/PEG molecular assemblies, intracellular delivery of model proteins was also examined.

Chapter 7

This chapter demonstrates the construction of novel complexes of liposomes with gold nanoparticles (Au NPs) for photo-responsive nanodevices. The stability of liposome-Au NP complex was investigated by time-dependent surface plasmon resonance (SPR). Formed complexes were also characterized using transmittance electron microscopy (TEM), dynamic laser scattering (DLS) and release of encapsulated molecules. Furthermore, the effect of lipid composition was examined on obtained liposome-Au NP complexes.

Chapter 8

This chapter summarizes all the conclusions in this thesis.

1. 5. References

1. J. D. Watson and F. H. C. Crick, *Nature* 1953, **171**, 737-738.
2. J. A. Thomson et al., *Science* 1998, **282**, 1145-1147.
3. K. Takahashi and S. Yamanaka, *Cell* 2006, **126,** 663-676.
4. K. Takahashi et al., *Cell* 2007, **131**, 861-872.
5. M. Stadtfeld et al., *Science* 2008, **322,** 945-949.
6. K. Okita et al., *Science* 2008, **322**, 949-953.
7. D. Huangfu et al. *Naure Biotechnology* 2008, **26**, 1269-1275.
8. T. Aasen et al., *Nature Biotechnology* 2008, **26**, 1276-1284.
9. Y. Yoshida et al., *Cell Stem Cell* 2009, **5**, 237-241.
10. J. Banchereau and A.K. Palucka, *Nat. Rev. Immunol.* 2005, **5**, 296–306.
11. N.S. Wilson and J.A. Viladangos, *Adv. Immunol.* 2005, **86**, 241–305.
12. A. Fire et al., *Nature* 1998, **391**, 806-811.

13. S. Yamanaka, *Nature* 2009, **460**, 49-52.

14. WF. Lai, MC. Lin, *J Control Release* 2009, **134**, 158-168.

15. R. Karinagaa et al., *Biomaterials* 2005, **26**, 4866–4873.

16. M. G. Svahn1 et al., *J. Gene Med*. 2004, **6**, 36–44.

17. S Abes et al., *Nucl. Aci. Res*. 2007, **35**, 4495–4502.

18. P. L. Felgner et al., *Proc. Nat. Acad. Sci. USA* 1987, **84**, 7413-7417.

19. O. Boussif et al., *Proc. Nat. Acad. Sci. USA* 1995, **92**, 7297–7301.

20. J. Gary et al., *Proc. Nat. Acad. Sci. USA* 1993, **90**, 11307-11311.

21. I. Koltover et al., *Science* 1998, **281**, 78-81.

22. R. Koynova and R. C. MacDonald, *Biochim. Biophy. Acta* 2005, **1714**, 63-70.

23. IS. Zuhorn et al., *Biophys. J*. 2002, **83**, 2096–2108.

24. DS. Friend et al., *Biochim. Biophys. Acta* 1996, **1278**, 41–50.

25. S. Akhtar and I. F. Benter, *J. Clinical Inves*. 2007, **117**, 3623-3632.

26. R. Bryan R. et al., *Adv. Drug Del. Rev*. 2007, **59**, 134–140.

27. E. John et al., *Proc. Nat. Acad. Sci. USA*. 1987, **84**, 4626-4630.

28. K.L, Berkner, *Bio. Techniques* 1988, **6**, 616.

29. L. Guy et al., *Biochim. Biophy. Acta* 2007, **1772**, 243–262.

30. A. El-Aneed, *J Control Release* 2004, **94**, 1– 14.

31. J. A. MacDiarmid et al., *Nature Biotechnology* 2009, **27**, 643-651.

32. A. D. Bangham and R. W. Horne, *J. Mol. Biol*. 1964, **8**, 660-668.

33. A. D. Bangham et al., *J. Mol. Biol.* 1965, **13**, 238-252.

34. T. M. Allen and A. Chonn, *FEBS Lett.* 1987, **223**, 42-46.

35. A. L. Kilbanov et al., *FEBS Lett.* 1990, **268**, 235-237.

36. M. Ogris et al., *Gene Ther*. 1999, **6**, 595–605.

37. Y. Lu and P. S. Low, *Adv. Drug Deliv. Rev*. 2002, **54**, 675– 693.

38. R. Wiewrodt et al., *Blood* 2002, **99**, 912-922.

39. A. G. Schätzlein, *J. Biomed. Biotechnol*. 2003, **2**, 149–158.

40. MB. Yatvin et al., *Science* 1978, **202**, 1290–1293.

41. K. Kono, *Adv. Drug Delivery Rev*. 2001, **53**, 307-319.

42. D. Liu and L. Huang, *Biochim. Biophys. Acta* 1990, **1022**, 348–354.

43. H. Ellens et al., *Biochemistry* 1984, **23**, 1532-1538.

44. S. Mukherjee et al., *Physiol. Rev.*1997. **77**, 759–803.

45. E. Viroonchatapan et al., *Life. Sci.* 1996, **58**, 2251-2261.

46. R. Suzuki et al., *Int. J. Pharm.* 2008, **354**, 49-55.

47. T. Nagasaki et al., *Bioconjugate Chem.* 2003, **14**, 513-516.

48. H. Ringsdorf et al., *Angew. Chem. Int. Ed. Engl.* 1988, **27**, 113-158.

49. J. Sunamoto et al., *Chem. Lett.*, 1988, **17**, 1781-1784.

50. K. Seki et al., *Macromolecules* 1984, **17**, 1692–1698.

51. M. Maeda et al., *J. Am. Chem. Soc.* 1988, **110**, 7455–7459.

52. M. Fujiwara et al., *J. Colloid Interface Sci.* 1997, **185**, 210–216.

53. N. Murthy et al., *J. Controlled Release* 1999, **61**, 137–143.

54. K. Kono et al., *Biochim. Biophys. Acta 1994,* **1193***,* 1–9.

55. N. Sakaguchi et al., *Bioconjugate Chem*., 2008, **19**, 1040-1048.

56. S. H. Park et al., *Colloid Surf. B*, 2006, **48**, 112-118.

Chapter 2

pH-Sensitive fusogenic polymer-modified liposomes as a carrier of antigenic proteins for activation of cellular immunity

2. 1. Introduction

Efficient vaccination strategies have been desired for overcoming new pathogens and for evolution of resistance of microorganisms. In addition, efficient vaccine delivery systems have been required for achievement of cancer immunotherapy. Dendritic cells (DCs) are known as potent professional antigen presenting cells; they play a crucial role in innate and adaptive immune responses [1–3]. The DCs recognize, take up, process and present antigens to native and resting T cells for induction of an antigen-specific immune response. Antigenic proteins internalized *via* endocytosis are degraded to peptide fragments. These peptides are presented by binding to major histocompatibility complex (MHC) class II molecules, which mainly activate $CD4^+$ T lymphocytes, thereby inducing humoral immunity. On the other hand, antigenic proteins introduced into cytosol of DCs are degraded by proteasomes after ubiquitination. These fragmented peptides are presented by MHC class I molecules on the surface of DCs. They mainly activate $CD8^+$ cytotoxic T lymphocytes (CTLs) to induce cellular immunity. To attain efficient target-specific immunity, induction of the antigen-specific CTLs is important because they eliminate the infected cells and pathogens directly. Therefore, carrier systems that can introduce antigenic proteins efficiently into the cytosol of DCs are necessary to establish effective immunotherapy.

Numerous attempts have been undertaken to achieve delivery of antigens into the DC's cytosol. For example, Akagi et al. reported that nanoparticles of γ-poly(glutamic acid) introduced entrapped antigenic ovalbumin (OVA) into cytosol of DC and induced antigen

specific CTLs [4,5]. In addition, Fre´chet and coworkers showed that acid-degradable, acrylamide-based nanoparticles achieved cytosolic delivery of OVA and presentation of OVA-derived peptides *via* the MHC class I pathway [6]. These nanoparticles might be taken up by DC *via* endocytosis and enhance transfer of their encapsulated antigen molecules from endosome and/or lysosome to cytosol by destabilization of the membranes of these acidic compartments through hydrophobic or electrostatic interactions [5,6].

One of the most effective strategies for efficient introduction of antigenic proteins into cytosol of DC might be to use membrane fusion especially for membrane-based nanoparticles, such as liposomes. To date, viral fusion proteins have been used frequently to provide liposomes with fusion ability [7,8]. Indeed, viral fusion protein-incorporated liposomes have been used to introduce encapsulated antigenic OVA into DC's cytosol and induced efficient cellular immunity [7,8]. However, viral proteins might provoke unexpected immune responses. Therefore, the use of synthetic carriers might be preferred for the delivery of antigens into DCs.

The author has developed pH-sensitive liposomes, which generate fusion ability under weakly acidic conditions, by surface modification of egg yolk phosphatidylcholine (EYPC) liposomes with poly(glycidol) derivatives having carboxyl groups (Fig. 2-1) [9,10]. In fact, these polymer-modified liposomes delivered a membrane impermeable fluorescent dye, calcein, into cytosol of HeLa cells after internalization *via* endocytosis and subsequent fusion with membrane of endosome or lysosome [9,10]. Especially, 3-methylglutarylated poly(glycidol) (MGluPG), which has hydrophobic side chains, exhibited higher fusion ability than succinylated poly(glycidol) (SucPG) [10].

Considering the excellent performance of these polymer-modified liposomes as a cytoplasmic delivery vehicle, the author attempted to apply these liposomes to the production of potent vaccines, which deliver antigenic proteins into cytosol of DCs and activate cellular immune response through their administration *via* nasal mucosa, which affords some

advantages, such as noninvasive needle-free administration and induction of both mucosal and systemic immune responses [11–14]. Correlation of fusogenic properties of the liposomes with their ability to activate cellular immunity was described.

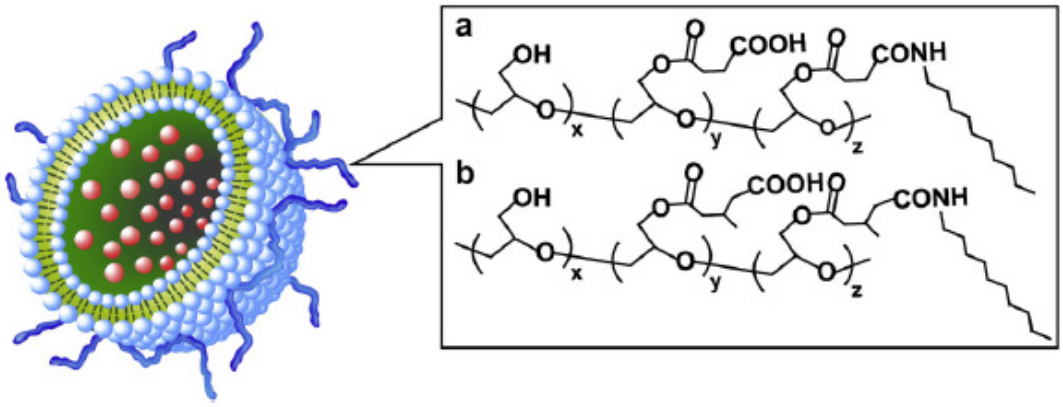

Figure 2-1. Structures of SucPG (a), MGluPG (b) and pH-sensitive polymer-modified liposome.

2. 2. Materials and Methods

2. 2. 1. Materials

EYPC and L-dioleoyl phosphatidylethanolamine (DOPE) were kindly donated by NOF Co. (Tokyo, Japan). N-(7-nitrobenz-2-oxa-1, 3-diazol-4-yl)dioleoyl phosphatidylethanolamine (NBD-PE) and lissamine rhodamine B-sulfonyl phosphatidylethanolamine (Rh-PE) were purchased from Avanti Polar Lipids (Birmingham, AL, USA). Monophosphoryl lipid A (MPL), Freund's complete adjuvant (CFA) and OVA were purchased from Sigma (St. Louis, MO.). SucPG and MGluPG were prepared using poly(glycidol) with number average and weight average molecular weights of 1.6×10^4 and 2.5×10^4, respectively, as previously reported [10,15]. Molar percentages of glycidol/carboxylated glycidol/n-decylamine-attached unit in the resultant SucPG and MGluPG were determined to be 18/74/8 and 9/81/10, respectively, using ^{1}HNMR.

2. 2. 2. Cell Lines Culture

DC2.4 cells, which were an immature murine DC line, were provided from Dr. K. L. Rock (Harvard Medical School, USA) and were grown in RPMI 1640 supplemented with 10% FBS (MP Biomedical, Inc.), 2 mM L-glutamine, 100 μM nonessential amino acid, 50 μM 2-mercaptoethanol (2-ME) and antibiotics at 37 °C [16]. EL4, a C57BL/6 mice-derived T lymphoma, was obtained from Tohoku University (Sendai, Japan). E.G7-OVA, which is a chicken egg OVA gene-transfected clone of EL4 and which presents OVA with MHC class I molecules, was obtained from the American Type Culture Collection (Manassas, VA) [17]. CD8-OVA1.3 cells, a T–T hybridoma against $OVA_{257–264}$/H-$2K^b$ complex, were kindly provided by Dr. C.V. Harding [18], and were grown in Dulbecco's modified Eagle's medium supplemented with 10% FBS, 50 μM 2-ME, and antibiotics. OT4H.1D5 cells, a T–T hybridoma against $OVA_{265–277}$/I-A^b complex, were kindly provided by Dr. J.A. Kapp [19], and were cultured in RPMI 1640 medium supplemented with 10% FBS, 50 μM 2-ME, and antibiotics.

2. 2. 3. Animals

Female C57BL/6 mice (H-2^b, 7 weeks old) were purchased from Oriental Yeast Co., Ltd. (Tokyo, Japan). The experiments were carried out in accordance with the guidelines for animal experimentation in Osaka Prefecture University.

2. 2. 4. Generation of Murine Bone Marrow-Derived DCs

Bone marrow-derived dendritic cells (BMDCs) were prepared according to the method of Lutz et al. with slight modification [20]. Briefly, bone marrow cells flushed from the femurs and tibias of C57BL/6 mice were seeded at 5×10^6 cells per sterile 100-mm bacterial grade culture dish in 10 ml of RPMI 1640 containing 10% FBS, 10 ng/ml recombinant murine granulocyte/macrophage colony-stimulating factor (GM-SCF, PeproTech EC Ltd.), 50 μM 2-ME, and antibiotics. On day 5, another 10 ml of culture medium was

added to the dish for medium replenishment. Nonadherent cells were harvested on days 6–8 as immature BMDCs.

2. 2. 5. Preparation of Liposomes

Liposomes were prepared by two kinds of methods, namely vortex and extrusion. Liposomes were prepared using vortex as follows: a dry thin membrane of a mixture of EYPC, DOPE, and SucPG or MGluPG (EYPC/DOPE. 1/1, mol/mol; lipids/polymer. 7/3, w/w) was dispersed in PBS by vortex to afford liposomes. Also, liposomes were prepared by extrusion method as follows: a dry thin membrane of a mixture of lipid and polymer was suspended by a brief sonication using a bath-type sonicator and the obtained liposome suspension was extruded through a polycarbonate membrane of pore sizes of 100 nm [9,10,15]. For liposomes encapsulating OVA, PBS containing OVA (4 mg/ml) was used for hydration of the lipid/polymer membranes. Free OVA was removed by ultracentrifuge for vortex method and by gel filtration using a Sepharose4B column for extrusion method. Unmodified liposomes were also prepared according to the above procedure using dry membrane of a lipid mixture without polymer.

2. 2. 6. Dynamic Light Scattering and Zeta Potential

Diameters and zeta potentials of the liposomes were measured using a Nicomp380 ZLS dynamic light scattering instrument (Particle Sizing Systems, Santa Barbara, CA) equipped with a 35 mW laser (632.8 nm wavelength). Zeta potentials were measured by equipped an Avalanche photodiode detector, and were detected at an 18.9 angle treated with 9.75 mV. Data was obtained as an average of more than three measurements on different samples.

2. 2. 7. Fusion Assay

Fusion between plain EYPC liposomes and polymer-modified liposomes was detected by measuring resonance energy transfer between NBD-PE and Rh-PE [21,22]. Polymer-modified liposomes containing NBD-PE and Rh-PE were prepared according to the above procedure using the lipid/polymer membrane containing NBD-PE (0.6 mol%) and Rh-PE (0.6 mol%) and extrusion through a polycarbonate membrane with a pore size of 50 nm. Probe-free plain liposomes were also prepared according to the same procedure. The labeled liposomes (final concentration of lipid 0.125 mM) were mixed with fluorescent probe-free EYPC liposomes (final concentration of lipid 0.25 mM) in 25 mM MES and 125 mM NaCl solution of varying pH. Their fusion was followed by monitoring the fluorescence intensity ratio of NBD-PE to Rh-PE (R). The excitation wavelength of NBD-PE was 450 nm and monitoring wavelengths for NBD-PE and Rh-PE were 520 nm and 580 nm, respectively. Percentage increase in R was defined as:

$$\text{Percentage increase in } R = (R_t - R_0)/(R_{100} - R_0) \times 100 \qquad (1)$$

where R_0 and R_t represent the initial and intermediary R values. R_{100} is the R of the labeled liposomes when the liposomes fused completely. The fluorescent lipid-labeled liposomes and the unlabeled liposomes were dissolved in methanol, dried by evaporation, and resuspended in MES buffer. The R value of the suspension was taken as R_{100} [21].

2. 2. 8. Cellular Uptake

The DC2.4 cells (1×10^5 cells) cultured for 2 days in a 12-well plate were washed with Hank's balanced salt solution (HBSS, Sigma) and then incubated in culture medium. The liposomes containing FITC-labeled OVA or the liposomes which lipids were substituted by Rh-PE (1 mol%) were added gently to the cells and incubated for 4 h at 37 °C. The cells were washed with HBSS three times, and then the detached cells using trypsin were applied to flow cytometry [23].

2. 2. 9. Microscopy

The DC2.4 cells (2×10^5 cells) cultured for 2 days in 35-mm glass-bottom dishes were washed with HBSS, and then incubated in serum-free medium. The liposomes containing FITC-labeled OVA (50 μg), in which lipids were substituted by Rh-PE (1 mol%), were added gently to the cells and incubated for 4 h at 37 °C. After the incubation, the cells were washed with HBSS three times and then replaced by serum-free medium. LysoTracker Red DND-99 (Molecular Probes) was used by the staining of intracellular acidic compartments according to the manufacturer's instructions. Briefly, LysoTracker Red was added to cells at the final concentration of 75 nM. After the 5 min-incubation, the cells were washed with HBSS three times. Confocal laser scanning microscopic (CLSM) analysis of these cells was performed using LSM 5 EXCITER (Carl Zeiss Co. Ltd.).

2. 2. 10. In Vitro Antigen Presentation Assay

The BMDCs were seeded in a 96-well culture plate at a density of 2×10^4 cells/well and cultured for 12 h at 37 °C. Each well was washed twice with HBSS, and then the cells were treated with various liposomes containing OVA or OVA solution at various OVA concentrations. After 3 h incubation at 37 °C, the cells were washed three times with HBSS. Subsequently, the cells were co-cultured with 2×10^4 CD8-OVA1.3 or OT4H.1D5 cells for 24 h at 37 °C. The response of stimulated CD8-OVA1.3 or OT4H.1D cells was assessed by determining the amount of IL-2 released into an aliquot of culture medium (100 μl) using a murine IL-2 ELISA KIT (PeproTech EC Ltd.).

2. 2.11. Immunization

Mice were nasally immunized with 10 μl aliquots of polymer-modified liposomes or unmodified liposomes containing 100 μg of OVA on days 0 and 14. Other group of mice was nasally immunized with OVA solution and another group of mice was subcutaneously

immunized with CFA/OVA emulsion.

2. 2. 12. CTL Assay

Splenocytes from immunized mice were suspended in RPMI 1640 medium supplemented with 10% FBS, 100 U/ml penicillin, 100 μg/ml streptomycin, 50 μM 2-ME, and 20 U/ml recombinant murine IL-2 (Peprotech, London, UK). Seven days after the second immunization, splenocytes were obtained from five mice, and the splenocytes were pooled and stimulated with mitomycin C-treated E.G7-OVA cells at a ratio of 10:1 for 5 days. The stimulated splenocytes were used as effector cells for the cytotoxicity assay. The CTL activity was evaluated at various ratios of effector cells to target cells (E.G7-OVA or EL4 cell), which were defined as E/T ratios, using a lactate dehydrogenase (LDH) cytotoxicity detection assay (Takara Biomedicals, Tokyo, Japan).

2. 3. Results and Discussion

2. 3. 1. Characterization of Liposomes

The author measured sizes and zeta potentials of prepared liposomes to characterize the liposomes. Table 2-1 presents particle sizes and zeta potentials of various liposomes prepared by vortex method or extrusion method. When the liposomes were prepared using the vortex method, unmodified liposomes were of about 1500 nm diameter. Although the SucPG-modified and MGluPG-modified liposomes were prepared according to the same method, they showed much smaller diameters of around 400–500 nm, probably because negatively charged polymers bound on the liposome surface enhanced hydration of themembrane surface and increased the colloidal stability of the liposomes. When prepared using the extrusion method, all liposomes showed similar particle sizes of around 110 nm, which corresponds to the pore size of the membrane used for their extrusion.

Regarding zeta potentials of the liposomes, the unmodified liposomes were nearly

zero, indicating that their surface was electrically neutral. However, the liposomes modified with SucPG or MGluPG showed negative zeta potentials of around -11 mV because of carboxylate anions on the polymer chains. This result demonstrates that these polymer-modified liposomes have electrically similar surface characteristics, irrespective of the polymers attached on their surface.

Table 2-1. Particle size and zeta potential of various liposomes.

Liposome	Method	Zeta potential/mV (SD)	Partide size/nm (SD)
Unmodified	Vortex	−0.51 (0.73)	1560 (817)
Unmodified	Extrusion	−0.92 (0.42)	116 (26.0)
SucPG	Vortex	−11 (2.4)	431 (112)
SucPG	Extrusion	−12 (2.5)	105 (18.0)
MGluPG	Vortex	−11 (3.5)	523 (78.0)
MGluPG	Extrusion	−11 (2.4)	110 (23.0)

2. 3. 2. Fusogenic Activities of Liposomes

In previous studies, it was showed that modification with SucPG and MGluPG provides pH-dependent fusion ability to stable EYPC liposomes [9,10]. In this study, the author used a mixture of EYPC and DOPE as liposomal lipids because inclusion of DOPE is shown to increase the fusion ability of liposomes [24]. The author examined the fusion abilities of these polymer-modified liposomes using resonance energy transfer between NBD-labeled and Rh-labeled lipids in the liposome membranes. The labeled liposomes were mixed withunlabeled plain EYPC liposomes and incubated for 1 h at various pH. Fusion between these liposomes was evaluated by monitoring the ratio of fluorescence intensity of NBD to that of Rh (*R* value).

Fig. 2-2 portrays the percent increase in the *R* value during 1 h incubation as a function of pH. The unmodified liposomes exhibit a very low extent of the increase in *R* throughout the experimental pH region, indicating the lack of fusion ability for unmodified liposomes. The SucPG-modified liposomes also showed a very low extent of the increase in *R* at neutral pH, but the *R* value increased below pH 6, suggesting that the SucPG-modified

liposomes generated fusion ability at weakly acidic pH. Although a similar pH-dependence of fusion was apparent for the MGluPG-modified liposomes, the extent of increase in the *R* value in the weakly acidic pH region was greater, indicating that the MGluPG-modified liposomes generated higher fusion ability than SucPG-modified liposomes. Because MGluPG has more hydrophobic side chains than SucPG, polymer chains of MGluPG might strongly disrupt the liposome membrane, resulting in more intensive fusion of the liposomes. These results indicate clearly that SucPG and MGluPG provided fusion ability to stable EYPC/DOPE liposomes and that the latter gave higher fusion ability than the former, which is consistent with our previous observation [10].

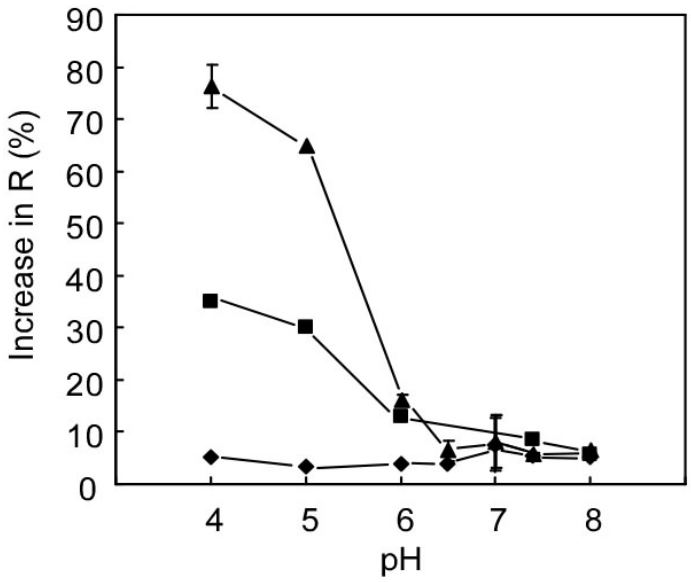

Figure 2-2. pH-dependent fusogenic properties of liposomes. Percent increase in R values for fluorescent lipid-labeled unmodified (diamonds), SucPG-modified (squares) and MGluPG-modified (triangles) EYPC/DOPE liposomes after 1 h incubation with the unlabeled plain EYPC liposomes at varying pH was shown. Measurements were performed in 25 mM MES and 125 mM NaCl at 37 °C. Each point is the mean ± SD (n = 3). Liposomes prepared by extrusion method were used.

2. 3. 3. Association of Liposomes with DCs

To estimate the performance of the polymer-modified liposomes as delivery vehicles

of antigenic proteins to cytoplasm of DC, the author examined the association of the liposomes with DCs after their incubation. The DC2.4 cells were incubated with various liposomes labeled with Rh-PE for 4 h; then fluorescence intensities of the cells were measured using a flow cytometer. As presented in Figs. 2-3a and 3b, cells treated with the labeled liposomes exhibited higher fluorescence intensities than intact cells, indicating the association of liposomes to the treated cells. In addition, the cells treated with SucPG-modified and MGluPG-modified liposomes displayed stronger fluorescence of Rh-PE, suggesting more efficient association of these polymer-modified liposomes to DCs. To evaluate their ability to associate DCs further, the average of cellular fluorescence intensities was calculated (Fig. 2-3c). Compared with the cellular association of the unmodified liposomes, on average, 6.6 and 6.2 times higher amounts of liposome association were observed, respectively, for SucPG-modified and MGluPG-modified liposomes. Actually, DCs are known to have scavenger receptors, which recognize the microorganisms or apoptotic cells with an anionic component [25]. As described in a previous report, these polymer-modified liposomes are likely to be taken up by DCs through interaction of their anionic surfaces with scavenger receptors [23].

Comparison of liposomes prepared by the extrusion method to those prepared by the vortex method shows that the former exhibited slightly higher cellular association than the latter, indicating that DCs engulf small liposomes more efficiently than large liposomes with diameters of 500–1500 nm, although the difference was slight.

2. 3. 4. Cytoplasmic Delivery of Antigenic Protein to DCs

The author examined the ability of the polymer-modified liposomes to deliver OVA, which was used as an antigenic protein into cytosol of DCs. To monitor the inracellular distribution of the liposomes, the encapsulated OVA and the liposome membrane were labeled, respectively, using FITC and Rh-PE. The labeled liposomes encapsulating

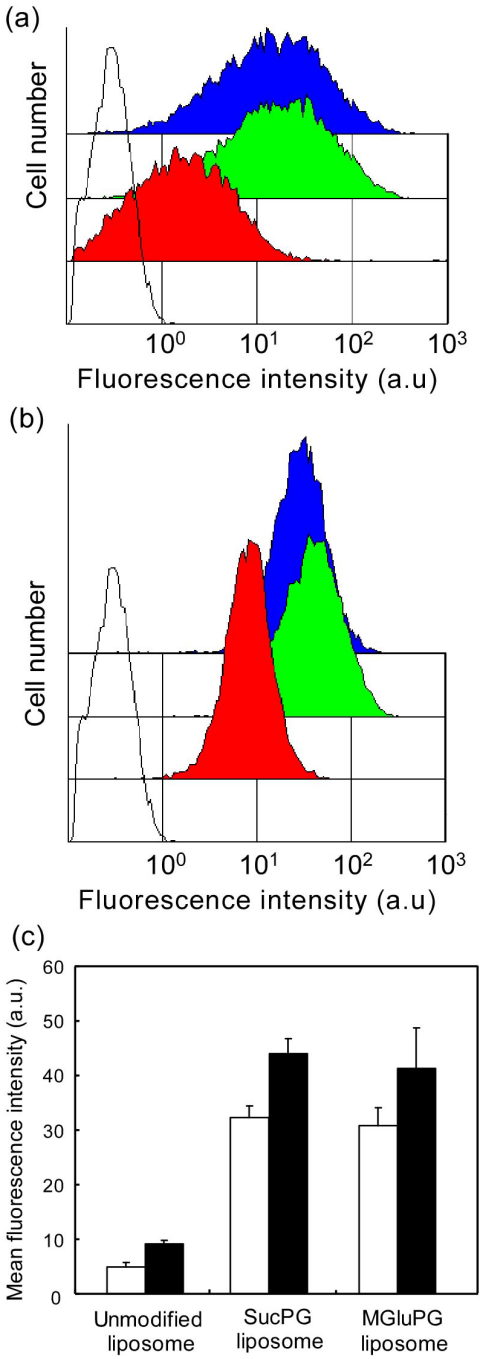

Figure 2-3. Evaluation of cellular association of various liposomes labeled with Rh-PE using flow cytometry. DC2.4 cells were treated with SucPG-modified (green), MGluPG-modified (blue) and unmodified (red) liposomes prepared by vortex method (a) or extrusion method (b). Fluorescence intensity of untreated cells (black lines) is also shown. (c) Mean fluorescence intensity of the liposome-treated DC2.4 cells. Each point is the mean ± SD (n = 3). Cellular treatment was performed by incubating with liposomes prepared by vortex method (open) or extrusion method (closed) in serum-free medium at 37 °C for 4 h.

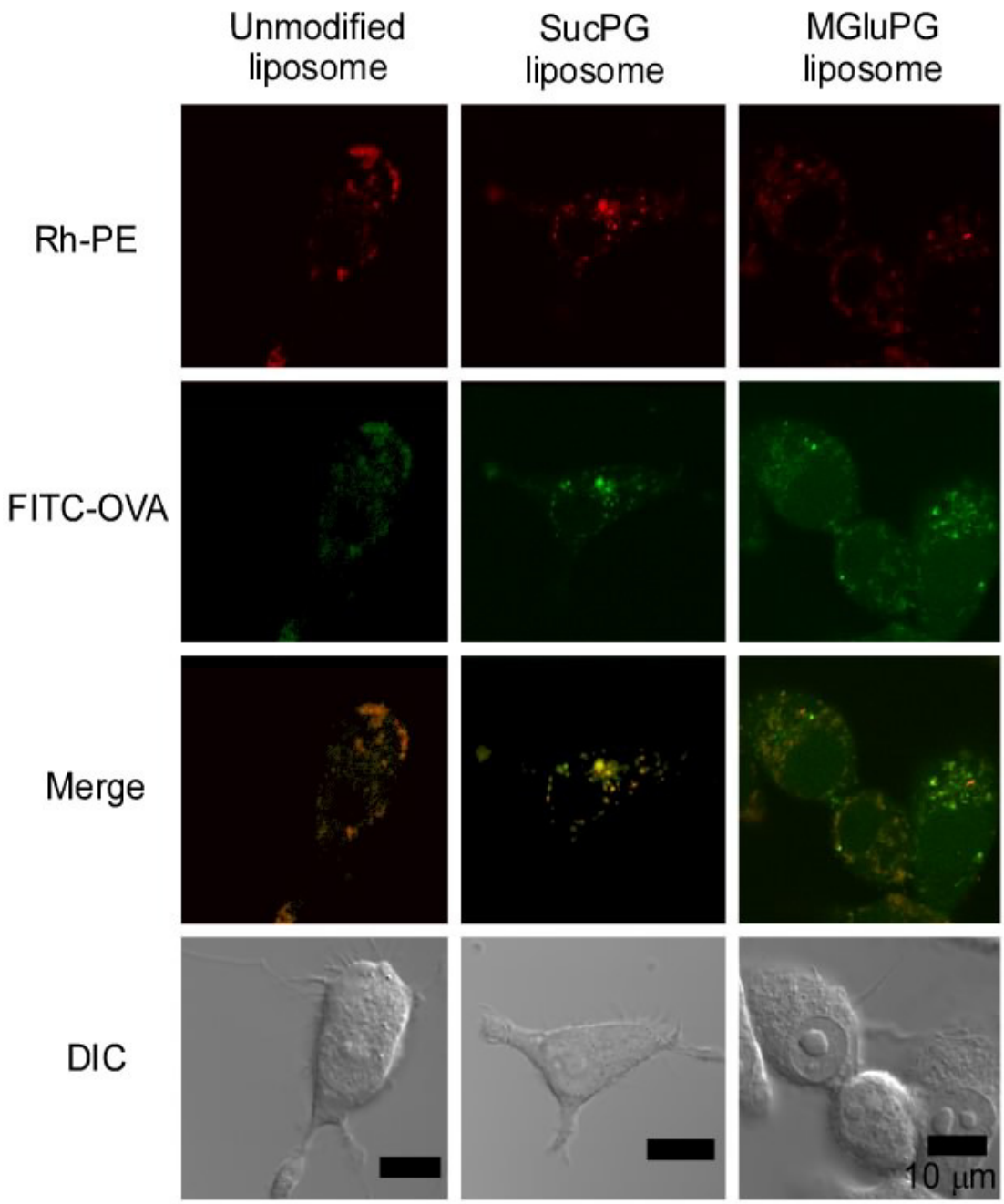

Figure 2-4. CLSM images of DC2.4 cells treated with various liposomes labeled with Rh-PE and loaded with FITC-OVA. Liposomes prepared by extrusion method were used. DC2.4 cells were incubated with liposomes at 37 °C for 4 h in the serum-free medium, washed with HBSS and observed with CLSM. Scale bar represents 10 μm. Concentration of liposomal lipids for cellular treatment was 0.1 mM.

FITC-OVA were added to DC2.4 cells and incubated for 4 h. Then, the cells were washed with buffer and observed using CLSM (Fig. 2-4). When DC2.4 cells were treated with the unmodified liposomes, punctate fluorescence of FITC-OVA was observed in the cells. In

addition, fluorescence of Rh was observed at the same places that FITC-OVA fluorescence appeared. This result suggests that OVA molecules loaded in the unmodified liposomes were still trapped in the endosomes and/or the lysosomes. For cells treated with the SucPG liposomes, the fluorescence of FITC-OVA was also mostly punctate and overlapped with Rh-PE fluorescence. In contrast, for cells treated with MGluPG liposomes, diffuse fluorescence of FITC-OVA was observed in the cells, while fluorescence of Rh-PE remained punctate, indicating that the labeled OVA molecules were transferred into cytosol from endosome, where liposomal membrane remained trapped. Probably, the highly fusogenic MGluPG liposomes generate strong fusion ability in the weakly acidic environments of endosome and fuse with endosomal membrane, resulting in the release of entrapped OVA molecules into cytosol [9,10]. The SucPG liposomes only slightly induced the transfer of OVA into cytosol. Therefore, it is implied that their fusion ability is insufficient to induce fusion or destabilization of endosomal membrane for efficient transfer of OVA molecules into cytosol (Fig. 2-2).

2. 3. 5. Induction of Cellular Immune Responses

The author examined the ability of these polymer-modified liposomes to activate cellular immunity. Although immunization is generally conducted *via* subcutaneous injection of antigen, the author exploited the administration of antigen through nasal mucosa because antigen administration can be achieved using a noninvasive, needleless method in this immunization. It can also induce both mucosal and systemic immunities [11–13].

For this study, the C57BL/6 mice were immunized nasally twice with OVA-loaded liposomes containing MPL in the membrane as an adjuvant. One week later, splenocytes were collected from the immunized mice and stimulated with mitomycin C-treated E.G7-OVA cells. Then their toxicity toward E.G7-OVA cells, which are OVA-presenting recombinant cells derived from EL4 cells, was measured to estimate the induction of OVA-specific CTLs.

Fig. 2-5a shows cellular toxicities of the stimulated splenocytes recovered from mice that had been immunized with various OVA-loaded liposomes or free OVA. When free OVA was used for the immunization, CTL activity was almost identical to that of the case of untreated mice, indicating that free OVA has no ability to induce cellular immunity under experimental conditions. In addition, administration of the OVA-loaded unmodified liposomes increased the CTL activity only slightly. In contrast, when the polymer-modified liposomes containing OVA were used for immunization, higher CTL activities were observed. Especially, MGluPG-modified liposomes more efficiently induced activation of CTLs than the SucPG-modified liposomes did. Indeed, the same stimulated splenocytes did not exhibit cellular toxicity toward EL4 cells (Fig. 2-5b). Therefore, immunization with these polymer-modified liposomes containing OVA induced activation of OVA-specific CTLs. Considering that these polymer-modified liposomes showed a similar degree of cellular association with DCs (Fig. 2-3), it is likely that the difference in fusion ability between these liposomes caused their different abilities for cellular immune activation.

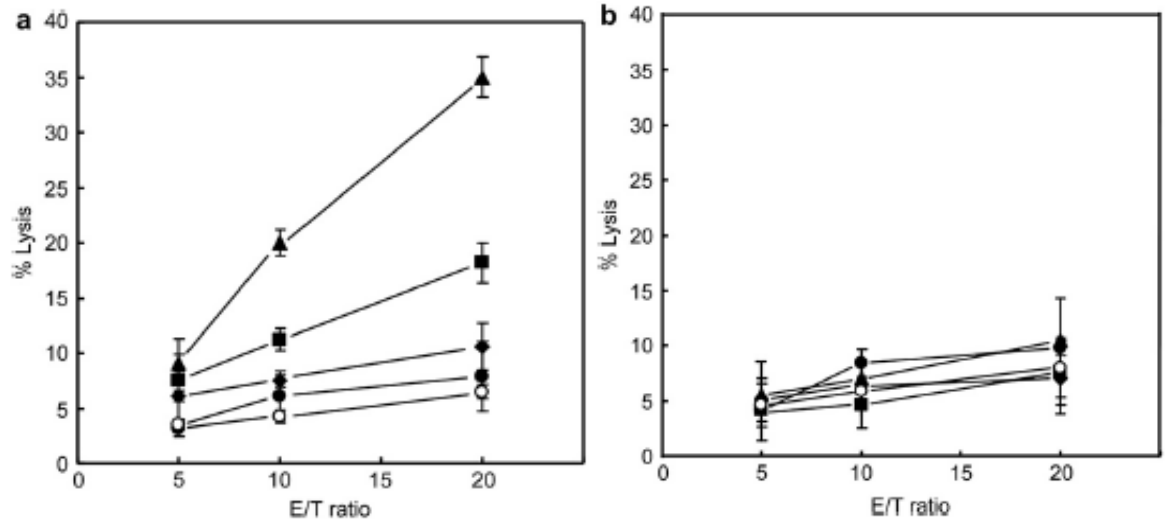

Figure 2-5. OVA-specific cytotoxic T cell responses in spleen at Day 21 after nasal immunization with OVA solution (●), polymer-unmodified liposomes (◆), SucPG liposomes (■) and MGluPG liposomes (▲). Liposomes prepared by vortex method were used. Cytotoxic activity was measured by a LDH assay at indicated E/T ratios. E.G7-OVA cells (a) and EL4 cells (b) were used as target cells. T cell responses from mice without treatment (○) were also shown as a negative control.

2. 3. 6. Estimation of Antigen Presentation

The highly fusogenic MGluPG-modified liposomes induced cellular immune response efficiently. Because the cellular immunity is activated through antigen presentation on the MHC class I molecules of antigen presenting cells (APCs), such as DCs, the author expected that the liposome-mediated delivery of OVA molecules into cytosol of APCs caused the antigen presentation on the MHC class I molecules, engendering activation of cellular immunity. To confirm this mechanism, the author further examined whether the MGluPG-modified liposomes actually possess the capability of inducing antigen presentation on the MHC class I on DCs.

The OVA-loaded liposomes or free OVA were added to BMDCs; then BMDCs were co-cultured with CD8-OVA1.3 or OT4H.1D5 cells, which respectively recognize MHC class I/peptide complexes or MHC class II/peptide complexes. Subsequently, MHC class-restricted antigen presentation was evaluated by detection of IL-2 secretion in supernatants of the co-cultured medium. Fig. 2-6 shows IL-2 production levels of the co-cultured medium of BMDCs treated with the OVA-loaded liposomes and free OVA. As depicted in Fig. 2-6a, interaction with BMDCs and OVA-loaded MGluPG-modified liposomes strongly enhanced IL-2 release from CD8-OVA1.3 cells. The BMDCs treated with either OVA-loaded in the plain liposomes or free OVA also promoted IL-2 release from the CD8-OVA1.3 cells, but the promotion occurred to a much lesser degree than the case of the OVA-loaded MGluPG-modified liposomes. This result suggests that the OVA-loaded MGluPG-modified liposomes induced antigen presentation through the MHC class I molecules on BMDCs more efficiently than free or plain liposome-encapsulated OVA. In contrast, BMDCs treated with these OVA-loaded liposomes or free OVA enhanced IL-2 release from OT4H.1D5 cells only slightly, suggesting that the OVA-loaded MGluPG-modified liposomes have no ability to induce MHC class II-mediated antigen presentation. These results demonstrate that the MGluPG-modified liposomes can induce

antigen presentation through MHC class I molecules.

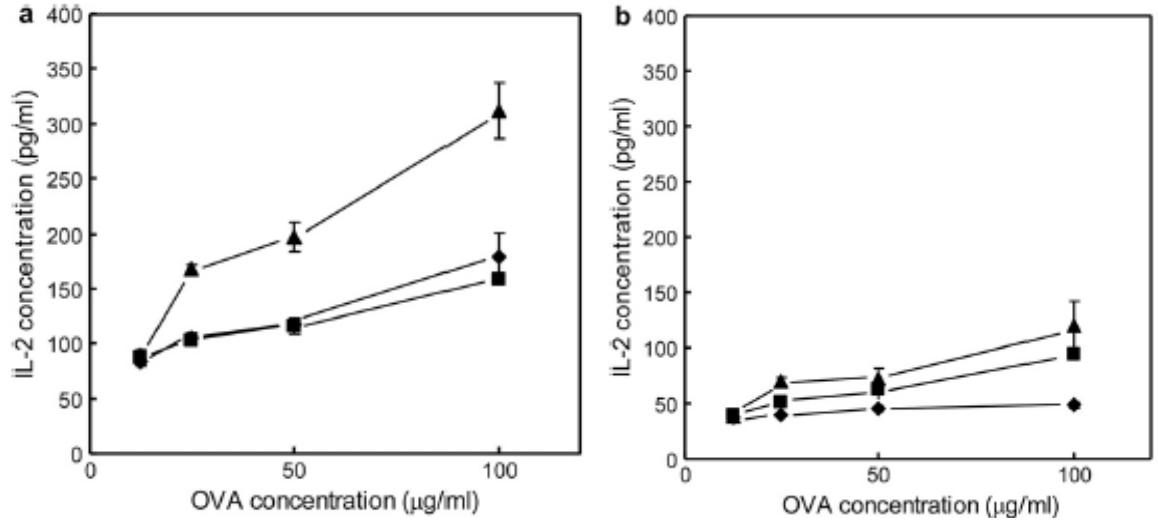

Figure 2-6. Presentation of OVA-derived epitope peptides *via* MHC molecules in BMDCs. BMDCs were incubated with free OVA (diamonds), and OVA-loaded MGluPG-modified (triangles) and unmodified (squares) liposomes at varying OVA concentrations for 3 h. Liposomes prepared by extrusion method were used. Concentrations of IL-2 in the medium after co-culture of OVA-treated BMDCs with (a) CD8-OVA1.3 (specific for $OVA_{257–264}$/H-$2K^b$ complex) and (b) OT4H.1D5 (specific for $OVA_{265–277}$/I-A^b complex) cells for 24 h as a function of OVA concentration during the BMDCs treatment were shown. Each point represents means ± SD.

2. 3. 7. Influence of Liposome Size on Cellular Immunity Activation

Finally, the author examined the influence of liposome size on their ability to activate cellular immunity. First, MGluPG liposomes with diameters around 500 nm and 110 nm were prepared, respectively, using vortex and extrusion methods (Table 2-1). The author compared the respective efficiencies of the intracellular OVA delivery of these liposomes with different sizes. The amounts of encapsulated OVA per 1 nmol of liposomal lipid were estimated to be 0.77 μg for the large liposomes and 0.2 μg for the small liposomes. When the same amount of FITC-OVA was added to DC2.4 cells as encapsulated in the liposomes, approximately double the amount of FITC-OVA was taken up by the cells using the large liposomes than those using the small liposomes (Fig. 2-7a).

The author also examined the intracellular distribution of OVA molecules delivered

by these MGluPG liposomes of different sizes. The DC2.4 cells were incubated with these MGluPG liposomes encapsulating FITC-OVA for 4 h and then observed using CLSM (Fig. 2-7b). Strong and punctate fluorescence of FITC-OVA was observed in cells treated with large MGluPG liposomes. Punctate fluorescence of FITC-OVA is mostly overlapped with fluorescence of LysoTracker Red. Therefore, most FITC-OVA molecules remained trapped in the endosomes and lysosomes. The punctate fluorescence of FITC-OVA was still observed in the liposome-treated cells even after 24 h incubation, indicating that FITC-OVA molecules were retained in endosome and lysosome for 24 h (data not shown). In contrast, cells treated with the small MGluPG liposomes displayed diffuse fluorescence of FITC-OVA, suggesting that these small liposomes delivered the antigenic protein efficiently into the cytosol.

The large MGluPG liposomes prepared by vortex showed less endosomal escape, compared to the small extruded MGluPG liposomes, although these liposomes were modified with the same fusogenic polymer MGluPG. Because the large liposome should have a multilamellar structure, only the outermost layer of the bilayer membranes with low curvature might contact with the target membrane, resulting in low efficiency of fusion. In fact, the author evaluated fusion ability of the large MGluPG liposome by the same method used for evaluation of the small MGluPG liposome fusion (Fig. 2-2) and observed only 10% increase in *R* value after 3.5 h incubation at pH4.0, indicating a low fusion ability of the large MGluPG liposome (data not shown).

These liposomes encapsulating OVA were administered nasally; then CTL responses were evaluated as described above (Fig. 2-7c). Splenocytes of the immunized mice exhibited high toxicity toward OVA-presenting E.G7-OVA cells but almost no toxicity toward their parent EL4 cells, indicating that both liposomes were able to induce OVA-specific CTLs, irrespective of their size difference. Moreover, the CTLs derived with these OVA-loaded liposomes showed an almost identical level of toxicity to E.G7-OVA cells within the error bars. The large MGluPG liposomes delivered more OVA molecules to cells than the small

liposomes. However, the latter introduced OVA molecules into the cytosol more efficiently than the former. Consequently, these liposomes might achieve CTL activation to a similar degree.

To evaluate the potential of MGluPG liposomes as an adjuvant, the author compared their induced CTLs activity with that of CFA, which is widely used for induction of immune responses [26]. The result is also presented in Fig. 2-7c. Apparently, CTL activity induced by CFA is of a comparable level to that of MGluPG liposomes.

2. 4. Conclusions

For this study, by modification of liposomes with carboxylated poly(glycidol) derivatives, such as SucPG and MGluPG, the author prepared pH-sensitive fusogenic liposomes that can deliver antigenic proteins into the cytosol of DCs. The author then investigated their ability to activate cellular immune response. Indeed, these polymer-modified liposomes were shown to have capabilities of delivering antigenic OVA into cytosol of DCs and inducing antigen presentation through the MHC class I molecules on DCs. Nasal administration of these liposomes encapsulating OVA activated the antigen-specific cellular immunity in mice. Especially, highly fusogenic MGluPG liposomes exhibited high ability for CTL activation, which is comparable to the widely used adjuvant CFA. Despite its high ability to activate immune response, CFA is known to induce inflammatory reactions at the site of administration. Consequently, CFA is not applicable to humans. In contrast, MGluPG liposomes comprise phospholipid and biocompatible poly(glycidol) derivatives [27]. For that reason, MGluPG liposomes and their relevant liposomes might be promising antigen carriers for establishment of cancer immunotherapy and mucosal vaccination.

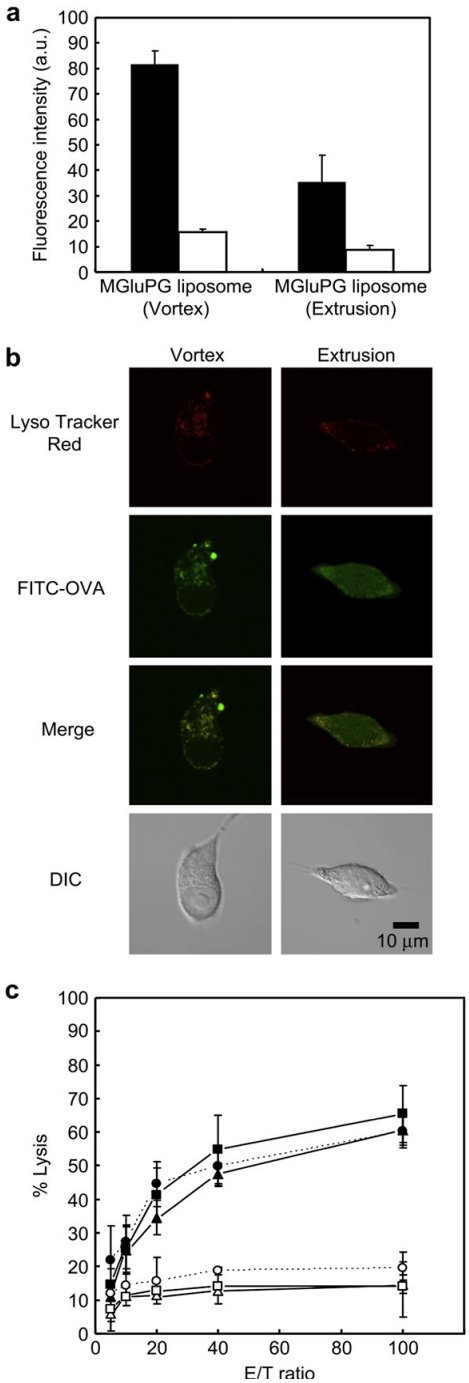

Figure 2-7. (a) Effect of liposome size on delivery of FITC-OVA by MGluPG liposomes. DC2.4 cells were treated with FITC-OVA-loaded liposomes prepared by extrusion or vortex method in the serum-free medium at 4 °C (open) and 37 °C (closed) for 4 h, and then cellular association of FITC-OVA was estimated using flow cytometry. Each point is the mean ± SD (n = 3). OVA concentration was 50 μg/ml. (b) CLSM images of DC2.4 cells treated with FITC-OVA-loaded liposomes prepared by vortex method or extrusion method. DC2.4 cells were incubated with MGluPG-modified liposomes encapsulating FITC-OVA (50 μg of OVA/ml) in the serum-free medium at 37 °C for 4 h. (c) Effect of liposome size on OVA-specific cytotoxic T cell response. Mice were nasally immunized with OVA-loaded MGluPG liposome prepared by vortex method (triangles) or by extrusion method (squares). Mice were also immunized with CFA/OVA emulsion subcutaneously (circles). Cytotoxic activity of splenocytes of the immunized mice was measured by a LDH assay at indicated E/T ratios. E.G7-OVA cells (closed symbols) and EL4 cells (open symbols) were used as target cells.

2. 5. References

1. J. Banchereau and RM. Steinman, *Nature* 1998, **392**, 245–252.

2. I. Mellman and RM. Steinman, *Cell* 2001, **106**, 255–258.

3. NC. Fernadez et al., *Nat. Med.* 1999, **5**, 405–411.

4. T. Akagi et al., *Biomaterials* 2007, **28**, 3427–3436.

5. T. Yoshikawa et al, *Biochem. Biophys. Res. Commun.* 2008, **366**, 408–413.

6. YJ. Kwon et al., *J. Control Release* 2005, **105**, 199–212.

7. J. Kunisawa et al., *J. Immunol.* 2001, **167**, 1406–1412.

8. L. Bungener et al., *Vaccine* 2002, **20**, 2287–2295.

9. K. Kono et al., *Biochim. Biophys. Acta.* 1997, **1325**, 143–154.

10. N. Sakaguchi et al., *Bioconjugate Chemistry* 2008, **19**, 1040–1048.

11. J. Mestecky et al., *Behring Inst. Mitt.* 1997, **98**, 33–43.

12. FR. Brennan et al., *J. Virol.* 1999, **73**, 930–938.

13. S. Sjolander et al., *Vaccine* 2001, **19**, 4072–4080.

14. MT. De Magistris et al., *Adv. Drug Del. Rev.* 2006, **58**, 52–67.

15. K. Kono et al., *Biochim. Biophys. Acta* 1994, **1193**, 1–9.

16. Z. Shen et al., *J. Immunol.* 1997, **158**, 2723–2730.

17. MW. Moore et al., *Cell* 1988, **54**, 777.

18. CV. Harding et al., *J. Immunol.* 1994, **153**, 4925–4933.

19. Y. Li et al., *J. Leukoc. Biol.* 1994, **56**, 616–624.

20. MB. Lutz et al., *J. Immunol.* Methods 1999, **223**, 77–92.

21. K. Kono et al., *Gene Ther.* 2001, **8**, 5–12.

22. DK. Struck et al., *Biochemistry* 1981, **20**, 4093–4099.

23. E. Yuba et al., *J. Controlled Release* 2008, **130**, 77–83.

24. N. Bergstrand et al., *Biophys. Chem.* 2003, **104**, 361–379.

25. ML. Albert et al., *J. Exp. Med.* 1998, **188**, 1359–1368.

26. Y. Ke et al., Eur. *J. Immunol.* 1995, **25**, 549–553.

27. RK. Kainthan et al., *Biomacromolecules* 2006, **7**, 703–709.

Chapter 3

Carboxylated Hyperbranched Poly(glycidol)s for Preparation of pH-Sensitive Liposomes

3. 1. Introduction

Cytoplasmic delivery of bioactive molecules such as proteins and nucleic acids, which are unable to permeate a cellular membrane themselves, is important to establish therapies—such as immunotherapy and gene therapy—based on these molecules. Although various systems have been attempted for application to cytoplasmic delivery, one of promising systems is pH-sensitive liposome, which induces destabilized and/or fusogenic activity under mildly acidic conditions. Various methods have been applied to produce pH-sensitive liposomes. For example, pH-sensitive amphiphiles, such as oleic acid and cholesteryl hemisuccinate, have been mixed with non-bilayer-forming phospholipid dioleoylphosphatidylethanolamine (DOPE) to yield pH-sensitive liposomes [1,2]. Another efficient method for pH-sensitization of liposome is modification of stable liposomes with pH-sensitive membrane active molecules such as fusion peptides derived from viral fusogenic proteins, or synthetic polymers with carboxyl groups such as poly(alkyl acrylic acid)s [3,4]. Earlier studies by the authors developed a series of carboxylated poly(glycidol) derivatives for pH-sensitization of liposomes [5–7]. These polymers have a linear backbone structure similar to that of poly(ethylene glycol) (PEG) and carboxyl groups on the side chains, which control interaction of the polymer backbone with lipid membranes in a pH-dependent manner. Earlier studies showed that these polymer-modified liposomes are stable at neutral pH, but that they exhibit considerable destabilization under mildly acidic conditions and deliver contents into cytosol by membrane fusion with endosome/lysosome membranes [5–7].

Generally, membrane fusion as a biological function is mediated by fusogenic proteins.

For example, enveloped viruses of various kinds have proteins that promote fusion of their envelope with cellular membranes to invade target cells. A very well studied viral fusion protein is influenza virus hemagglutinin (HA), which forms a fusion-active trimeric structure in the intracellular acidic compartment endosome and causes membrane fusion [8]. Considering these protein-mediated fusion processes, it might be important that fusogenic proteins having a bulky steric structure interact with a membrane for efficient membrane fusion because such interaction might generate a defective area and initiate membrane fusion.

Synthetic polymers of various kinds reportedly interact with membranes and induce membrane fusion [4,5,7,9,10]. Considering that these synthetic polymers generally have a linear structure, it is presumed that their interaction with membranes might not be so effective to generate defective regions for initiation of membrane fusion as sterically bulky proteins do. To date, the influence of the backbone structure of fusogenic polymers on their membrane fusion activity remains unknown. Hyperbranched polymers tend to take on a three-dimensional and spherical structure, which differs from those of linear polymers taking on a random coil structure [11–15]. Recently, 3-methyl-glutarylated poly(glycidol) was synthesized by the authors. It destabilizes phospholipid membranes under a weakly acidic environment and causes membrane fusion [7]. For the present study, its analogous polymers were prepared using hyperbranched poly(glycidol)s (HPGs) with different degrees of polymerization (DP), 3-methyl-glutarylated HPGs (MGlu-HPGs). Results described herein demonstrate that the DP and backbone structure of the pH-sensitive polymers affected their pH-sensitive fusion properties and their performance as intracellular delivery vehicles.

3. 2. Materials and Methods

3. 2. 1. Materials

HPGs with DPs of 10, 20, 40 and 60, which are respectively designated as HPG10, HPG20, HPG40 and HPG60, were provided by Daicel Chemical Industries, Ltd. (Osaka,

Japan). Egg yolk phosphatidylcholine (EYPC) and L-dioleoyl phosphatidylethanolamine (DOPE) were kindly donated by NOF Co. (Tokyo, Japan). Pyrene, pyranine, 1-aminodecane and Triton X-100 were obtained from Tokyo Chemical Industries Ltd. (Tokyo, Japan). *p*-Xylene-bis-pyridinium bromide (DPX) was from Molecular Probes (Oregon, USA). *N*-(7-Nitrobenz-2-oxa-1,3-diazol-4-yl)dioleoyl phosphatidylethanolamine (NBD-PE) and lissamine rhodamine B-sulfonyl phosphatidylethanolamine (Rh-PE) were purchased from Avanti Polar Lipids (Birmingham, AL, USA). 3-Methylglutaric anhydride was obtained from Aldrich (Milwaukee, WI). 4-(4,6-Dimethoxy-1,3,5-triazin-2-yl)-4-methyl morpholinium chloride (DMT-MM) was from Wako Pure Chemical Industries Ltd. (Osaka, Japan). Ovalbumin (OVA) and fluorescein isothiocyanate (FITC) were purchased from Sigma (St. Louis, MO.). 3-Methylglutarylated linear poly(glycidol) (MGluPG) (Fig. 1) was prepared as previously reported using two kinds of poly(glycidol)s with different molecular weights: PG76 with number average molecular weight (Mn) of 5.6×10^3 and weight average molecular weight (Mw) of 8.7×10^3, and PG222 with Mn of 1.6×10^4 and Mw of 2.5×10^4, which were evaluated using gel permeation chromatography with Shodex KD-803 and KF805L columns (Showa Denko) and poly(ethylene glycol)s as the standard. Obtained polymers were designated as MGluPG76 and MGluPG222, respectively [7]. FITC-OVA was prepared by reacting OVA (10 mg) with FITC (11.8 mg) in 0.5 M $NaHCO_3$ (4 mL, pH 9) at 4 °C for three days and subsequent dialysis.

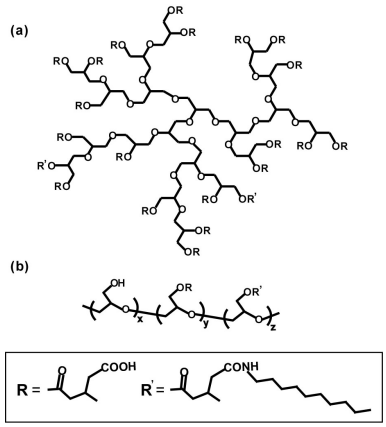

Figure 3-1. Structures of MGlu-HPG20-C_{10} (a) and linear MGluPG-C_{10} (b).

3. 2. 2. Synthesis of Hyperbranched Poly(glycidol) Derivatives

3-Methyl-glutarylated hyperbranched poly(glycidol) (MGlu-HPG) was prepared by reaction of HPG with varying DP with 3-methylglutaric anhydride. HPG10 (0.765 g) and LiCl (0.765 g) were dissolved in pyridine (18 mL) and 3.0 equiv. of 3-methylglutaric anhydride (3.98 g) was added to the solution. The mixed solution was kept at 115 °C for 24 h with stirring. Then, the reaction mixture was evaporated and dialyzed against water for 3 days. The product was recovered by freeze-drying. HPG20, HPG40 and HPG60 were also reacted with 3-methylglutaric anhydride by the same procedure. As anchor moieties for fixation of MGlu-HPG onto liposome membranes, 1-aminodecane was combined with carboxyl groups of MGlu-HPG. Each polymer was dissolved in water around pH 7.4, and 1-aminodecane (0.18 equiv. to carboxyl group of polymer) was reacted to carboxyl groups of the polymer using DMT-MM (0.18 equiv. to carboxyl groups of polymers) at room temperature for three days with stirring. The obtained polymers were purified by dialysis in water.

3. 2. 3. Cell Culture

DC2.4 cells, which were an immature murine DC line, were provided from Dr. K. L. Rock (Harvard Medical School, USA) and were grown in RPMI 1640 supplemented with 10% FBS (MP Biomedical, Inc.), 2 mM L-glutamine, 100 μM non-essential amino acids (Gibco, Inc.), 50 μM 2-mercaptoethanol (2-ME) and antibiotics at 37 °C [16].

3. 2. 4. Precipitation pH

Precipitation pH of polymers was determined by measuring the optical density of aqueous polymer solutions (0.25 mg/mL) at various pH. Polymers were dissolved in 30 mM sodium acetate and 120 mM NaCl aqueous solution of various pH. After 5 min incubation at 25 °C, optical densities of the polymer solutions at 500 nm were measured by using a spectrophotometer (Jasco V-520). Precipitation pH was determined using optical density-pH

profiles as the pH at which OD drastically rose.

3. 2. 5. Pyrene Fluorescence

A given amount of pyrene in acetone solution was added to an empty flask, and acetone was removed under vacuum. Polymer (0.2 mg/mL) dissolving in 25 mM MES and 125 mM NaCl solution of a given pH was added to the flask, yielding 1 μM concentration of pyrene. The sample solution was stirred overnight at room temperature, and emission spectra with excitation at 337 nm were recorded. The fluorescence intensity ratio of the first band at 373 nm to the third band at 384 nm (I_1/I_3) was analyzed as a function of pH of the solution.

3. 2. 6. Preparation of Pyranine-Loaded Liposomes

To a dry, thin membrane of EYPC (7 mg) was added 500 μL of aqueous 35 mM pyranine, 50 mM DPX, and 25 mM MES solution (pH 7.4), and the mixture was sonicated for 2 min using a bath-type sonicator. The liposome suspension was further hydrated by freeze and thaw, and was extruded through a polycarbonate membrane with a pore size of 100 nm. The liposome suspension was applied to a sepharose4B column to remove free pyranine from the pyranine-loaded liposomes. Polymer-modified liposomes were also prepared according to the above procedure using dry membrane of a lipid mixture with polymers (lipids/polymer = 7/3, w/w).

3. 2. 7. Release of Pyranine from Liposome

Release of pyranine from liposome was measured as previously reported [7,17]. Pyranine fluorescence was quenched by DPX inside of the liposomes, but this molecule exhibits intense fluorescence when released from the liposome [17]. For study of interaction of polymers with lipid membranes, to a suspension of pyranine-loaded liposomes (lipid concentration: 2.0×10^{-5} M) in 25 mM MES and 125 mM NaCl buffer of varying pH was

added a given amount of the polymer dissolved in the same buffer (final concentration: 0.013 mg/mL) at 25 °C, and fluorescence intensity (512 nm) of the mixed suspension was followed with excitation at 416 nm using a spectrofluorometer (Jasco FP-6500). For study of release behavior of polymer-modified liposomes, polymer-modified liposomes encapsulating pyranine were added to 25 mM MES and 125 mM NaCl buffer of varying pHs at 37 °C and fluorescence intensity of the suspension was monitored (lipid concentration: 2.0×10^{-5} M). The percent release of pyranine from liposomes was defined as

$$\text{Release (\%)} = (F_t - F_i) / (F_f - F_i) \times 100$$

where F_i and F_t mean the initial and intermediary fluorescence intensities of the liposome suspension, respectively. F_f is the fluorescent intensity of the liposome suspension after the addition of TritonX-100 (final concentration: 0.1%).

3. 2. 8. Liposome Size Change

EYPC liposomes were prepared as described above without pyranine and DPX. EYPC liposomes (4.1 mM, 103.4 μL, pH 7.4) were added to 25 mM MES and 125 mM NaCl buffer of various pHs (2370 μL). And then, 26.6 μL of polymer solution of the same buffer (10 mg/mL, pH 7.4) was added. The mixed solutions were incubated overnight. pH of the mixed solution was measured and liposome diameters were evaluated using a Nicomp 380 ZLS dynamic light scattering instrument (Particle Sizing Systems, Santa Barbara, CA) equipped with a 35 mW laser (λ=632.8 nm). Data was obtained as an average of more than three measurements on different samples.

3. 2. 9. Intracellular Behavior of Liposomes

The FITC-OVA-loaded liposomes containing Rh-PE were prepared as described above except that mixtures of polymers and EYPC containing Rh-PE (0.1 mol%) was dispersed in phosphate-buffered saline containing FITC-OVA (4 mg/mL). The DC2.4 cells (2

$\times 10^5$ cells) cultured for 2 days in 35-mm glass-bottom dishes were washed with Hank's balanced salt solution (HBSS, Sigma), and then incubated in serum-free RPMI medium (500 μL). The FITC-OVA-loaded liposomes (100 μg/mL of FITC-OVA, 500 μL) were added gently to the cells and incubated for 4 h at 37 °C. After the incubation, the cells were washed with HBSS three times. Confocal laser scanning microscopic (CLSM) analysis of these cells was performed using LSM 5 EXCITER (Carl Zeiss Co. Ltd.). Fluorescence intensity of these cells was also determined using a Coulter Epics XL Flow Cytometer (Coulter Corporation, Florida, USA) [18].

3. 2. 10. Fusion of Liposomes in Cell

Liposomes containing NBD-PE and Rh-PE (each 0.6 mol%) were prepared as described above using DOPE as an additional lipid component and suspended in PBS. The DC2.4 cells (2×10^5 cells) cultured for 2 days in 35-mm glass-bottom dishes were washed with HBSS, and then incubated in serum-free RPMI medium (500 μL). Then, the liposomes suspension (1.0 mM of liposomal lipid, 500 μL) were added gently to the medium of the cells and incubated for 4 h at 37 °C. After the incubation, the cells were washed with HBSS three times and analyzed by CLSM. Fluorescence of NBD-PE and Rh-PE was observed through specific path filters (λ_{em} = 500–530 nm for NBD-PE and λ_{em} > 560 nm for Rh-PE) with excitation at 488 nm. Fluorescence intensities of these cells were also determined by flow cytometry with excitation at 488nm. The fluorescence intensity ratio of NBD-PE to Rh-PE was defined as

$$\mathrm{NBD/Rh} = (I_{\mathrm{NBD}} - I_{\mathrm{NBD},0}) / (I_{\mathrm{Rh}} - I_{\mathrm{Rh},0})$$

where I_{NBD} and I_{Rh} are the fluorescence intensities of the liposome-treated cells detected by FL1 (λ_{em} = 505–545 nm) and FL2 channel (λ_{em} = 560–590 nm), respectively. $I_{\mathrm{NBD},0}$ and $I_{\mathrm{Rh},0}$ are the fluorescence intensities of untreated cells detected by FL1 and FL2 channel, respectively.

3. 3. Results and Discussion

3. 3. 1. Characterization of HPG Derivatives

Previous studies developed and assessed a series of carboxylated linear poly(glycidol) derivatives for pH-sensitization of liposome [5–7]. Especially, MGluPG-modified liposomes were stable at neutral pH and showed strong fusogenic activity under weakly acidic conditions [7]. Considering the function of viral fusogenic proteins for viral membrane fusion, it was assumed that a polymer with a three-dimensional backbone structure can interact with membranes more effectively and intensively than a linear polymer. Therefore, a hyperbranched polymer was selected as a backbone structure. We prepared four kinds of MGlu-HPGs with different molecular sizes, namely MGlu-HPG10, MGlu-HPG20, MGlu-HPG40, and MGlu-HPG60, using HPGs with DPs of 10, 20, 40, and 60, as pH-sensitive polymers with a hyperbranched structure. Also, two kinds of MGluPGs with different chain lengths, namely MGluPG76 and MGluPG222, were prepared as pH-sensitive polymers with a linear structure, using PG76 and PG222. Hydrodynamic diameters of HPG10, HPG20, HPG40, HPG60, PG76, and PG222 were estimated to be 2.0, 2.6, 3.2, 3.6, 4.8, and 8.6 nm, respectively, according to the method of Hester and Mitchell using GPC with PEG standards [19].

Compositions of these polymers, which were estimated using ^{1}H NMR, are resented in Table 3-1. For all polymers, only low percentages of unreacted glycidol units remained on the polymer backbone after the reaction of HPG with 3-methylglutaric anhydride, demonstrating the high efficiency of these reactions, which is consistent with a previous report [7]. Fundamentally, every repeating unit possesses a carboxyl group in the resultant polymers. Results of an earlier study showed that attachment of 1-aminodecane to about 8 unit% of a carboxylated poly(glycidol) chain is sufficient to fix the polymer chain onto an EYPC liposome membrane [5,7]. Based on previous studies, 1-aminodecane was combined to about 10 unit% of the polymer chains in this study (Table 3-1).

Table 3-1. Compositions of Various Hyperbranched and Linear Poly(glycidol) Derivatives

Polymer	Hydroxyl unit/%	Carboxylated unit/%	Anchor unit/%
MGlu-HPG10	0	100	-
MGlu-HPG20	0	100	-
MGlu-HPG40	0	100	-
MGlu-HPG60	5	95	-
Linear MGluPG76	10	90	-
Linear MGluPG222	6	94	-
MGlu-HPG10-C_{10}	0	88	12
MGlu-HPG20-C_{10}	0	90	10
MGlu-HPG40-C_{10}	0	90	10
MGlu-HPG60-C_{10}	5	85	10
Linear MGluPG76-C_{10}	10	75	15
Linear MGluPG222-C_{10}	9	81	10

Estimated by ^{1}H NMR.

Acid-base titration of these polymers was performed to estimate the p*K*a values. As presented in Table 2, MGlu-HPGs had p*K*a values around 5.9–6.5 and p*K*a slightly increased concomitantly with increasing DP. For polymers with a hyperbranched structure, their chain density increases concomitantly with increasing DP. Therefore, hydrophobic interactions among these crowded polymer chains of HPG with higher DP might engender a more compact conformation. Such a compact conformation of HPGs increases spatial density of carboxyl groups in the polymer chains, which might suppress dissociation of carboxyl groups to avoid repulsive electrostatic forces among carboxylate anions. In addition, hydrophobic environment of the crowded polymer chains may induce suppression of dissociation of carboxyl groups. As a result, pKa of the MGlu-HPGs might increase with increasing DP.

Table 3-2. p*K*a and Precipitation pH of Various Hyperbranched and Linear Poly(glycidol) Derivatives

Polymer	pKa	Precipitation pH	Degree of protonation at precipitation pH
MGlu-HPG10	5.9	4.4	0.98
MGlu-HPG20	6.2	4.6	0.98
MGlu-HPG40	6.5	4.7	0.99
MGlu-HPG60	6.5	4.9	0.94
Linear MGluPG76	6.2	4.9	0.99
Linear MGluPG222	6.1	4.8	0.99

Hydrophobicity of carboxylated polymers affects their precipitation behaviors [20]. For that reason, it was estimated that the pH at which the polymers precipitate using the following optical densities of these polymer solutions as the solution pH was decreased (Fig. 3-2). These polymers were soluble in water at neutral pH; their solutions were transparent. However, the polymer solutions suddenly became turbid at a specific pH, which was defined as the precipitation pH. The precipitation pH thresholds for MGlu-HPGs were estimated as presented in Table 3-2. The precipitation pH shifted to slightly higher pH values with increasing DP of MGlu-HPGs, indicating that hydrophobicity of MGlu-HPG increases concomitantly with increasing DP, consistent with previous observations for methacrylic acid copolymers with varying hydrophobicities and a previous report by the authors [7,20]. Acid–base titration for these polymers revealed that the degree of protonation for their

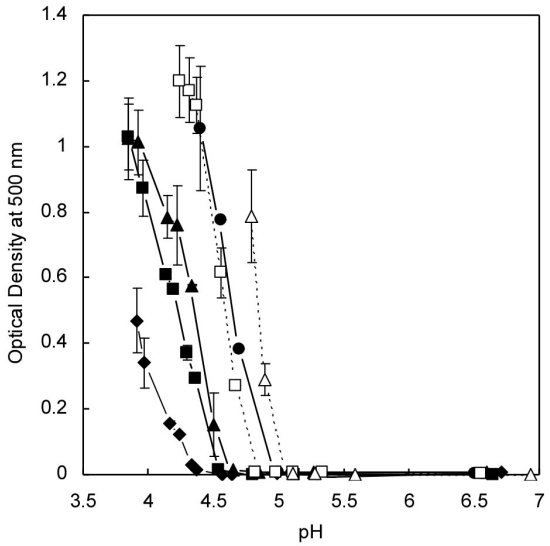

Figure 3-2. Optical densities at 500 nm for solutions of MGlu-HPG10 (closed diamonds), MGlu-HPG20 (closed squares), MGlu-HPG40 (closed triangles), MGlu-HPG60 (closed circles), linear MGluPG76 (open triangles), and linear MGluPG222 (open squares) dissolved in 30 mM sodium acetate and 120 mM NaCl of various pH (0.25 mg/mL) at 25 °C. Each point is the mean ± SD (n = 3).

carboxyl groups was around 0.94–0.99 at the precipitation pH: most carboxyl groups must be protonated to elicit precipitation of these polymers.

Hydrophobicity of the polymers was further investigated using a fluorescence probe

pyrene. An emission intensity ratio of the first (373 nm) to the third (384 nm) peaks of pyrene, I_1/I_3, is known to be sensitive to the micro-environmental polarity surrounding the pyrene molecule [21]. Consequently, this ratio has been widely used to estimate the hydrophobic nature of polymers [22,23]. Figure 3-3 depicts the I_1/I_3 ratio of pyrene fluorescence in the buffer dissolving various polymers as a function of pH. In buffers dissolving MGlu-HPG10 or MGlu-HPG20, the I_1/I_3 ratios of pyrene were around 1.75 at pH 5, suggesting that these polymers formed few domains with a hydrophobic nature, even after protonation of carboxyl groups of the polymer chain. On the other hand, a significant decrease in the I_1/I_3 ratio is seen in the presence of MGlu-HPG40 or MGlu-HPG60 under weakly acidic conditions. These results suggest that MGlu-HPGs with higher DP formed more hydrophobic domains probably because of their globular structure. The presence of linear MGluPGs also affected the I_1/I_3 ratio, which tends to decrease below pH 6.0. However, their I_1/I_3 values were generally higher than those of MGlu-HPGs with similar DP. Linear MGluPGs might be unable to form hydrophobic domains as much as MGlu-HPGs because of their linear backbone structure.

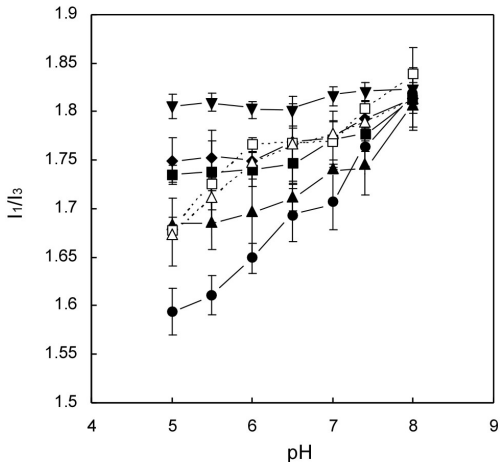

Figure 3-3. pH-Dependence of I_1/I_3 of pyrene fluorescence in the absence (closed inverted triangles) or presence of MGlu-HPG10 (closed diamonds), MGlu-HPG20 (closed squares), MGlu-HPG40 (closed triangles), MGlu-HPG60 (closed circles), linear MGluPG76 (open triangles), and linear MGluPG222 (open squares) dissolving in 25 mM MES and 125 mM NaCl solution. Concentration of polymers and pyrene were 0.2 mg/mL and 1 μM, respectively. I_1/I_3 was defined as the fluorescence intensity ratio of the first band at 373 nm to the third band at 384 nm.

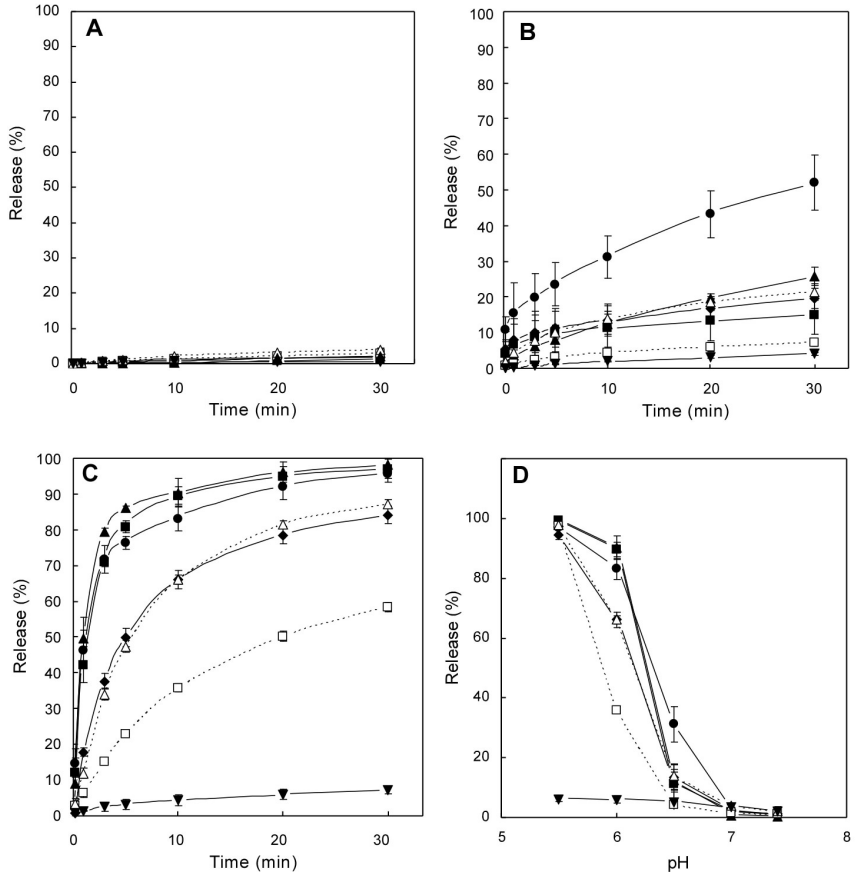

Figure 3-4. Pyranine release from EYPC liposomes induced by various hyperbranched poly(glycidol) derivatives. Time courses at pH 7.4 (A), pH 6.5 (B), and pH 6.0 (C), and pH-dependence (D) of pyranine release induced by MGlu-HPG10 (closed diamonds), MGlu-HPG20 (closed squares), MGlu-HPG40 (closed triangles), MGlu-HPG60 (closed circles), linear MGluPG76 (open triangles), and linear MGluPG222 (open squares) or without polymer (closed and inverted triangles). Percent release of pyranine after 10 min-incubation was shown (D). Polymer and lipid concentrations were 0.013 mg/mL and 2.0×10^{-5} M, respectively. Each point is the mean ± SD (n = 3).

3. 3. 2. Interaction of HPG Derivatives with Lipid Membrane

The author has shown that anchoring moiety into liposomes was necessary for poly(glycidol) derivatives to interact with liposomal membrane [7]. MGlu-HPG with anchor moieties (MGlu-HPG-C_{10}) were added to liposomes encapsulating both pyranine and its quencher DPX, and fluorescence of the released pyranine was monitored (Fig. 3-4). At neutral pH, no polymer showed a content release (Fig. 3-4A), indicating that these polymers did not

disrupt liposome membrane under this condition. On the other hand, release of the contents was observed for all MGlu-HPG-C_{10} at pH 6.5 (Fig. 3-4B). Complete release was achieved below pH 6.0 (Fig. 3-4C), indicating that protonated polymers disrupt the liposome membrane. As portrayed in Fig. 4D, the content release in the weakly acidic region increased in the order of DP of MGlu-HPGs-C_{10}, indicating that the polymer with higher hydrophobicity triggers release more strongly. In addition, MGlu-HPGs-C_{10} triggered the content release more strongly than linear MGluPG-C_{10} under the weakly acidic condition, demonstrating that the hyperbranched polymers can destabilize the liposome membrane more strongly than linear polymers.

Interaction of the polymers with the liposomes was also investigated through inspection of the liposome size change. EYPC liposomes were incubated with MGlu-HPGs-C_{10} or linear MGluPGs-C_{10} at various pHs overnight; their diameters were evaluated by DLS (Fig. 3-5). The liposome size changed only slightly after incubation with MGlu-HPGs-C_{10} at pHs 7.4 and

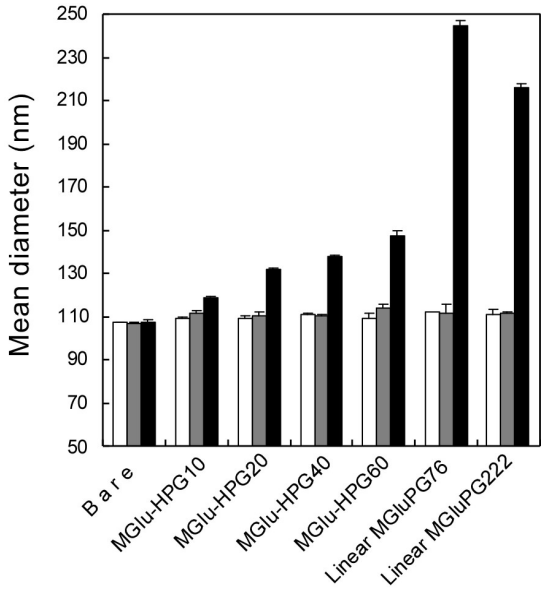

Figure 3-5. Mean diameters of EYPC liposomes after overnight incubation with various polymers or without polymer at pH 7.4 (open bars), pH 6.5 (gray bars) and pH 5.5 (closed bars). Polymer and lipid concentrations were 0.11 mg/mL and 1.7×10^{-4} M, respectively. Each point is the mean ± SD (n = 3).

6.5, but incubation at pH 5.5 increased their diameter to some extent. This range of increase rose with increasing DP. On the other hand, incubation with linear MGluPGs-C_{10} induced remarkable liposome size change at pH 5.5. Because linear MGluPG-C_{10} has a high degree of freedom on their conformation, they might promote intervesicular interaction, engendering aggregation of liposomes. In contrast, MGlu-HPGs-C_{10} might interact with the membrane in single liposome because of their compact conformation.

3. 3. 3. Preparation of pH-Sensitive Liposomes Using HPG

Figure 3-6 depicts pH-sensitive content release behaviors of liposomes modified with

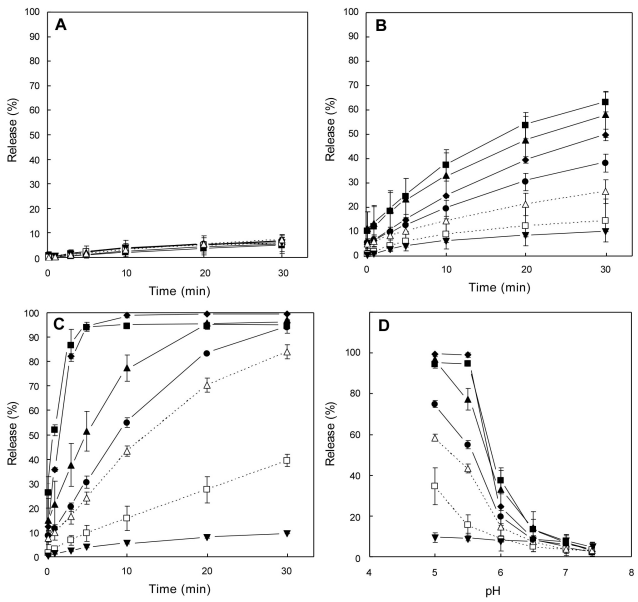

Figure 3-6. Pyranine release from EYPC liposomes modified with various hyperbranched and linear poly(glycidol) derivatives. Time courses at pH 7.4 (A), pH 6.0 (B), and pH 5.5 (C), and pH-dependence (D) of pyranine release from EYPC liposomes modified with MGlu-HPG10 (closed diamonds), MGlu-HPG20 (closed squares), MGlu-HPG40 (closed triangles), MGlu-HPG60 (closed circles), linear MGluPG76 (open triangles), linear MGluPG222 (open squares), and unmodified EYPC liposomes (closed and inverted triangles). Percent release of pyranine after 10 min-incubation was shown (D). Lipid concentrations were 2.0×10^{-5} M. Each point is the mean ± SD (n = 3).

MGlu-HPGs-C_{10} or linear MGluPGs-C_{10}. All liposomes retained pyranine at pH 7.4 (Fig.

3-6A). However, MGlu-HPGs-C_{10}-modified liposomes enhanced their content release below pH 6.0; almost complete release was achieved at pH 5.5 (Figs. 3-6B and 6C). As portrayed in Fig. 3-6D, liposomes modified with MGlu-HPGs-C_{10} of low DP exhibited higher content release in acidic pH than MGlu-HPGs-C_{10} of high DP. These observations differ from the case of content release induced by addition of these polymers into the liposome suspensions (Fig. 3-4). These might be resulted from the difference of protonation behavior of polymers between on the liposome surface and in an aqueous medium. It is possible that the protonation of MGlu-HPG-C_{10} with low DP is enhanced on the liposome membrane because carboxylate anions of the small-size polymer might exist in close vicinity of the membrane. Comparison of liposomes modified with linear and hyperbranched polymers shows that MGlu-HPG-C_{10}-modified liposomes induced the content release at a higher pH region than linear MGluPG-C_{10}-modified liposomes. Therefore, the liposomes having the hyperbranched polymers might destabilize the endosome in the early stage of endocytic pathway after their uptake by a cell.

3. 3. 4. Cytoplasmic Delivery by Polymer-Modified Liposomes

Previously, the author has shown that liposomes modified with linear MGluPG can be used for cytoplasmic delivery of antigenic proteins, such as OVA, into dendritic cells for induction of antigen-specific immune responses [24]. Therefore, the author compared the performance of the MGlu-HPG-modified liposomes as antigenic protein delivery vehicles with that of the linear MGluPG-modified liposomes.

The author prepared the MGlu-HPGs-C_{10}-modified liposomes labeled with Rh-PE and loaded with FITC-OVA, and their interaction with DC2.4 cells was compared with that for the linear MGluPG-C_{10}-modified EYPC liposomes or bare EYPC liposomes labeled with Rh-PE and loaded with FITC-OVA. As presented in Fig. 3-7A, cells treated with the bare liposome displayed weak and punctate fluorescence of Rh-PE and FITC-OVA. Considering

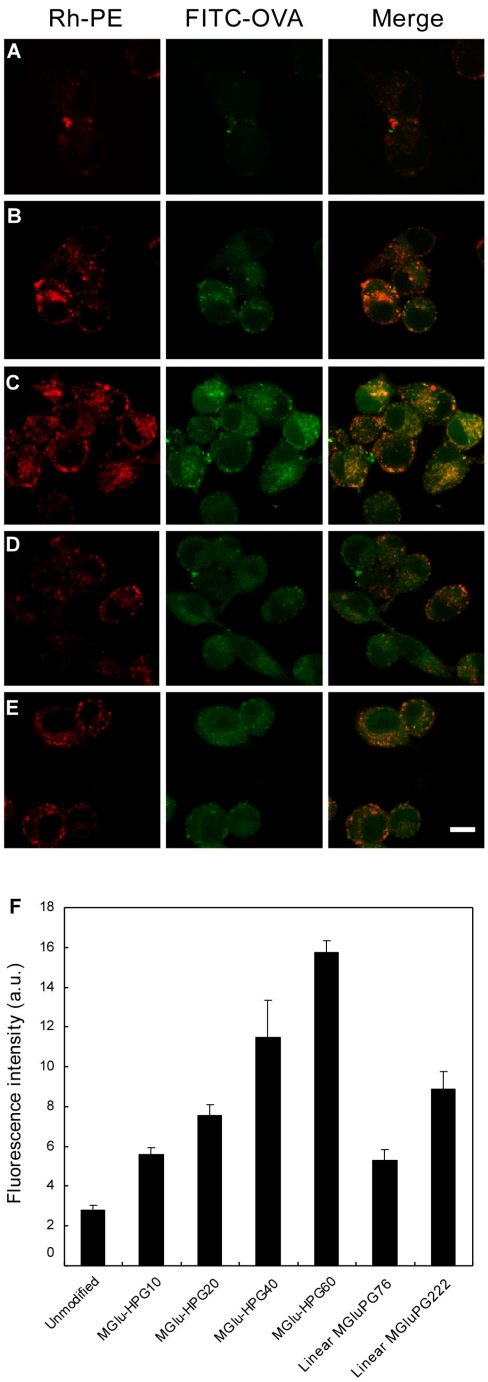

Figure 3-7. Confocal laser scanning microscopic (CLSM) images of DC2.4 cells treated with Rh-PE-labeled and FITC-OVA-loaded EYPC liposomes of various types: plain liposomes (A); liposomes modified with MGlu-HPG20-C_{10} (B), MGlu-HPG60-C_{10} (C), linear MGluPG76-C_{10} (D), or linear MGluPG222-C_{10} (E). FITC-OVA concentration was 50 μg/mL. Intracellular localization of Rh-PE (red) and FITC-OVA (green) was observed using a CLSM. Scale bar represents 10 μm. (F) Fluorescence intensities of DC2.4 cells treated with Rh-PE-labeled EYPC liposomes modified with or without polymers of various types. The fluorescence intensities of Rh-PE were determined by a flow cytometer.

that the liposomes were generally taken up by a cell *via* endocytosis, it is highly likely that

FITC-OVA molecules were still trapped in endosome and/or lysosome. In contrast, cells treated with MGlu-HPG-C_{10}-modified liposomes showed punctate fluorescence of Rh-PE but diffuse fluorescence of FITC-OVA (Figs. 3-7B and 3-7C), indicating that lipid molecules existed in endosome and lysosome but that FITC-OVA molecules existed in cytoplasm. These liposomes have the capability of destabilizing lipid membranes under a weakly acidic environment. Therefore, it is likely that FITC-OVA molecules were transferred from endosome into cytoplasm. Furthermore, the fluorescence from cells treated with MGlu-HPG60-C_{10}-modified liposomes was much brighter than that from cells treated with MGlu-HPG20-C_{10}. Although diffuse fluorescence of FITC-OVA was also observed for cells treated with the linear MGluPG-C_{10}-modified liposomes (Figs. 3-7D and 7E), their fluorescence was weaker than the case of MGlu-HPG60-C_{10}-modified liposomes.

The Rh-fluorescence intensity of the liposome-treated cells was evaluated by flow cytometry (Fig. 3-7F). The Rh-fluorescence intensity increased concomitantly with increasing DP of MGlu-HPGs-C_{10}, indicating that liposomes modified with MGlu-HPG-C_{10} of higher DP were taken up more efficiently. In addition, cells treated with the MGlu-HPG60-C_{10}–modified liposomes showed higher intensity than those treated with the linear MGluPGs-C_{10}–modified liposomes. This result suggests that liposomes having polymers of a hyperbranched structure were taken up by cells more efficiently than those with the polymers of a linear structure. The author has shown that linear MGluPG-modified liposomes are taken up by DC2.4 cells through their interaction with the cellular scavenger receptors, which recognize carboxylate anions of polymers [18, 24]. Negatively charged carboxylate groups of the hyperbranched polymer tend to locate in the peripheral region of the polymer. Therefore, these groups might be recognized by scavenger receptors efficiently, thereby promoting their uptake by the cells. These results demonstrate that modification of liposomes with MGlu-HPG-C_{10} can produce pH-sensitive liposomes that achieve efficient cytoplasmic delivery of proteins.

3. 3. 5. Fusion of Polymer-Modified Liposomes within Cell

Finally, the author attempted to verify the fusion of MGlu-HPG-C_{10}-modified liposomes in the cells. The polymer-modified liposomes containing NBD-PE and Rh-PE were prepared to detect fusion of the liposomes with intracellular membranes [6,25]. Fusion of the labeled liposomes with endosomal membranes causes dilution of these fluorescent lipids in the membrane, resulting in decrease of energy transfer efficiency between these fluorescent lipids. The fluorescent lipid-labeled liposomes with or without polymers were applied to DC2.4 cells and incubated for 4 h. Then cellular fluorescence was observed using a CLSM under irradiation of light with wavelength of 488 nm, which is for excitation of NBD-PE (Fig. 3-8). As Fig. 3-8A shows, cells treated with the bare liposomes displayed only fluorescence of Rh-PE, suggesting that fluorescence of NBD-PE was quenched by energy transfer to Rh-PE and hence the bare liposomes did not fuse with the endosomal membrane. In contrast, the cells treated with MGlu-HPG60-C_{10}-modified or linear MGluPG76-C_{10}-modified liposomes exhibited not only Rh-PE-fluorescence but also NBD-PE-fluorescence, indicating that fusion between these liposomes and the endosomal membranes occurred (Figs. 3-8B and 3-8C). However, the fluorescence of NBD-PE was very weak, suggesting that their fusion was not efficient.

The intracellular fusion behavior of the liposomes containing a non-bilayer-forming lipid DOPE, which is known to enhance membrane fusion, was also examined (Figs. 3-8D–F). For cells treated with the bare EYPC/DOPE liposomes, fluorescence of NBD-PE remained very weak (Fig. 3-8D). However, intensive fluorescence of NBD-PE was detected from cells treated with the DOPE-containing liposomes having either MGlu-HPG60-C_{10} or linear MGluPG76-C_{10}, indicating that these polymer-modified liposomes fused efficiently with endosomal membranes (Figs. 3-8E and 3-8F).

The fluorescence intensity ratios of NBD-PE to Rh-PE for the liposome-treated cells

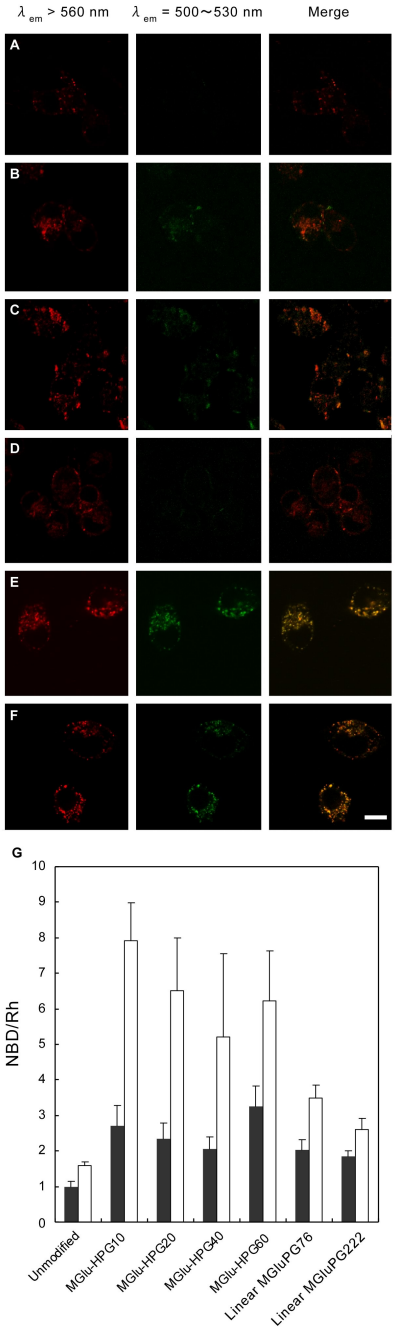

Figure 3-8. CLSM images of DC2.4 cells treated with EYPC (A-C) or EYPC/DOPE (1/1, mol/mol) (D-F) plain liposomes (A, D) or liposomes modified with MGlu-HPG60-C_{10} (B, E), and linear MGluPG76-C_{10} (C, F). Liposomal lipid concentration was 0.5 mM. Fluorescence of NBD and Rh upon excitation at 488 nm was observed using a CLSM. Scale bar represents 10 μm. (G) Fluorescence intensity ratios of NBD-PE to Rh-PE for DC2.4 cells treated with EYPC (closed symbols) or EYPC/DOPE (open symbols) liposomes modified with or without polymers. Fluorescence intensity ratios were evaluated by a flow cytometer and were expressed as relative values using the ratio of the plain EYPC liposome-treated cells as the standard.

were evaluated by flow cytometry and were expressed as relative values using the ratio of the

bare EYPC liposome-treated cells as the standard (Fig. 3-8G). The cells treated with either polymer-modified EYPC liposomes showed a 2–3 times increase in the NBD/Rh ratio compared with those treated with the base EYPC liposomes. Furthermore, no significant difference was found between the cells treated with any MGlu-HPG-C_{10}-modified and linear MGluPG-C_{10}-modified EYPC liposomes. These results indicate that these polymer-modified EYPC liposomes possess similar abilities to fuse with the endosomal membrane. Indeed, the EYPC/DOPE liposomes modified with these polymers caused a more significant increase in the NBD/Rh ratio than EYPC liposomes having the same polymers (Fig. 3-8G). In particular, the EYPC/DOPE liposomes modified with the hyperbranched polymers showed a higher NBD/Rh ratio than linear polymers, indicating that the backbone structure of the polymer affects their ability to generate the fusion ability of EYPC/DOPE liposomes.

The performance of MGlu-HPG-modified liposomes as a cytoplasmic delivery system was shown to increase as MGlu-HPG with higher DP was used for liposome modification. There might be various modes of interaction between MGlu-HPG with lipid membranes, such as absorption onto the membrane, penetration into the membrane, and solubilization lipid molecules. Therefore, their ability to destabilize lipid membranes might be influenced by their size. Optimization of molecular size may generate MGlu-HPG-modified liposomes with even higher performance.

3. 4. Conclusion

A new type of pH-sensitive polymer with a hyperbranched backbone—MGlu-HPG-C_{10}—was synthesized. Its feasibility for production of pH-sensitive liposomes was then investigated. Their ability for pH-sensitization of liposomes was enhanced with increasing DP. Modification of liposomes with MGlu-HPG-C_{10} produced highly pH-sensitive liposomes that undergo content release at mildly acidic pH. The MGlu-HPG-C_{10}-modified liposomes encapsulating OVA delivered their contents efficiently

into the cytosol of DC2.4 cells. Especially, liposomes having MGlu-HPG-C_{10} with high DP exhibited higher fusion ability and more efficient cellular internalization property than the liposomes modified with the counterpart polymers with a linear backbone structure. This is the first report describing the importance of the polymer backbone structure for polymer-based functionalization of liposomes. The MGlu-HPG-C_{10}-modified liposomes showed excellent ability to deliver the loaded proteins into cytosol of dendritic cell-derived cells. Therefore, they might have potential usefulness for the delivery of antigenic proteins.

3. 5. References

1. D. Liu and L. Huang, *Biochim. Biophys. Acta* 1990, **1022**, 348-354.

2. H. Ellens et al., *Biochemistry* 1984, **23**, 1532-1538.

3. J. Kunisawa et al., *J. Immunol.* 2001, **167**, 1406-1412.

4. K. Seki and D. A. Tirrell, *Macromolecules* 1984, **17**, 1692-1698.

5. K. Kono et al., *Biochim. Biophys. Acta* 1994, **1193**, 1-9.

6. K. Kono et al., *Biochim. Biophys. Acta* 1997, **1325**, 143-154.

7. N. Sakaguchi et al., *Bioconjugate Chem.* 2008, **19**, 1040-1048.

8. P. A. Bullough et al., *Nature* 1994, **371**, 37-43.

9. N. Murthy et al., *J. Controlled Release* 1999, **61**, 137–143.

10. C. A. Lackey et al., *Bioconjugate Chem*. 1999, **10**, 401–405.

11. C. C. Lee et al., *Nat. Biotech.* 2005, **12**, 1517-1526.

12. U. Boas et al., *Chem, Soc. Rev.* 2004, **33**, 43-63.

13. A. Sunder et al., *Adv. Mater.* 2000, **12**, 235-239.

14. A. Sunder et al., *Chem.sEur. J.* 2000, **6**, 2499-2506.

15. H. Frey and R. Haag, *Rev. Mol. Biotechnol.* 2002, **90**, 257-267.

16. Z. Shen et al., *J. Immunol.* 1997, **158**, 2723-2730.

17. D. L. Daleke et al., *Biochim. Biophys. Acta* 1990, **1024**, 352-366.

18. E. Yuba et al., *J. Controlled Release* 2008, **130**, 77-83.

19. R. D. Hester et al., *J. Polym. Sci. Chem. Ed*. 1980, **18**, 1727-1738.

20. M. A. Yassine et al., *Biochim. Biophys. Acta* 2003, **1613**, 28-38.

21. K. Kalyanasundaram et al., *J. Am. Chem. Soc.* 1977, **99**, 2039-2044.

22. H. G. Schild and D. A. *Langmuir* 1991, **7**, 1319-1324.

23. K. Tamano et al., *J. Phys. Chem. B* 2005, **109**, 1226-1230.

24. E. Yuba et al., *Biomaterials* 2010, **31**, 943-951.

25. D. K. Struck et al., *Biochemistry* 1981, **20**, 4093-4099.

Chapter 4

Gene delivery to dendritic cells mediated by complexes of lipoplexes and pH-sensitive fusogenic polymer-modified liposomes

4. 1. Introduction

Dendritic cells (DCs) are potent professional antigen presenting cells. They play a crucial role in innate and adaptive immune responses [1–3]. In fact, DCs recognize, acquire, process and present antigens to native and resting T cells for induction of an antigen-specific immune response. Because DCs presenting tumor-associated antigens (TAAs) can activate TAA-specific immune response, many researchers have been attracted to TAA-presenting DCs as a vaccine for cancer immunotherapy [4,5].

A key for vaccine production is delivery of TAA into DCs. The most extensively studied approach for TAA-loading of DCs is to expose them to defined antigenic proteins or the entire contents of tumor cells. Antigenic proteins are internalized *via* endocytosis and degraded to peptide fragments. These peptides are presented by binding to major histocompatibility complex (MHC) class II molecules, which mainly activate $CD4^+$ T cells, thereby inducing humoral immunity. Nevertheless, these vaccines have not been useful for cancer immunotherapy to date, because fragmented antigen peptides do not necessarily bind to MHC class II molecules efficiently because of the MHC molecules' diversity [6].

Another promising strategy for supplying DCs with TAA is the delivery of TAA-coded DNA or mRNA to express TAA in DCs as an endogenous antigen. The TAAs expressed in DCs are degraded by proteasomes after ubiquitination. These fragmented peptides are presented by binding to MHC class I molecules, which mainly activate $CD8^+$ T cells to induce cellular immunity. Antigen peptides processed from endogenous proteins bind

efficiently to MHC molecules. Reportedly, some cancer cells present their own TAA on the surface *via* MHC class I molecules for recognition by CD8+ T cells. Therefore, the preparation of TAA-loading DCs by gene delivery can induce antitumor immune responses in a practical manner, constituting a powerful tool for cancer immunotherapy [5,7].

Attempts have been made to develop efficient vectors for DCs from adenovirus [8,9]. Although the transfection efficiency of a conventional adenovirus is not high, toward DCs, Okada et al. achieved efficient transfection of 90% DC2.4 cells using the fiber-mutant adenoviral vector [8], indicating that modification of adenovirus might engender production of efficient vectors for DCs. However, adenoviruses induced not only gene transfer, but also dispensable immune responses [10]. Consequently, non-viral vectors have been attractive for gene delivery into DCs because of their low immunogenicity and lack of pathogenicity, even though they have lower transfection activity than virus-based vectors.

Recent progress in the area of non-viral vector-mediated gene delivery has revealed various cellular processes that are involved in the vector-mediated transfection of cells. They include cellular binding and subsequent internalization, transfer from endosome into cytosol, nuclear entry, and gene transcription [11,12]. Therefore, to achieve efficient transfection of DCs, vectors must be rationally designed specifically for DC to pass through these cellular processes efficiently. Among these cellular processes, efficient cellular binding and endosomal escape greatly affect the efficiency of non-viral vector-mediated transfection [11–13].

Previously, the author prepared hybrid complexes comprising lipoplexes and liposomes modified with pH-sensitive fusogenic polymers, such as succinylated poly(glycidol) (SucPG) and 3-methylglutarylated poly(glycidol) (MGluPG) [14–17]. These complexes, which are designated respectively as SucPG complex and MGluPG complex, generate fusion capability under mildly acidic conditions. In addition, these complexes have a structure in which the positively charged lipoplexes are covered with negatively charged

polymer-modified liposomes. Consequently, once an appropriate ligand, such as transferrin, was conjugated, they achieved efficient transfection of various cancer-derived cell lines, such as HeLa and K562 cells, through efficient cellular association via receptor-mediated endocytosis and through endosomal escape by membrane fusion with endosome (Fig. 4-1) [14–17].

To advance the development of potent vectors that are designed specifically for DCs based on the hybrid complexes consisting of pH-sensitive fusogenic liposomes and lipoplexes, the author attempted to optimize their structure from the viewpoints of ligand and pH-sensitive properties, which would contribute to high cellular uptake and efficient endosomal escape, respectively, using DC2.4 cells, a murine DC line, as a model of DCs. The authors' results demonstrated that the structural optimization of the complexes was able to produce an efficient non-viral vector for DCs.

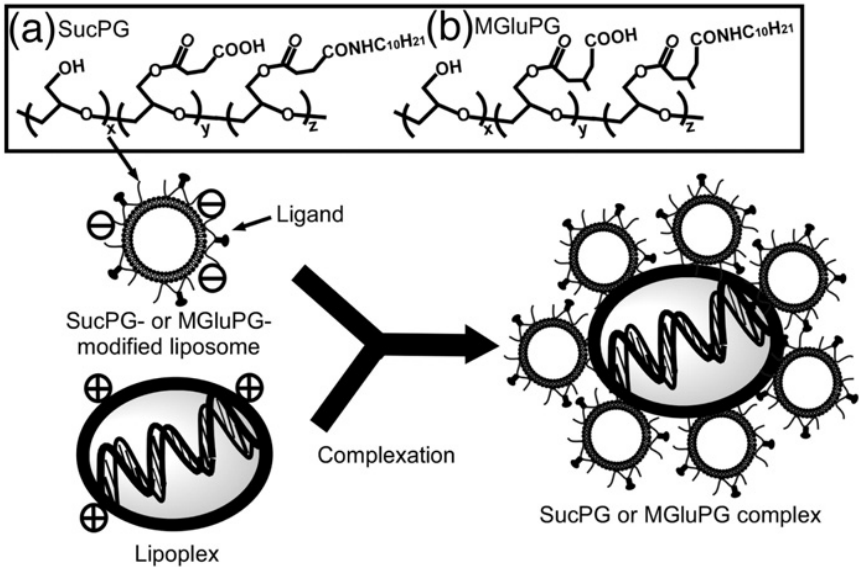

Figure 4-1. SucPG (a) and MGluPG (b) complexes.

4. 2. Materials and Methods

4. 2. 1. Materials

SucPG and MGluPG were synthesized according to previous reports [18,19]. SucPG and MGluPG with the composition (*x:y:z*, Fig. 4-1) of 18:74:8 and 9:81:10 (mol/mol/mol),

respectively. TRX-20 (Fig. 4-2a) [20] and L-dioleoyl phosphatidylethanolamine (DOPE) were provided from Terumo corp. and NOF corp., respectively. Dilauroyl phosphatidylcholine (DLPC) and transferrin were purchased from Aldrich. Aminoethylcarbamylmethyl mannan (Fig. 4-2b) was synthesized as previously reported [21]. The obtained product was estimated to have an amino group per 22 mannose units using fluorescamine assay [22].

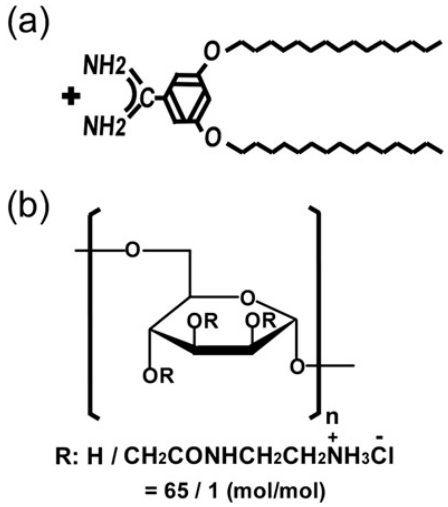

Figure 4-2. Structures of TRX-20 (a) and aminoethylcarbamylmethyl mannan (b).

4. 2. 2. Cell Culture

DC2.4 cells, which were an immature murine DC line, were provided from Dr. K. L. Rock (Harvard Medical School, USA) and were grown in RPMI 1640 supplemented with 10% FBS (MP Biomedical, Inc.), 2 mM L-glutamine, 100 μM nonessential amino acid, 50 μM 2-mercaptoethanol and antibiotics at 37 °C [23].

4. 2. 3. Preparation of pH-Sensitive Polymer-Modified Liposome–Lipoplex Complexes

Lipoplexes were prepared as reported previously [16]. In brief, plasmid DNA, pCMV-Luc or pEGFP-C1, was added to a suspension of cationic liposome consisting of TRX-20, DLPC and DOPE at the ratio of 1/1/2 (mol/mol/mol) in 5% glucose solution, and incubated for 10 min on ice. SucPG or MGluPG-modified liposomes were prepared by

suspending a mixture of SucPG or MGluPG and EYPC at the weight ratio of 3/7 in 5% glucose containing 5 mM Hepes (pH 7.4) and subsequent extrusion through a polycarbonate membrane with a pore size of 50 nm. Transferrin or aminoethylcarbamylmethyl mannan was conjugated to SucPG or MGluPG using EDC as previously reported [14]. To the liposome suspension was added EDC (0.7 mg) at pH 6.0 and stirred for 2 h at 4 °C. Then, transferrin (3 mg) and 0.5 M ferric citrate (5 μl) or aminoethylcarbamylmethyl mannan (3 mg) was added to the liposome suspension and the suspension was kept at 4 °C overnight. After the liposome suspension was adjusted to pH 7.4, the transferring or aminoethylcarbamylmethyl mannan-conjugated SucPG or MGluPG-modified liposome was purified using a Sepharose4B column at 4 °C with 5 mM Hepes and 5% glucose (pH 7.4). A suspension of SucPG or MGluPG-modified liposome either bearing or not bearing ligand (0.2 mM) was added to the lipoplex suspension and incubated for 10 min in an ice bath.

4. 2. 4. Dynamic Light Scattering and Zeta Potential

Diameters and zeta potentials of the complexes were measured using a Nicomp 370 ZLS dynamic light scattering instrument (Particle Sizing Systems, Santa Barbara, CA). Data were obtained as an average of more than three measurements on different samples.

4. 2. 5. Transfection

For luciferase assay, DC2.4 cells (7.5×10^4 cells) cultured for 2 days in a 24-well plate were washed with Hank's balanced salt solution (HBSS, Sigma) and then incubated in culture medium. The complexes or the lipoplexes containing pCMV-Luc (0.75 μg) were added to the cells and incubated for 4 h at 37 °C. The cells were washed with HBSS three times, followed by incubation in culture medium at 37 °C for 40 h. Then, transfected cells were evaluated by luciferase assay [14]. For GFP expression, the complexes or the lipoplexes containing pEGFP-C1 (0.75 μg) were added gently to the DC2.4 cells (1.5×10^5 cells)

incubated for 2 days in a 12-well plate. After 4 h-incubation at 37 °C, the cells were washed with HBSS three times, followed by the incubation in culture medium at 37 °C for 24 h. Then, GFP-transfected cells were evaluated using flow cytometer [16]. SuperFect (QIAGEN) and Lipofetamine2000 (Invitrogen) were also used according to the manufacturer's instructions.

4. 2. 6. Cellular Uptake

The DC2.4 cells (1×10^5 cells) cultured for 2 days in a 12-well plate were washed with HBSS and then incubated in culture medium. The complexes or the lipoplexes containing plasmid DNA (1 μg), in which DOPE was substituted by NBD-PE (3 mol%), were added gently to the cells and incubated for 4 h at 37 °C. The cells were washed with HBSS three times, and then fluorescence intensity of the cells was measured using a flow cytometer [16]. For inhibition assay, free transferrin, mannan or dextran sulfate at different concentrations was preincubated to cell for an hour before the incubation of these complexes labeled with NBD-PE.

4. 2. 7. Microscopic Analysis

The DC2.4 cells (1.5×10^5 cells) cultured for 2 days in 35-mm glass bottom dishes were washed with HBSS, and then incubated in culture medium. The complexes or lipoplexes containing FITC-labeled plasmid DNA (0.5 μg) were added gently to the cells and incubated for 4 h at 37 °C. After the incubation, the cells were washed with HBSS three times, and then replaced by serum-free medium. LysoTracker Red DND-99 (Molecular Probes) was used for the staining of intracellular acidic compartments according to the manufacturer's instructions. Confocal laser scanning microscopic analysis of the cells was performed using LSM 5 EXCITER (Carl Zeiss).

4. 2. 8. Cytotoxicity

The cells were treated with the complexes for 4 h and incubated for 40 h according to the transfection procedures. Then, the culture medium was carefully replaced with 0.11 ml of fresh RPMI containing 10% FCS and 10 μl of WST-8 (5 mg/ml) was added to each well. After 2 h-incubation at 37 °C, the survived cells was determined by absorbance at 450 nm using Wallac 1420 ARVO SX multilabel counter (Perkin Elmer Life Sciences) [24].

4. 2. 9. MHC Class I Presentation

Surface marker expression was analyzed according to the previous report [8]. DC2.4 cells were treated under the transfection condition. DC2.4 cells treated with 10 mg/ml lipopolysaccharide (LPS; Nacalai Tesque, Inc., Kyoto, Japan) and 100 U/ml recombinant murine interferon-γ (IFN-γ; Pepro Tech EC LTD., London, England) for 4 h were used as positive controls for DC maturation. At 24 h after transfection, cells were analyzed by flow cytometry. The cells (1×10^4) suspended in 100 μl of staining buffer (phosphate-buffered saline containing 0.1% BSA and 0.01% NaN_3) were incubated with the anti-mouse CD16/32-block Fc binding (eBioscience, CA, USA) for 30 min on ice to block nonspecific binding of the antibody. After three times wash with the staining buffer, the cells were incubated with biotin-conjugated mouse anti-mouse H-$2K^b$/H-$2D^b$ (MHC class I) monoclonal antibody (BD Bioscience, NJ, USA) in the staining buffer for 30 min on ice according to the manufacturer's instruction. After three times wash with the staining buffer, MHC class I expressed at the surface was detected by the 30 min-incubation with phycoerythrin (PE)-conjugated streptavidin (SIGMA, Missouri, USA) at a 1:200 dilution.

4. 3. Results and Discussion

4. 3. 1. Transfection of DC2.4 Cells

The author performed luciferase assay to examine the transfection activity of the SucPG complexes to DC2.4 cells. Our previous reports described that the most effective

SucPG complexes toward the transfection of HeLa cells were composed of the lipoplexes of TRX-20, DLPC, and DOPE at the molar ratio of 1/1/2 and transferrin-conjugated SucPG liposomes [16]. Accordingly, the author first performed transfection of DC2.4 cells using SucPG complexes consisting of the same components. Then the author optimized their composition for maximum transfection activity.

Fig. 4-3 shows that transfection activity of SucPG complexes is affected by both the cationic lipid/nucleotide unit ratio (N/P ratio) of the lipoplex and the SucPG-modified liposomes/lipoplex ratio, which is defined as the ratio of the SucPG carboxylated unit to DNA nucleotide unit of the complexes. The SucPG complexes achieved the highest transfection activities when the lipoplex with the N/P ratio of 4 was used for their preparation, indicating that greater amounts of lipid components to DNA were necessary for efficient transfection of DC2.4 cells. The decreasing activities at higher N/P ratio might result from higher toxicity of the complex. This figure also shows that the SucPG complexes at the N/P ratio of 4 exhibited more efficient transfection than the parent lipoplex, indicating that the complexation of SucPG-modified liposomes was as effective for transfection of DC2.4 cells as for cancer cells [14–17]. The following assay was performed using lipoplexes and SucPG complexes at the N/P ratio of 4.

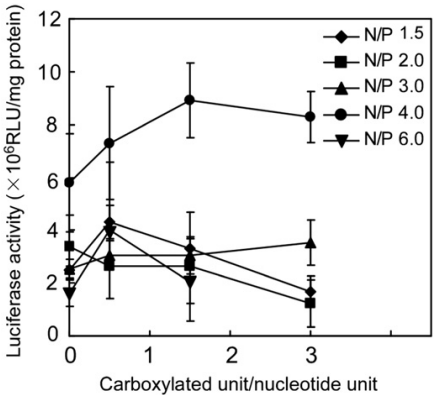

Figure 4-3. Expression of luciferase in DC2.4 cells treated with SucPG complexes with various compositions prepared using TRX-20 lipoplexes of varying N/P ratios. Compositions of SucPG complexes are expressed as molar ratios of succinylated units (carboxylated units) of SucPG-modified liposomes and DNA nucleotide units of TRX-20 lipoplexes.

4. 3. 2. Ligand Effect on Transfection of DC2.4 cells

The SucPG complexes with transferrin exhibited higher transfection activities than the intact lipoplexes (Fig. 4-3). Although DCs have transferrin receptors, mannose receptors are known to be largely expressed in DCs. Mannan, as a ligand for mannose receptors, has been used for delivery to DCs [10,25–27]. Therefore, mannan was incorporated to the SucPG complexes to increase their transfection activity. Mannan derivatives with amino groups were synthesized [21] and bound to carboxyl groups of SucPG using a condensation reagent, as in the method of attachment of transferrin to the complexes [14–17].

Fig. 4-4 shows that the transfection activities of both the complexes bearing transferrin and mannan were unexpectedly almost equivalent over a wide range of carboxylated unit/nucleotide unit ratios. In addition, the complex without ligands also exhibited activity at the same level. This figure indicates that ligands such as transferrin and mannan were not effective to improve transfection activity of SucPG complexes to DC2.4 cells.

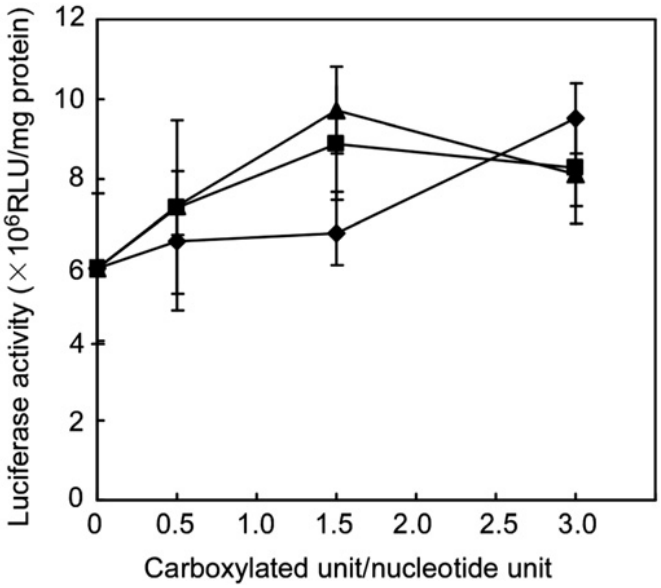

Figure 4-4. Comparison of transfection activities of SucPG complexes modified with various ligands, transferrin (square) and mannan (triangle). Plain SucPG complexes without ligands were also shown as a control (diamond).

Complexation of plain SucPG-modified liposomes with the lipoplex also tends to increase the transfection activity (Fig. 4-4). Our previous study showed that their complexation resulted in significant reduction of the transfection activity toward HeLa cells because of reduction of affinity to cell [14,16]. These facts imply that the negatively charged surface derived from the SucPG-modified liposomes might not suppress interaction between the complex and DCs.

The author next investigated the cellular association of SucPG complexes to elucidate the ligand effect. Fig. 4-5a shows that the amount of plain SucPG complex associated to DCs was almost equal to those of ligand-bearing complexes and was equal to that of the parent lipoplex. The auhors' previous studies showed that the SucPG complexes without transferring to HeLa cells exhibited a much lower level of association to HeLa cells than the parent lipoplex because the positively charged surface of the lipoplex was shielded

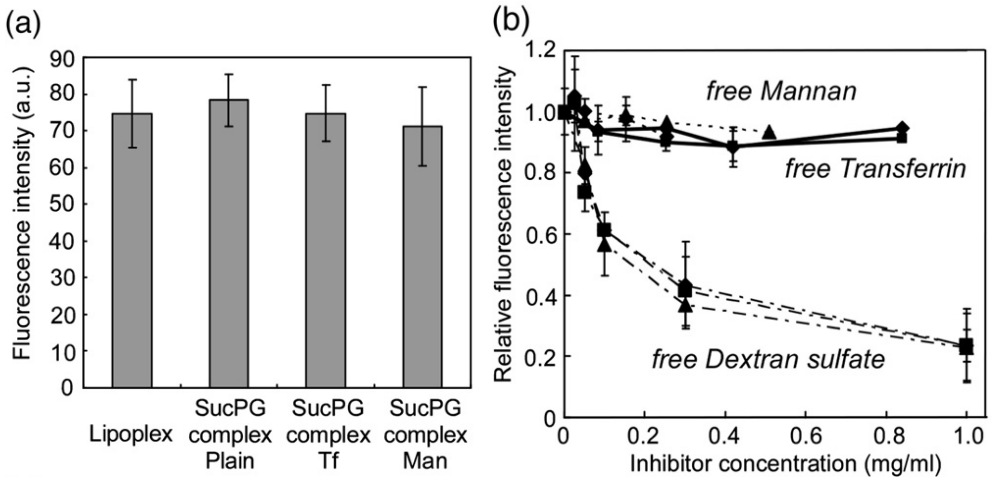

Figure 4-5. Cell association of the lipoplexes and SucPG complexes modified with various ligands. (a) The amount of cell association of the lipoplexes and SucPG complexes containing transferrin (Tf) and mannan (Man) at the carboxylated unit/nucleotide unit of 1.5. The complex without ligands (Plain) was also shown as a control. (b) Inhibition of the complexes with transferrin (square) and mannan (triangle) to the cell association. The complexes without ligands were also shown as a control (diamond). Free transferrin (solid lines), free mannan (dotted lines) and dextran sulfate (dash lines) were preincubated with DCs as an inhibitor. Relative fluorescence intensity was calculated as the ratios of the amount of association in the presence of ligands to that in the absence of ligands.

by negatively charged polymer-modified liposomes [14,16]. Indeed, the SucPG complexes without ligand showed lower association to the HeLa cells than those with ligand. Therefore, Fig. 4-5a suggests that the negatively charged liposomes of the complex might be involved in its association to DC2.4 cells.

Inhibition assay was also performed using free transferrin and free mannan (Fig. 4-5b), which indicates that neither free transferrin nor free mannan inhibited the association of these complexes. This result further confirms that transferrin and mannan in the complexes only slightly affected association of the complexes to DC2.4 cells. It is known that DCs engulf microorganisms or apoptotic cells with an anionic component via scavenger receptors [28]. Considering that SucPG complexes contain negatively charged moieties derived from SucPG-modified liposomes, involvement of scavenger receptors is possible. Therefore, the author also examined inhibitory effects of dextran sulfate, which has been used as an inhibitor of interaction between negatively charged compounds and scavenger receptors [29]. Fig. 4-5b shows that the addition of dextran sulfate strongly suppressed cellular association of the SucPG complexes, depending on the concentration. Consequently, the SucPG complexes were likely to have been internalized mainly *via* scavenger receptors. In fact, enhanced uptake by macrophages through scavenger receptors was also reported for poly(acrylic acid)-coated liposomes [29].

Although the author conjugated mannan and transferrin to the complexes, they only slightly affected their association to the cells. Instead, the complexes were taken up efficiently by DC2.4 cells through interaction with scavenger receptors, which bind to anionic molecules [30]. In fact, DCs are known to have many kinds of scavenger receptors [30]. Therefore, multivalent binding between these receptors and many carboxylate anions of the polymer chains fixed on the complexes might cause their strong interaction, resulting in the highly efficient association of the complexes to DCs.

4. 3. 3. Effect of pH-Sensitive Fusogenic Polymers on Transfection Activity of Complexes

The author next examined the effect of fusion ability of the polymers to improve transfection activities of the complexes. The MGluPG has more hydrophobic side groups than SucPG and is more fusogenic than SucPG [19]. In addition, the MGluPG complexes exhibit greater fusion ability under mildly acidic conditions than the SucPG complexes [17]. Thus, the author evaluated transfection activity of these fusogenic polymer-incorporated complexes toward DC2.4 cells.

The SucPG complexes at N/P ratios of 4 exhibited the most efficient transfection (Fig. 4-3). Therefore, the author prepared the MGluPG complexes at the same N/P ratio with varying ratios of carboxylated unit of MGluPG liposomes to the DNA nucleotide unit of the lipoplex. Fig. 4-6a shows that the complexation of MGluPG liposomes improved the transfection activity of the parent lipoplex. In addition, the MGluPG complex with the carboxylated unit/nucleotide unit ratio of 2 exhibited the highest transfection activity. At that ratio, 25% of GFP-expressed cells were observed.

Transfection activities of the complexes with optimal composition were compared to those of commercially available reagents, such as Lipofectamine2000 and SuperFect. Fluorescence intensity of EGFP for the transfected cells was evaluated using a flow cytometer (Fig. 4-6b). A larger population of the cells displayed more intensive fluorescence for the cells treated with MGluPG complex than cells treated with other complexes or reagents. Percentages of EGFP-positive cells and mean fluorescence intensity of the treated cells are shown in Fig. 4-6c. The MGluPG complex induced a much higher percentage and much higher mean fluorescence intensity to DC2.4 cells than other reagents and complexes.

To confirm the high transfection activity of MGluPG complex, the author further examined the transfection using luciferase gene. The author found that luciferase activities of DC2.4 cells treated with SucPG complex and MGluPG complex were $1.16 \pm 0.14 \times 10^7$ RLU/mg protein and $2.02 \pm 0.17 \times 10^7$ RLU/mg protein, respectively, indicating that

MGluPG complex induced twice-higher luciferase activity than the SucPG complex.

The cytotoxicities of the complexes and the parent lipoplex were also examined. The survived cells after transfection with these complexes and lipoplex were estimated respectively as 50%, 54%, and 39%. Although these complexes exhibited some toxicity to DC2.4 cells during the cellular treatment, their cytotoxicity was still lower than that of the parent lipoplex. It is likely that the negatively charged liposomes shielded positively charged surface of the lipoplex, resulting in the lower toxicity for these complexes than for the

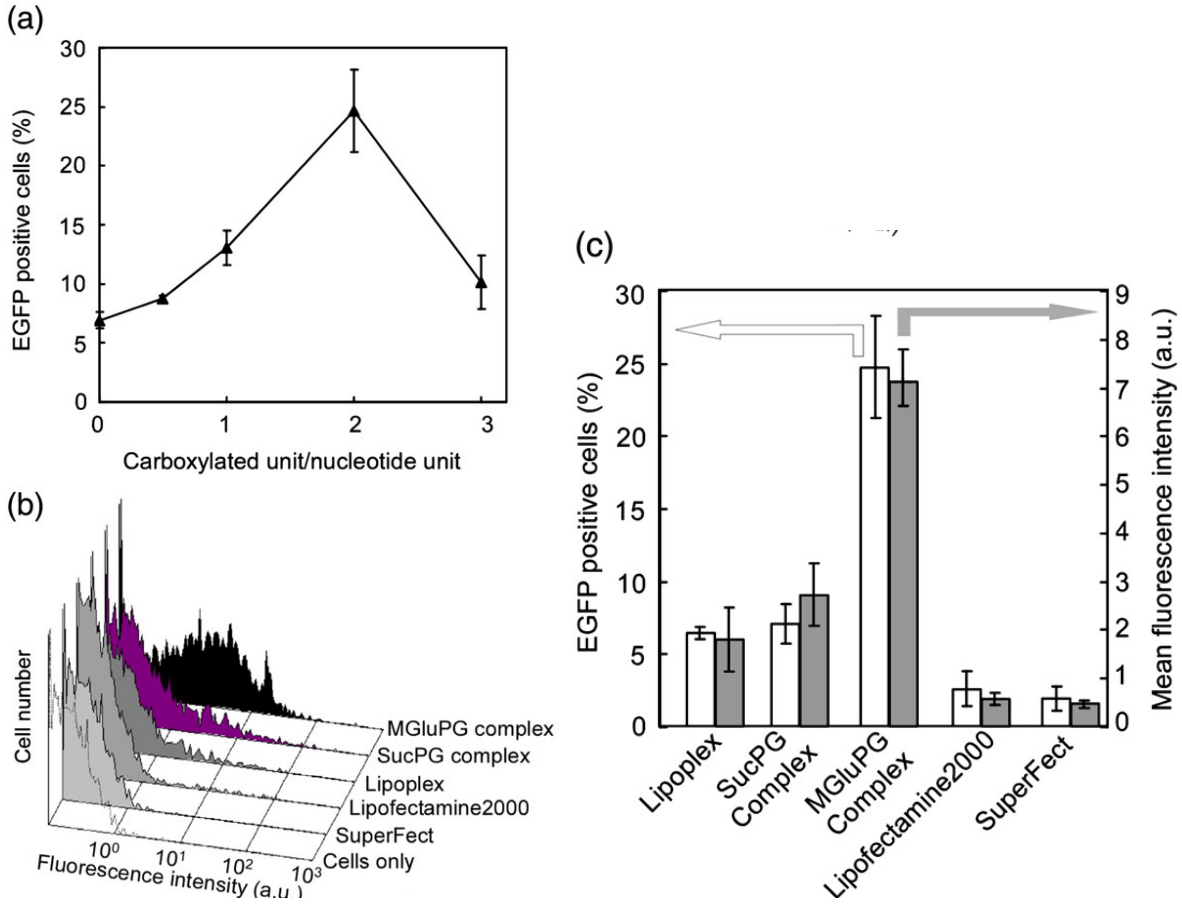

Figure 4-6. Transfection activities of the MGluPG complexes containing EGFP gene. (a) Expression of EGFP in DC2.4 cells treated with MGluPG complexes with various compositions prepared using TRX-20 lipoplexes with N/P ratio of 4. Compositions of MGluPG complexes are expressed as molar ratios of carboxylated units of MGluPG-modified liposomes and DNA nucleotide units of TRX-20 lipoplexes. (b) Expression levels of EGFP among various transfection reagents. (c) Comparison of transfection activities and gene expression levels among various transfection reagents. Percentage of EGFP-positive cells (open bars) and mean fluorescence intensity of cells (closed bars) are shown.

lipoplex.

4. 3. 4. Mechanism of the Efficient Transfection Activity by the MGluPG Complexes

The author examined the cell association and the intracellular localization of these complexes to elucidate the cause of their high transfection activity. Fig. 4-7a shows mean fluorescence intensities of DC2.4 cells treated with the fluorescent-lipid-labeled lipoplex or the complexes. The mean fluorescence intensities of these treated cells were almost the same, indicating that approximately equal amounts of the complexes and lipoplex were associated with DC2.4 cells. Mean diameters and zeta potentials of these complexes were estimated as 258 ± 13 nm and 19.6 ± 1.0 mV (SucPG complex) and 258 ± 15 nm and 19.8 ± 6.0 mV (MGluPG complex), respectively, indicating that these complexes have similar particle size and surface charge. The author already mentioned that the SucPG complexes are taken up by DC2.4 cells through interaction with scavenger receptors. Therefore, the MGluPG complex might be taken up by the cells through the same interaction. In addition, considering their surfaces were positively charged, electrostatic interaction might contribute their association to the cells. Consequently, it is likely that these complexes are taken up by the cells at similar efficiencies.

The author also examined the subcellular distribution of these complexes containing FITC-labeled DNA in DC2.4 cells, in which the acidic compartments were stained using LysoTracker. Fig. 4-7b shows that many yellow dots were observed by treatment with lipoplexes, indicating that the lipoplexes were localized dominantly at acidic compartments such as endosomes/lysosomes. In cells treated with the SucPG or MGluPG complexes, green fluorescence was observed at different locations from those of the red dots, suggesting that these complexes were able to escape from endosomal compartments. No large difference was found in the intracellular localization of these complexes. Indeed, it might be difficult to identify small differences in amounts of DNA existing in the cytosol using this technique. The

authors observed that the MGluPG complex had about three-times-higher ability to induce membrane fusion than the SucPG complex at around pH 5–4.5 [17]. Such a high fusion ability of MGluPG complexes might strongly promote the transfer of plasmid DNA from endosomes to cytosol, resulting in the high transfection activities to DC2.4 cells.

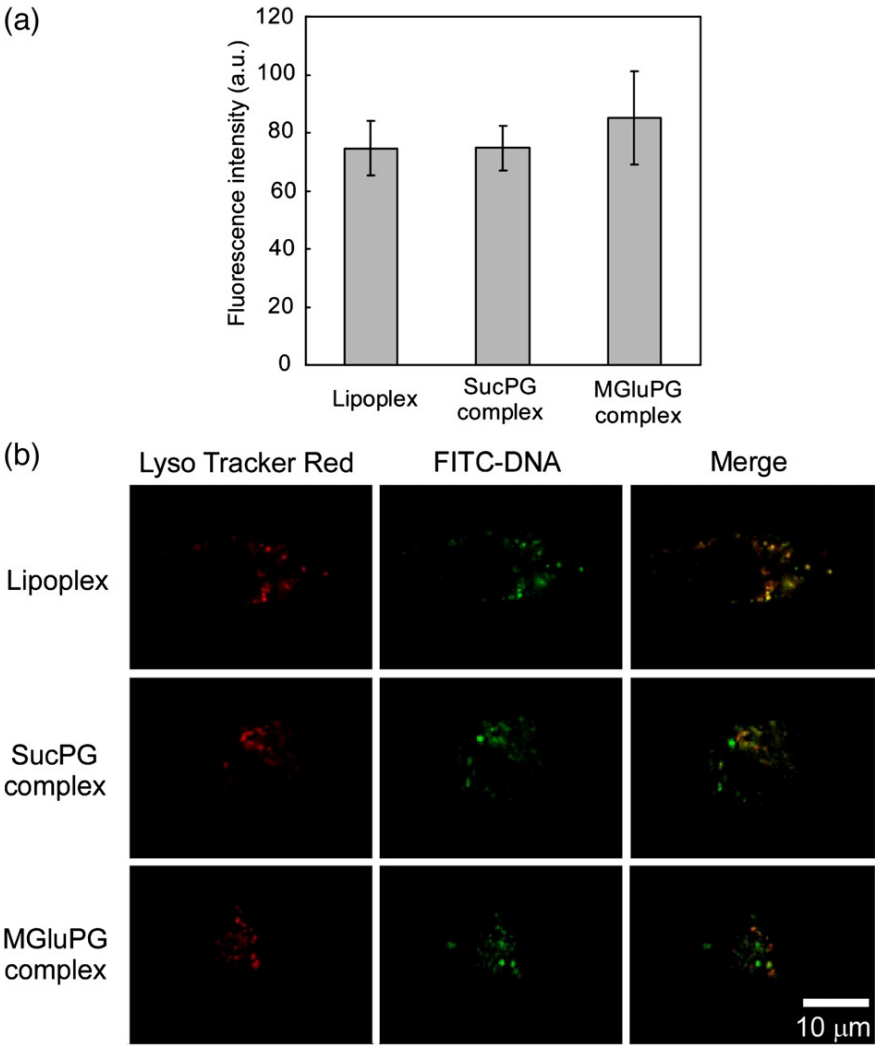

Figure 4-7. Comparison of cell association (a), and intracellular localization (b) between lipoplexes, the SucPG complexes and MGluPG complexes

4. 3. 5. Toward Application to Immunotherapy

Considering use of the complexes as a vector for DC-mediated immunotherapy, MHC class I presentation for transgenes is important. Therefore, the author finally evaluated expression of MHC class I on the DC2.4 cell surface after transfection with the complexes or the parent lipoplex containing luciferase gene. Fig. 4-8 shows that the expression level of

MHC class I was up-regulated by transfection with the lipoplex, SucPG complex or MGluPG complex, suggesting the MHC class I presentation responded to the transgene expression. It is also possible that the enhancement of MHC class I molecules is related with CpG motif in the plasmid. However, higher concentration of intracellular transgene product might induce more efficient presentation of the epitope presentation.

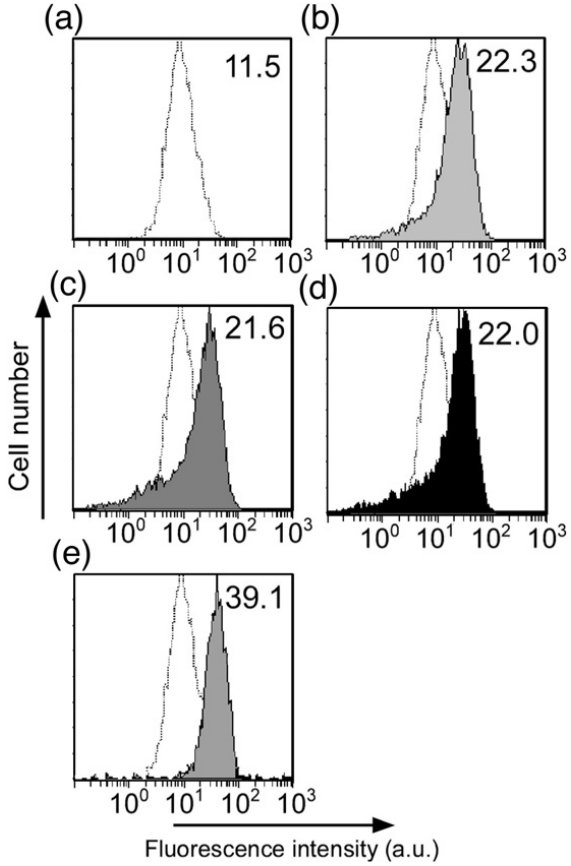

Figure 4-8. Immunofluorescence analysis of DC2.4 cells treated with (a) no treatment, (b) lipoplex, (c) SucPG complex and (d) MGluPG complex. DC2.4 cells treated with 10 mg/ml LPS plus 100 U/ml IFN-γ for 24 h were used as positive control for phenotypical DC maturation (e). Cells were stained by indirect immunofluorescence using biotinylated monoclonal antibodies of H-2K^b/H-2D^b (MHC class I) followed by PE-conjugated streptavidin. Value in the upper right-hand corner of each panel represents the mean fluorescence intensity in flow cytometry analysis in the presence of specific antibodies.

4. 4. Conclusion

In this study, the author prepared hybrid complexes of lipoplex and pH-sensitive polymer-modified liposomes designed for transfection of DCs from the viewpoints of ligand and pH-sensitive fusogenic properties. Irrespective of possession of ligands, the complexes

were taken up efficiently by DC2.4 cells, probably because carboxylate anions of the polymers on the complexes were recognized by scavenger receptors of the cells. The complexes with higher fusion ability exhibited more efficient transfection of DC2.4 cells. Especially, the MGluPG complexes achieved much higher level of transgene production than some commercially available transfection reagents. Because these complexes might introduce high concentration of intracellular antigen in DCs, induction of efficient presentation of epitope and strong immune response may be expected. The authors are currently attempting evaluation of their potency for activation of transgene-specific cellular immune systems to confirm their usefulness for DC-mediated immunotherapy.

4. 5. References

1. J. Banchereau and R.M. Steinman, *Nature* 1998, **392**, 245–252.

2. I. Mellman and R.M. Steinman, *Cell* 2001, **106**, 255–258.

3. N.C. Fernadez et al. *Nat. Med.* 1999, **5**, 405–411.

4. J. Banchereau and A.K. Palucka, *Nat. Rev. Immunol.* 2005, **5**, 296–306.

5. N.S. Wilson and J.A. Viladangos, *Adv. Immunol.* 2005, **86**, 241–305.

6. P.J. Kuebler and D.F. Nixon, *Vaccine* 1996, **14**, 1664–1670.

7. A.Y. Huang et al., *Science* 1994, **264**, 961–965.

8. N. Okada et al., *Cancer Res.* 2001, **61**, 7913–7919.

9. N. Okada, *Biol. Pharm. Bull.* 2005, **28**, 1543–1550.

10. P.H. Tan et al., *Mol. Ther.* 2005, **11**, 790–800.

11. L. Wasungu et al, *J. Control. Release* 2006, **116**, 255–264.

12. L.K. Medina-Kauwe et al., *Gene Ther.* 2005, **12**, 1734–1751.

13. R. Kircheis et al., *J. Control. Release* 2001, **72**, 165–170.

14. K. Kono et al., *Gene Ther*. 2001, **8**, 5–12.

15. N. Sakaguchi et al., *Int. J. Pharm.* 2006, **325**, 186–190.

16. N. Sakaguchi et al., *Biomaterials* 2008, **29**, 1262–1272.

17. N. Sakaguchi et al., *Biomaterials* 2008, **29**, 4029-4036.

18. K. Kono et al., *Biochim. Biophys. Acta* 1994, **1193**, 1–9.

19. N. Sakaguchi et al., *Bioconjugate Chem.* 2008, **19**, 1040–1048.

20. T. Harigai et al., *Pharm. Res.* 2001, **18**, 1284–1290.

21. J. Sunamoto et al., *Biochim. Biophys. Acta* 1987, **898**, 323–330.

22. S. Udenfriend et al., *Science* 1972, **173**, 871–872.

23. Z. Shen et al., *J. Immunol.* 1997, **158**, 2723–2730.

24. T. Miyamoto et al., *Avian Dis*. 2002, **46**, 10–16.

25. S.S. Diebold et al., *J. Biol. Chem.* 1999, **274**, 19087–19094.

26. Z. Cui et al., *Pharm. Res.* 2004, **21**, 1018–1025.

27. Y. Hattori et al., *Biochem. Biophys. Res. Commun.* 2004, **317**, 992–999.

28. M.L. Albert et al., *J. Exp. Med.* 1998, **188**, 1359–1368.

29. M. Fujiwara et al., *Biochim. Biophys. Acta* 1996, **1278**, 59–67.

30. N. Platt et al., *Chem. Biol.* 1998, **5**, R193–R203.

Chapter 5

Modification of liposome surface with pH-responsive polyampholytes for the controlled-release of drugs

5. 1. Introduction

Liposomes are nano-/microscopic particles derivable from natural non-toxic phospholipids and cholesterol. The walls of liposomes are made of bilayers of phospholipids and are capable of encapsulating hydrophilic drugs internally and adsorbing hydrophobic drugs on their double lipid membrane. Due to these inherent positive properties they possess, researchers from various parts of the world have further enhanced the functions of liposomes to enable them to successfully serve as carriers for different purposes such as drugs carriers for targeting specific sites that cause the disease [1, 2] and gene carriers for carrying normal genes into a cell to replace defective disease causing genes [3, 4].

Liposomes have been modified to become pH sensitive [5–8], light sensitive [9, 10] and temperature sensitive [11–13] functional liposomes mainly through the incorporation of functional polymers onto the membranes of liposomes. Seki and Tirrell [8] who modified liposomes with poly(acrylic acid) (PAA) suggested that the possible attractive forces operating between the partially ionized acid polymer and the liposomes are (i) charge-dipole interactions involving polymer-bound carboxylate anions and the phosphocholine dipole, (ii) hydrophobic interactions between the hydrophobic portions of the polymers and the liposome membranes, and (iii) hydrogen bonding involving the un-ionized carboxyl groups of the polymer and the phosphodiester head group of the liposomal lipids.

Kono and co-workers had incorporated poly(*N*-isopropylacrylamide) [poly(NIPAM)], a known thermosensitive polymer and copolymers of NIPAM onto EYPC and dipalmitoylphosphatidylcholine (DPPC) liposome membranes [11–13]. They had shown that

when a homopolymer or copolymers of NIPAM were incorporated onto the surface of either EYPC or DPPC liposomes, content within the liposomes can be triggered to release by increasing the temperature above the LCST of the thermosensitive polymers.

In this study, pH-responsive polymers comprised of poly(2-diethylamino)ethyl methacrylate (PDEAEMA) as well as the copolymers of DEAEMA and AA (varying molar ratios) were used to modify the surface of EYPC for the purpose of studying the effect of these pH-sensitive polymers on the trend of the release of pyranine, a model drug in acidic and basic environments. The structure of DEAEMA/AA copolymer is depicted in Fig. 5-1. The amino group which is present in DEAEMA will undergo protonation in acidic medium resulting in the formation of a cationic moiety. On the other hand, AA, a carboxylic acid will undergo deprotonation in a basic environment leading to the formation of a carboxylic anion.

Pyranine, a fluorescent dye was encapsulated into EYPC before the surface of the liposome was being modified. A small quantity (2 mol%) of stearyl acrylate (SA) which served as anchors for the polymers onto the liposome membranes [14] was included in the polymer formulation. A spectrofluorometer was used to quantitatively determine the amount of pyranine released.

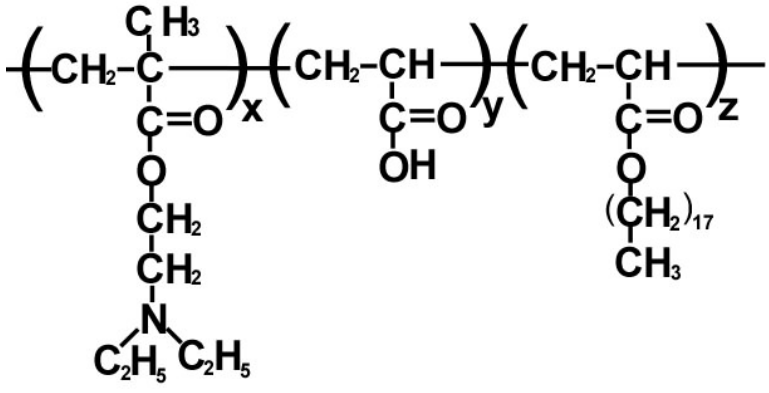

DEAEMA/AA/SA copolymer

Figure 5-1. Structure of DEAEMA/AA/SA copolymer.

5. 2. Materials and Methods

5. 2. 1. Materials

EYPC was kindly donated by Nippon Oil and Fats Co, Tokyo, Japan. The monomers, DEAEMA, AA and SA of high purity grade were purchased from Sigma-Aldrich, NSW, Australia, and were used as received. The photoinitiator, Irgacure 819 was a gift from Ciba Specialty Chemicals, Victoria, Australia. Pyranine was obtained from Tokyo Chemical Industry, Tokyo, Japan and Triton X-100 was supplied by Kishida Chemical Industry, Osaka, Japan. Phospholipids C-test Wako reagent kit for the determination of phospholipids concentration was procured from Wako Pure Chemical Industries, Osaka, Japan. DPX was obtained from Sigma-Aldrich.

5. 2. 2. Synthesis of PDEAEMA and Polyampholytes of Varying DEAEMA:AA Ratios

PDEAEMA and the five polyampholytes were prepared with SA and Irgacure 819 fixed at 2 mol% and 0.02 mol%, respectively. Percentage mole ratio of DEAEMA:AA in the polyampholyte formulations varied as follows: 0%:98% (PAA), 20%:78% (Polymer 1), 38%:60% (Polymer 2), 49%:49% (Polymer 3), 59%:39% (Polymer 4), 78%:20% (Polymer 5) and 98%:0% (PDEAEMA). These polymers were prepared using the same procedure as described in another publication [15]. Essentially, 1.0 mL of the reacting solution was placed in a non-pigmented polypropylene straw with a bore diameter of 0.5 cm, sealed at one end and subjected to UV exposure with a 90 W medium pressure mercury lamp model 93110E2 mounted in a vertical configuration. All experiments were performed at room temperature at a distance of 30 cm from the radiation source with a peak irradiance of 0.80 mW/cm^2 as measured by a 1L390A curing radiometer from International Light.

The water soluble polymers, Polymers 2–5 and PDEAEMA were dissolved in water and dialyzed against deionised water for 24 h, and then recovered by lyophilization. For convenience of referencing, Polymers 2–5 and PDEAEMA are abbreviated as P-2 to P-6, and

liposomes modified with Polymers 2–5 and PDEAEMA as LP-2 to LP-6 respectively.

5. 2. 3. Analysis of Polymers Using NMR Technique

The ratios of DEAEMA:AA in Polymers 2–5 were qualitatively evaluated using 1H NMR spectroscopy employing the Varian Mercury 400 MHz High Resolutions Solution NMR Spectrometer at 25 °C. CH_3OD (99.5% D) was the lock solvent used. The signal corresponding to $–CH_3$ in this solvent has been referenced to 3.31 ppm. The ^1H NMR spectra of all polymers have been consistently referenced in this manner.

5. 2. 4. Titration of Polymers

To 30 mL of an aqueous solution of each copolymer (1 mg/mL) was added an appropriate amount of 1 M HCl solution to make pH 2.5. The acidic polymer solution was titrated with 0.01 M NaOH solution. The titration was carried out by the stepwise addition of 0.01 M NaOH and conductivity of the resultant solution was measured using a digital conduct meter (Model CM-15A, TOA Electronics Ltd, Tokyo, Japan).

5. 2. 5. Encapsulation of Pyranine and Liposome Modification

EYPC liposome was first of all encapsulated with the model drug, pyranine by adding 500 μL of an aqueous solution of pyranine (35 mM) and DPX (50 mM) in 25 mM MES buffer (pH 7.4) to 7 mg of EYPC obtained from the evaporation of 700 μL of the stock solution in chloroform (10 mg/mL). The liposomes in pyranine solution were dispersed by sonication for approximately 2 min and then underwent 5 times of ‘freeze-thaw’ process for the purpose of encapsulating pyranine into the liposome molecules. In order to control the size of the liposome molecules for surface modification, the pyranine encapsulated liposomes were extruded through a polycarbonate membrane with pore diameter of 100 nm. The free un-encapsulated pyranine was separated from the pyranine-loaded liposomes through a

Sepharose 4B column eluted using 10 mM Tris-HCl-buffered (Tris = Tris(hydroxymethyl) aminoethane) solution containing 140 mM NaCl at pH 7.4. The separation was aided using a UV detector with the liposome/pyranine fraction eluted first and detected at the wavelength of 280 nm. The surface modification of the liposomes was carried out by mixing the pyranine-loaded liposome (3 mM) with a polymer solution (10 mg/mL) at pH 5 and incubating at 4 °C overnight and subsequent centrifugation at 20,000 rpm for 1 h three times. The volume ratio of the pyranine-loaded liposome suspension to the polymer solution was 5:3.

5. 2. 6. Estimation of Lipid Concentration in Liposome

Phospholipid concentration was evaluated by an assay using the phospholipids C-test Wako reagent. This evaluation was to ensure that all the test solutions had almost equal quantity of phospholipid.

5. 2. 7. Pyranine Release from Liposome

Since the modified liposome molecules were pH-responsive, release tests were carried out in acidic as well as basic buffer solutions. This enabled the evaluation to be made on the effect of pH on the release of pyranine encapsulated in the inner aqueous phase of liposome. Tris was used for the preparation of basic buffer solutions, and acidic buffer solutions were prepared using NaH_2PO_4. The pH of these buffer solutions could be adjusted using either HCl or NaOH solutions.

Essentially in the pyranine release test, polymer-modified liposomes encapsulated with pyranine were dispersed in a buffer solution containing 140 mM NaCl (to maintain physiological osmotic pressure) and the fluorescence change caused by the pyranine release was monitored using a spectrofluorometer (JASCO FP-6200 model) at 37 °C. Triton X-100 (final concentration 0.15%) was added in the final stage to ensure total release of pyranine.

The excitation and monitoring wavelengths of pyranine were 416 and 512 nm respectively. The percent leakage of the fluorescent dye from liposome was defined according to Eq. 1:

$$\% \text{ Leakage} = (F^t - F^0)/(F^f - F^0) \times 100 \qquad (1)$$

where F^0 and F^t represent the initial and intermediate fluorescence intensities of liposome suspension respectively. F^f is the fluorescence intensity after the addition of Triton X-100.

5. 3. Results and Discussion

5. 3. 1. ^{1}H NMR Analysis of Copolymers

The quantitative analysis of Polymers 2–5 using NMR was not possible because of broad resonances. However, there are clear variations of peak intensities belonging to DEAEMA and AA as the ratios of these two monomers varied. Figure 5-2 depicts the expanded 1H NMR spectra for Polymers 2–5 in the region of 0.7–1.5 ppm which shows the variation of DEAEMA:AA mole ratios in these polymers.

By comparing these NMR spectra to that of the monomers, DEAEMA and AA (not shown), the peak in the region 1.06–1.20 ppm belongs to protons of the two terminal methyl groups (attached to the two $–CH_2$ groups which are bonded to the N) in DEAEMA. The peak at 1.22–1.32 ppm belongs to the protons which are attached to the C–C single bonds in the AA unit after the loss of the double bond due to polymerization. Each of these spectra indicate clearly that as the peak in the region of 1.06–1.2 ppm increases with the increase in DEAEMA content, the peak in the region 1.22–1.32 ppm decreases.

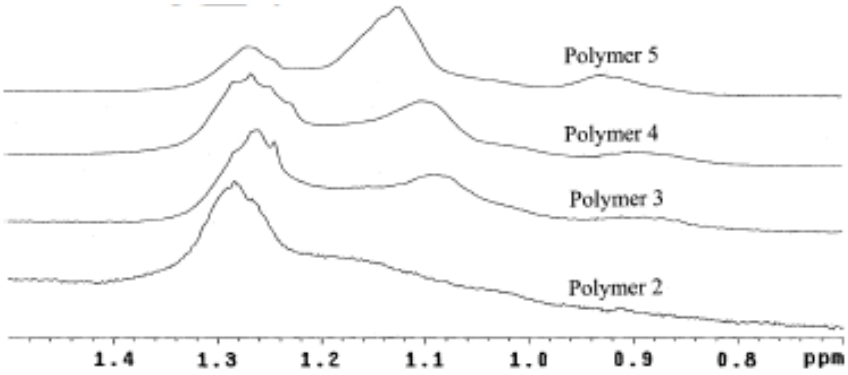

Figure 5-2. ^{1}H NMR spectra for Polymers 2–5 in the region of 0.7–1.5 ppm

5. 3. 2. Titration of Copolymers

DEAEMA is a monomer of weakly basic nature with a pK_b value 6.4 (pK_a = 7.6) [16] attributed to the lone pair of electrons on the nitrogen in the amino group. The copolymers formed from DEAEMA and AA contained both acidic and basic moieties in the structures and were thus considered as ampholytic polymers (polyampholytes). They were therefore expected to be responsive to both acidic and basic environments. However, the extent of responsiveness would depend to a large degree on the monomeric compositions of the polyampholyte formulations. In a basic medium, the acidic moieties (AA) in the polyampholytes would undergo deprotonation to form the anionic carboxylate ions (AA^-). On the contrary, in an acidic medium, the amino groups in DEAEMA units would undergo protonation to form quaternary ammonium cations ($DEAEMAH^+$).

Release of content encapsulated in liposomes modified with a polymer is generally reported to be caused by the destabilization of liposome membranes triggered off by a change in the chemical nature of the polymer such as the change from hydrophilicity to hydrophobicity characteristics under the experimental conditions [11]. In the current study, EYPC liposomes were modified with a pH sensitive polymer as well as four polyampholytes. Polyampholytes when placed in an acidic or basic environment would give rise to cationic or anionic moieties which contribute to the charge density (amount of charge present). It was anticipated that the charge density of polyampholytes could be a factor contributing to the destabilization of the liposome membrane.

To determine the change in charge density of the polyampholytes, we examined the titration of these polyampholytes in acidic medium (pH adjusted to 2.5) against a NaOH solution (0.01 M) and measured the conductivities. Figure 5-3 depicts the dissociation curves of P-2 to P-6. For P-6, DEAEMA quaternary ammonium cations, $DEAEMAH^+$ were expected to form in pH 2.5, and according to the dissociation curve, these cations deprotonated from pH 5.0 to 7.1. This indicates that at pH 5.0 all DEAEMA units were protonated and remained

cationic. However, at pH 7.2, all $DEAEMAH^+$ were deprotonated to form neutral uncharged DEAEMA units. As the AA content in the polymers increased from P-5 to P-2, the dissociation curves exhibited a shift to higher pH. This shift could possibly be due to the interaction between the anionic carboxylate ions, AA^- and the cationic $DEAEMAH^+$ ions.

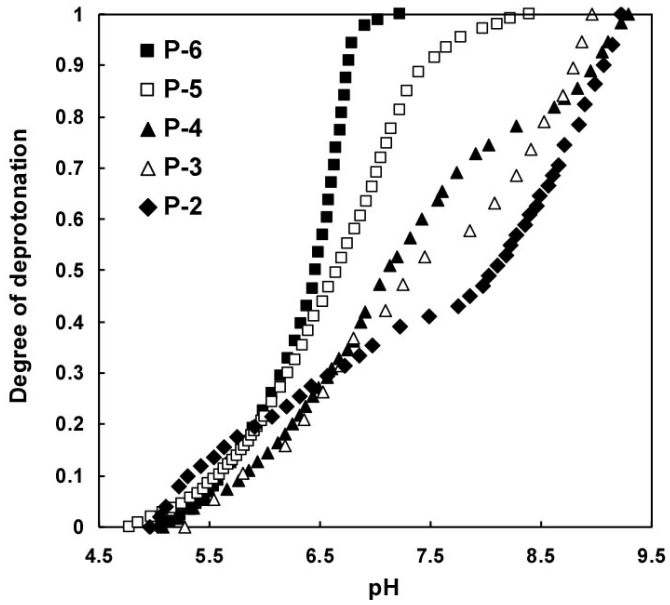

Figure 5-3. Deprotonation curves of P-2 to P-6.

5. 3. 3. Pyranine Release from Neat and Polymer-Modified Liposomes

Pyranine release tests were carried out in buffer solutions with pH values ranged from 4 to 10 on polymer-modified as well as the neat liposomes which served as the control. The addition of Triton X-100 to the neat as well as polymer-modified liposomes in buffer solutions indicated that the polymers did not act as the carrier of pyranine. However, the pyranine molecules were loaded in the liposomes and were totally released by the addition of this detergent.

Figure 5-4 depicts the profiles of the encapsulated pyranine release from EYPC liposomes modified with the above-mentioned pH-responsive polymers in buffer solutions with pH ranging from 4 to 10 at 37 °C. Data in Fig. 5-4 show that the unmodified EYPC liposomes which served as the control appeared to be pH insensitive and released less than

10% pyranine in either the acidic or basic environments (pH 4–10). However, under the same conditions, LP-2 to LP-6 exhibited a trend in 'critical pH' for pyranine release. Critical pH in this case refers to the pH at which the pyranine was released from the modified liposomes. It was observed that the critical pH values (in parentheses) increased in the order of LP-6 (5) < LP-5 (5.5) < LP-4 (6) ~ LP-3 (6.2) < LP-2 (7). These data indicate that P-2 to P-6 that were conjugated on the liposome surfaces had interacted with the liposome membranes in these respective pH environments and destabilized the membranes, leading to the leakage of the encapsulated pyranine.

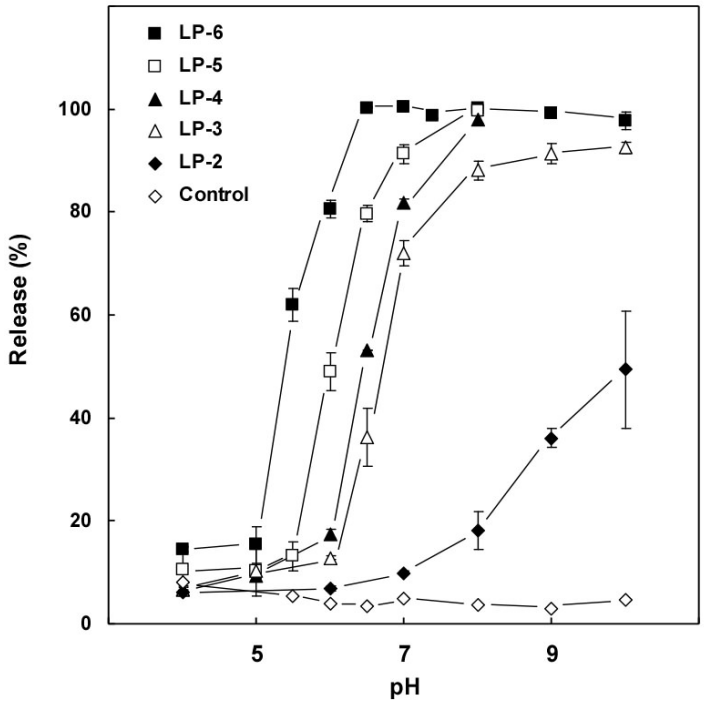

Figure 5-4. Profiles of the encapsulated pyranine release from the control and LP-2 to LP-6 in buffer solutions with pH ranging from 4 to 10 at 37 °C.

In our current study, it is demonstrated that critical pH values increased with increase in AA content in the polyampholytes that were used to complex with the liposome vesicles. LP-6 with the liposome surface being modified with neat PDEAEMA had a critical pH of 5. This means that in this pH environment, the liposome membrane was destabilized by interaction with PDEAEMA. The amine functional groups in PDEAEMA are expected to

undergo protonation to form quaternary ammonium cations in acidic medium. Data in Fig. 5-4 revealed that pyranine release was detectable at pH 5, and a significant release of approximately 60% of pyranine was observed at pH 5.5 although pyranine release was not detected in a pH 4 buffer solution. A plausible explanation for such a phenomenon could be an enhancement in the hydrophobicity of DEAEMA units when the pH was increased to 5 and less DEAEMA units underwent protonation. Hence comparatively less amount of the cationic $DEAEMAH^+$ ions were formed. This increase in hydrophobicity could be sufficient to bring about the hydrophobic interactions between the hydrophobic portions of PDEAEMA and the outer leaflet of the liposome membrane leading to the destabilization of the liposome. The deprotonation curve for P-6, which indicates deprotonation of $DEAEMAH^+$ ions took place from pH 5 to pH 7.1, correlated well with the pH-dependent content release curve for the P-6-modified liposomes, indicating that the uncharged DEAEMA units are responsible for the content release.

Regarding liposomes modified with copolymers containing AA units, they initiated the contents release at higher pH comparing to LP-6. Apparently, the critical pH for the contents release increased with increasing AA content of the polymers. This fact indicates that AA units should be responsible for the observed increase of the critical pH. For the liposomes modified with P-5 (DEAEMA:AA = 80:20), the critical pH for the content release was estimated to be 5.5, which is slightly higher than that of LP-6. PAA was shown to change its charge density between pH 4 and pH 10 [17]: deprotonation of AA units would be enhanced to form anionic AA^- with increasing pH from pH 4 to 10. Although AA content in P-5 is small, once these AA units are deprotonated, these negatively charged ions might stabilize positive charges of $DEAEMAH^+$ groups to some extent and suppress their deprotonation, resulting in the slight increase of the critical pH for the content release of LP-5.

For LP-4 and LP-3, the pH values at which pyranine release was triggered were estimated to be pH 6.0 and 6.2, respectively. Although the difference in the DEAEMA and

AA contents in these two liposome-polymer complexes was not significant, critical pH for the initiation of the content release was still affected by the composition of the polymers; P-4 and P-3 present in LP-4 and LP-3 had the mole ratios of 60:40 and 50:50 with respect to the ratio of DEAEMA:AA. Although P-4 and P-3 had comparatively larger contents of AA than P-5, almost complete release of pyranine was achieved above pH 7 for both polymer-modified liposomes. This fact indicates that when became uncharged, the DEAEMA units present in P-4 and P-3 could interact strongly with the liposome membrane to cause destabilization of the latter [18].

The critical pH for LP-2 was estimated to have a value of 7, which is higher than that of LP-3. This fact suggests that AA^- ions of the polymer chain with a high content of AA units in P-2 (DEAEMA:AA = 40:60) strongly suppressed deprotonation of $DEAEMAH^+$. In addition, the extent of pyranine release was low. For example, only 50% of content was released at pH 10, where $DEAEMAH^+$ units are completely deprotonated (Fig. 5-3). Probably, inclusion of a large amount of AA ions in the polymer chain suppressed binding of the polymer chain onto the liposome membrane and decrease interaction of the uncharged DEAEMA units with the liposome membrane.

5. 3. 4. Proposed Mechanism of Contents Release Induced by Polymers

Previously, Thomas and Tirrell [19] examined release of 6-carboxyfluoresence (CF) encapsulated in EYPC induced by a pH sensitive polymer, poly(2-ethylacrylic acid) (PEAA) and observed that PEAA induced the content release below pH 6.5. They proposed a mechanism for the content release of the liposomes induced by PEAA as follows. At the reduced pH, protonation of PEAA increase hydrophobicity of the polymer, which enhancing adsorption of the polymer chains onto the outer leaflet of the liposome membrane. The absorbed PEAA chains could lead to expansion of the outer leaflet. However, the inner layer may resist the expansion of the outer membrane and resulted in the tension within this layer.

The accumulated stress in the outer membrane might be relieved by the buckling of the outer membrane or the rupture of the inner leaflet, leading to the release of the encapsulated fluorescent compound.

Fujiwara et al. [20] researched on the pH-dependent complexation of PAA with phospholipids vesicles and reported the complexation was minimal around pH 7, where PAA was negatively charged. However, the complexation was pronounced below pH 4, where the anionic character of the polymer decreased and its hydrophobic character increased when the polymer carboxyl groups were protonated. Seki and Tirrell [8] in their studies on pH-dependent complexation of PAA derivatives with phospholipids vesicle membranes suggested that the attractive forces that brought about the complexation could be the hydrophobic interactions between the hydrophobic portions of the polymer and lipid molecules as well as the hydrogen bondings between carboxyl groups and head groups of lipid molecules.

Based on the findings of these researchers, our study suggests that the hydrophobic interactions between the deprotonated DEAEMA units in the polyampholytes and the liposome membranes caused content release of the liposome. It also demonstrates that the interaction between the DEAEMA units and the liposome membrane was being controlled by the amount of AA^- ions present in the polyampholyte. The results of this work thus imply that the ampholytic nature of the polymer plays an important role in governing the critical pH of polyampholyte-modified liposome when the liposome-polymer complex is placed in a certain pH environment.

5. 4. Conclusions

In this study, the author has modified the EYPC liposome surface with polyampholytic polymers comprised of varying mole ratios of DEAEMA and AA as well as with PDEAEMA, and successfully established the pH sensitivity of these polymer-liposome

complexes. The critical pH for the pyranine release from these polymer-liposome complexes tested in buffer solutions ranged from pH 4 to 10 decreased with increasing DEAEMA content in the polymers. This phenomenon is very likely due to the increase in hydrophobicity of the polymer contributed by increasing in DEAEMA units present. This would lead to increase in hydrophobic interaction between the polymer and liposome membrane causing the latter to be destabilized. This study contributes to the knowledge that pH responsive polyampholytes are a class of polymers that can be used to modify the surface of liposomes. The results from this work are of significance as the information derived is expected to be useful for the future synthesis of pH responsive polymer-liposome complexes with a desired critical value in mind. As certain damaged tissues (e.g. solid tumors) are of lower pH than normal, drugs adsorbed on the modified liposomes may be experimented to target the pH sensitive damaged tissues. This research potentially widens the scope of technology on surface modification of nanoparticles for drug delivery.

5. 5. References

1. V. Sihorkara and S.P. Vyas, *J. Pharm. Pharaceut. Sci*. 2001, **4**, 138–158.

2. G. Gregoriadis, *Liposomes as Drug Carriers, Wiley, New York*, 1988.

3. K. Kono et al., *Gene Ther.* 2001, **8**, 5–12.

4. N. Sakaguchi et al., *Biomaterials* 2008, **29**, 1262–1272.

5. N. Sakaguchi et al., *Bioconjugate Chem.* 2008, **19**, 1040–1048.

6. H. Kitano et al., *Molecules* 1991, **24**, 42–46.

7. M. Maeda, et al., *J. Am. Chem. Soc.* 1998, **110**, 7455–7459.

8. K. Seki and D.A. *Macromolecules* 1984, **17**, 1692–1698.

9. A. Kusumi et al., *Chem. Lett.* 1989, **18**, 433–436.

10. C. Pidgeon and C.A. Hunt, *Photochem. Photobiol.* 1983, **37**, 491–494.

11. H. Hayashi et al., *Bioconjugate Chem.* 1999, **10**, 412–418.

12. K. Kono et al., *J. Control. Release* 1994, **30**, 69–75.

13. T. Tomita et al., *Biochim. Biophys. Acta* 1989, **978**, 185–190.

14. K. Kono et al., *Biochim. Biophys. Acta* 1994, **1193**, 1–9.

15. L.-T. Ng et al., *Radiat.Phys. Chem*. 2006, **75**, 604–612.

16. H. Feil et al., *Molecules* 1992, **25**, 5528–5530.

17. K. Kono et al., *J. Membr. Sci.* 1993, **76**, 233–243.

18. J.M. Boggs, Can. *J. Biochem.* 1980, **58**, 755–770.

19. J. Thomas and D.A. Tirrell, *Acc. Chem. Res.* 1992, **25**, 336–342.

20. M. Fujiwara et al., *J. Colloid. Interface Sci.* 1997, **185**, 210–216.

Chapter 6

pH-Sensitive Vesicles That Undergo Transition to Micelles for Intracellular Delivery

6. 1. Introduction

Numerous lipid-based delivery systems have been studied to establish advanced medical technology, such as gene therapy, stem cell-based regenerative medicine and cell therapy. For these therapies, it is crucial to deliver bioactive molecules to specific sites where they work, in many cases, inside of the cells. Therefore, the development of efficient intracellular delivery systems was desired. Most major obstacle for efficient intracellular delivery is the degradation in endosome/lysosome. Inside of endosome/lysosome, which are cellular compartments involved in the internalization and degradation of exogenous materials, is weakly acidic environments [1]. To escape from endosome/lysosome pathway, pH-sensitive carriers have been developed. pH-Sensitive carriers are stable at physiological pH, but become destabilized and/or fusogenic under acidic conditions.

Many studies have been reported to establish the pH-sensitive drug delivery systems. For example, pH-sensitive liposomes were prepared by mixing non-bilayer-forming lipid, such as dioleoyl phosphatidylethanolamine (DOPE) and carboxyl group-containing amphiphilies, such as oleic acid or cholesteryl hemisuccinate (CHEMS) [2,3]. At neutral pH, deprotonated carboxyl groups promote the hydration degree of liposome surface and generate the electrostatic repulsion between liposomes, resulting in formation of stable liposomes. However, at acidic pH, liposomes are destabilized by the protonation of carboxyl groups. Other groups constructed pH-sensitive liposomes by conjugation of poly(carboxylic acid)

with liposomes [4-9]. At neutral pH, deprotonated carboxyl groups don't interact with liposome membrane. However, at acidic pH, protonated carboxyl groups destabilize liposome membrane rapidly.

The utility of pH-sensitive liposomes have been well shown. However, their performance as a delivery system depends on the property of pH-responsive molecules and is often insufficient because these molecules make carrier leaky or destabilized state but the carrier itself mostly retain their original formation. On the other hands, if amphiphilies change the balance between hydrophilic groups and hydrophobic groups by change of pH, it is expected that their assembling structure dramatically change, resulting in the release of their whole contents. Oleic acid and CHEMS is such examples, however they don't form stable vesicles by themselves. Hence, the amphiphiles which form stable carrier at neutral pH and change their assembling structure in response to pH is desired.

The author previously reported novel amphiphilic cationic lipid, poly(amidoamine) (PAMAM)-dendron-bearing lipid (DL, Fig. 6-1), which has PAMAM-dendron as a polar head group and two long alkyl groups as hydrophobic groups, and evaluated their application on gene delivery systems [10-14]. In addition, the properties of DL as an amphiphilic molecule were classified [15]. Because DL has PAMAM-dendron head group, which contains primary and tertiary amines, DL changed its hydration state responding to change of pH, resulting in changing its self-assembling structure: vesicles to micelles. This drastic change led us to apply DL to pH-sensitive drug delivery systems. However, DL formed the aggregates in a physiological condition. To evaluate the function of DL molecular assemblies as a drug delivery system, the method to make DL disperse stably is required.

In this study, poly(ethylene glycol) (PEG)-bearing lipid was introduced in molecular assemblies of DL to prevent the aggregation of DL. The effects of PEG-inclusion on DL dispersion and its properties were evaluated. Besides, the application of DL/PEG mixtures to intracellular system was examined.

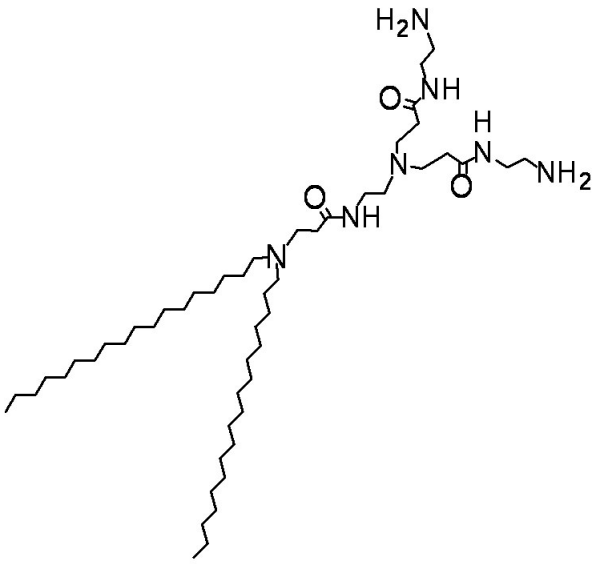

Figure 6-1. Structure of DL.

6. 2. Materials and Methods

6. 2. 1. Materials

DL-G1-2C_{18} (DL) was synthesized as previously reported (Fig. 6-1) [13]. Egg yolk phosphatidylcholine (EYPC) was kindly donated by NOF Co. (Tokyo, Japan). N-(carbonyl-methoxy poly(ethylene glycol)$_{2000}$)-1,2-distearoyl-*sn*-glycero-3-phosphoethanolamine, sodium salt (PEG_{2000}-PE) were purchased from NOF Co. (Tokyo, Japan). Lissamine rhodamine B-sulfonyl phosphatidylethanolamine (Rh-PE) were purchased from Avanti Polar Lipids (Birmingham, AL, USA). Ovalbumin (OVA) and fluorescein isothiocyanate (FITC) were purchased from Sigma (St. Louis, MO.). FITC-OVA was prepared by reacting OVA (10 mg) with FITC (11.8 mg) in 0.5 M $NaHCO_3$ (4 mL, pH 9.0) at 4 °C for three days and subsequent dialysis.

6. 2. 2. Cell Culture

DC2.4 cells, which were an immature murine DC line, were provided from Dr. K. L. Rock (Harvard Medical School, USA) and were grown in RPMI 1640 supplemented with 10% FBS (MP Biomedical, Inc.), 2 mM L-glutamine, 100 μM nonessential amino acid, 50

μM 2-mercaptoethanol and antibiotics at 37 °C [16].

6. 2. 3. DL/PEG Dispersion Preparation

DL/PEG dispersion was prepared as follows. A dry thin membrane of mixture of DL and PEG_{2000}-PE (DL/PEG_{2000}-PE = 96/4, mol/mol) was made by evaporation of solution of the lipids in chloroform and subsequent drying under vacuum. The membrane was dispersed in aqueous solution containing 20 mM Hepes and 150 mM NaCl (pH 7.4) by a bath type sonicator at 45 °C. Lipids suspension was subsequently extruded through a polycarbonate membrane of pore sizes of 100 nm at 45 °C.

6. 2. 4. Differential Scanning Calorimetry (DSC)

A given amount of DL and PEG_{2000}-PE was dissolved in chloroform and added onto Ag pan. After solvent was drying under vacuum, a given pH of aqueous solution containing 20 mM Hepes and 150 mM NaCl was added to sample. DSC measurements were performed with a DSC 120 microcalorimeter (Seiko Electronics). The heating rate was 1.25 °C/min.

6. 2. 5. Optical Density Measurement

Optical density at 500 nm of the DL/PEG dispersion (5 mg/mL) at various pH was measured by a Jasco Model V-560 spectrophotometer equipped with a peltier type thermostatic cell holder coupled with a controller ETC-505T.

6. 2. 6. Dynamic Light Scattering (DLS)

Diameters of the DL/PEG dispersion (0.5 mg/mL) at various pH were measured using a DLS-6000 (Otsuka Elec. Co., Ltd, Osaka, Japan) equipped with a Ar laser (488 nm wavelength). Data was obtained as an average of more than three measurements on different samples and analyzed by a modified Marquardt method.

6. 2. 7. Transmission Electron Microscopy (TEM)

TEM analysis of the DL/PEG dispersion (5 mg/mL) at various pH was performed using JEM-2000FEX II (Nihon Elec. Co., Ltd, Tokyo, Japan) with carbon-coated copper grids.

6. 2. 8. Release Assay

Release contents from the DL/PEG or EYPC/PEG dispersion was measured as follows. The pH of FITC-OVA containing DL/PEG or EYPC/PEG dispersion was adjusted to a given pH and incubated for 5 min or 120 min. After incubation, the pH was adjusted to 7.4. DL/PEG or EYPC/PEG dispersion was ultracentrifuged (55000 rpm, 30 min) and the fluorescence of FITC from each supernatant was measured by a fluorospectrometer. Total release was determined as the fluorescence from sample added TritonX-100.

6. 2. 9. Microscopy

The DC2.4 cells (2×10^5 cells) cultured for 2 days in 35-mm glass-bottom dishes were washed with Hank's balanced salt solution (HBSS, Sigma), and then incubated in serum-free medium. The DL/PEG or EYPC/PEG dispersion (60 nM) containing FITC-OVA, in which lipids were substituted by Rh-PE (0.6 mol%), were added gently to the cells and incubated for 4 h at 37 °C. After the incubation, the cells were washed with HBSS three times and confocal laser scanning microscopic (CLSM) analysis of these cells was performed using LSM 5 EXCITER (Carl Zeiss Co. Ltd.). EYPC liposome containing FITC-OVA, in which lipids were substituted by Rh-PE (0.6 mol%), were also added as a control.

6. 3. Results and Discussions

6. 3. 1. DSC Analysis of DL/PEG Dispersion

In a previous study, it was reported that DL exhibited pH-responsive structural transition by the change in hydration state of head group [15]. However, DL formed aggregates in a physiological environment. To obtain stable DL suspension in a physiological environment is crucial for its application to drug delivery system. Hence, a given amount of PEG-lipid was incorporated in DL molecular assemblies to promote the colloidal stability in a physiological environment.

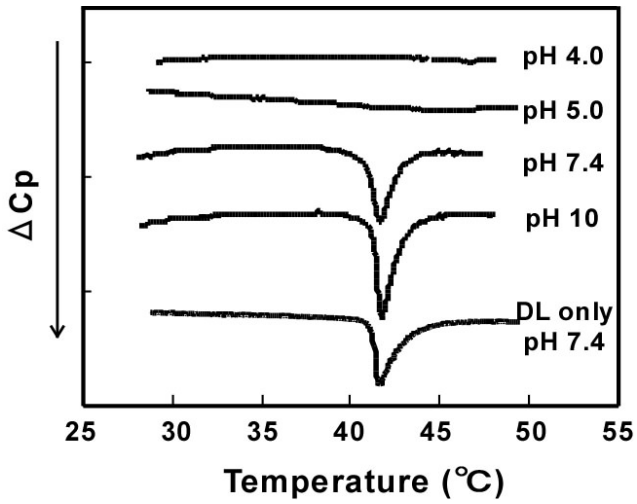

Figure 6-2. DSC thermograms for molecular assemblies of DL and DL/PEG. The DSC traces were obtained in the upward scan mode at the rate of 1.25 °C /min. The scan base line was corrected by using a buffer blank. DSC thermogram for molecular assemblies of DL at pH 7.4 was also shown as a control.

As a previous study, DL showed gel-liquid crystalline transition at around 43 °C. This was reproducible in a current study: DL exhibited sharp endothermic peak at 42 °C (Fig. 6-2). DSC analysis of lipid mixtures consisting of DL and PEG_{2000}-PE at various pH was examined to investigate effects of the inclusion of PEG-lipid on molecular assemblies. Figure 6-2 shows DSC thermograms of molecular assemblies consisting of DL and PEG_{2000}-PE at various pH. At pH 10 and 7.4, an endothermic peak was observed around at 42 °C. At pH 5 and 4, an endothermic peak was not observed. These indicate that molecular assemblies of DL/PEG may form lamellar phases at pH 10 and 7.4 and cause the gel-liquid crystalline phase transition around at 42 °C. In addition, at pH 5 and 4, these lamellar phases seem to be broken.

These data are almost consistent with previous report [15]. The values of transition enthalpy are 48.6 J/g (pH 10) and 39.9 J/g (pH 7.4). This may result in tight packing of DL molecules due to the relaxation of electrorepulsion between polar head groups by decreasing of the charge in head groups with increasing pH. Thus, the inclusion of PEG-lipid in molecular assemblies didn't inhibit phase-transition and vesicle-micelle transition of DL. Rather, the vesicle-micelle transition seems to be more critical than that of DL only.

6. 3. 2. pH-Dependent Change of Optical Density of DL/PEG Dispension

To evaluate pH-sensitivity of the molecular assemblies comprising of DL/PEG, optical density of DL/PEG dispersion at various pH was measured (Fig. 6-3). In a previous study, DL immediately aggregated at pH 7.4 and 37 °C [15]. Surprisingly, optical density of DL/PEG suspension was a consistent value of 0.14 at pH 7.4: the solution was almost transparent. When pH was raised to alkaline pH, optical density slightly rose to about 0.2, while at acidic pH, optical density decreased promptly. Figure 6-3B shows optical density of DL/PEG suspension at 10 min after as a function of pH. Drastic drop of optical density was observed between pH 7.0 and 6.7, indicating that some kinds of structural change occurred in this pH region. DL exhibited vesicle-micelle transition around this pH region [15], suggesting that DL/PEG may cause vesicle-micelle transition similarly.

6. 3. 3. Structural Analysis of DL/PEG Dispersion

Next, DLS and TEM of molecular assemblies comprising of DL/PEG were measured to elucidate the structural change by change of pH. Figure 6-4 shows the results of DLS about DL/PEG suspension at various pH. Consistence with optical density analysis, the sizes of molecular assemblies of DL/PEG increased with increasing pH and showed drastic decreasing around at pH 6.5 (Figure 6-4). Figure 6-5 shows TEM analysis of molecular assemblies of DL/PEG prepared at various pH. At pH 7.4, some particles of spherical structure which sizes

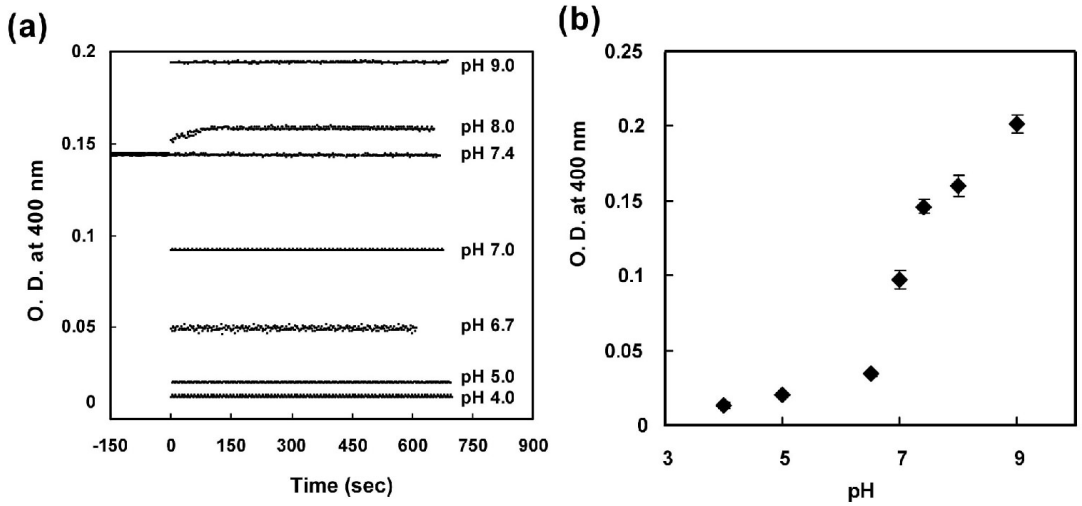

Figure 6-3. (a) Time courses of optical density of DL/PEG suspended in 20 mM Hepes and 150 mM NaCl aqueous solution at 37 °C as various pH. Time zero represents the time where NaOH or HCl solution was added to adjust the solution pH to indicating pH. (b) Optical density at 10 min after of DL/PEG suspended in 20 mM Hepes and 150 mM NaCl aqueous solution at 37 °C as a function of pH. Each point is the mean ± SD (n = 3).

of around 100 nm were observed. At pH 9.0, some aggregates were observed. At pH of 6.5 and 4.0 small particles which sizes of 10 to 20 nm were observed. Combined with these results, molecular assemblies of DL/PEG form stable bilayer vesicles which sizes are 100 nm at pH 7.4. When the pH was raised, these vesicles might aggregate between particles, resulting in formation of size of about 200 nm aggregates. This aggregate may result from membrane fusion between particles to make up for membrane defect resulting from tight packing of DL molecules which lost their charge. On the other hand, at acidic pH, the vesicles changed to smaller structures. At acidic pH, the tertiary amines of DL are well protonated [15] and its critical packing parameter may decrease, resulting in the structural transition from vesicles to smaller structure, probably micelles. As a result, the optical density of dispersion of DL/PEG at acidic pH became very small (Fig. 6-3) and an endothermic peak disappeared (Fig. 6-2). Thus, the inclusion of PEG-lipid in molecular assemblies provided DL colloidal stability in a physiological environment and very sharp responsiveness to pH.

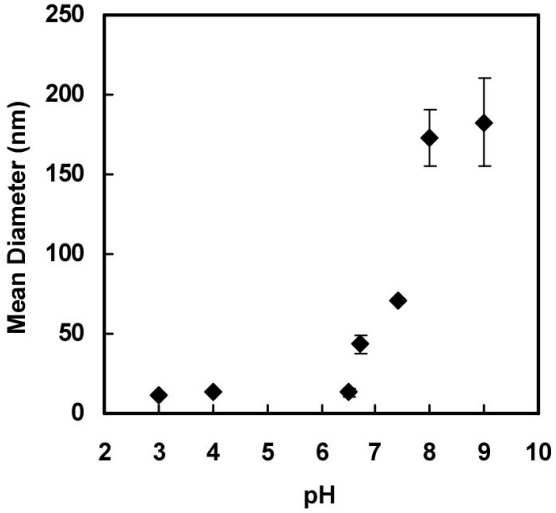

Figure 6-4. Particle sizes of DL/PEG suspended in 20 mM Hepes and 150 mM NaCl aqueous solution with various pH at 37 °C. Each point is the mean ± SD (n = 3).

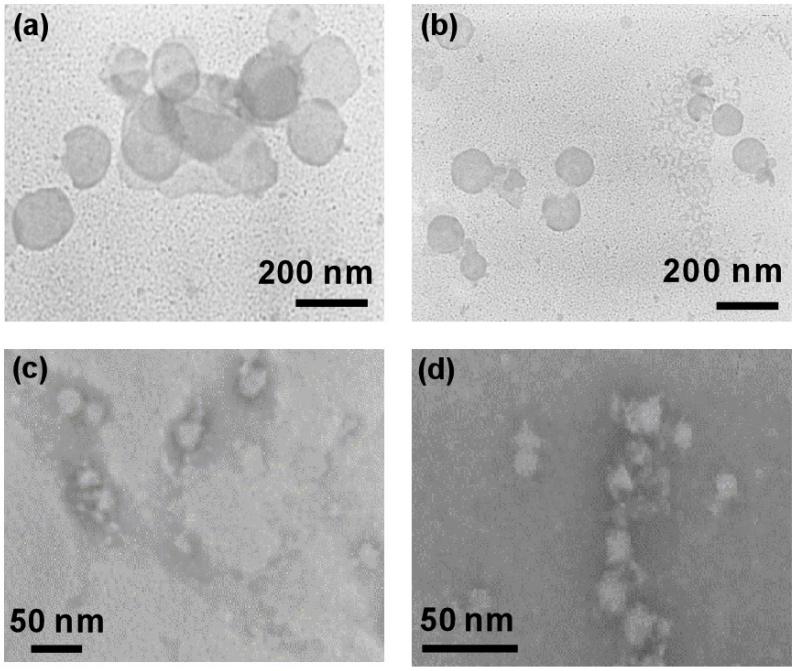

Figure 6-5. Transmission electron micrographs of DL/PEG suspended in 20 mM Hepes and 150 mM NaCl aqueous solution with pH of (a) 9.0, (b) 7.4, (c) 6.5 and (d) 4.0 at 37 °C.

6. 3. 4. Accurate Release Contents Responding to pH-Change

To evaluate the utility of these structural changes as a drug delivery system, drug release from DL/PEG vesicles was examined. OVA were used as a model protein drug. OVA were also fluorescence-labeled by FITC. Figure 6-6 shows FITC-OVA release from DL/PEG

vesicles. EYPC/PEG liposomes were also used as a control. The pH of FITC-OVA-loaded vesicles prepared at pH 7.4 was changed to a given pH and incubated 5 min or 120 min. Molecular assemblies were deposited by an ultracentrifuge and the fluorescence of supernatant were measured. In the case of EYPC/PEG liposomes (Fig. 6-6b), no change about fluorescence of supernatant was observed by change of incubation pH, indicating that EYPC/PEG liposomes were stable and didn't release their contents. On the other hand, in the case of DL/PEG vesicles (Fig. 6-6a), FITC-OVA were released at pH 6.0 or 4.0, indicating that the vesicle-micelle transition induced the release of contents coincidently. No significant difference was observed about percent release between 5 min incubation and 120 min incubation. This indicates that the content release from DL/PEG vesicles is very rapid.

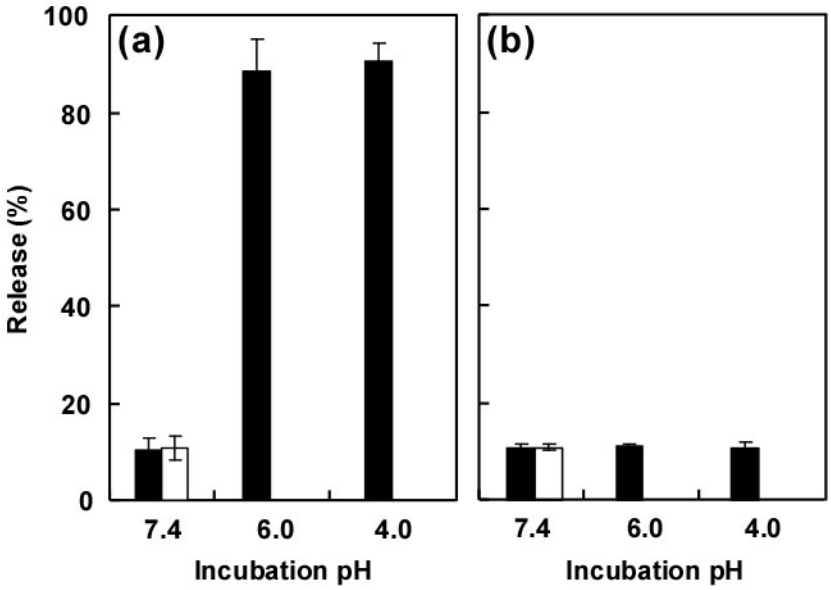

Figure 6-6. Release of FITC-OVA from (a) DL/PEG and (b) EYPC/PEG liposome induced by incubation at indicating pH for 5 min (closed bars) or 120 min (open bars) at 37 °C. After incubation, solution pH was adjusted to pH 7.4 and liposomes were precipitated by ultracentrifuge and then the fluorescence of supernatant was measured. Each point is the mean ± SD (n = 3).

6. 3. 5. Application to Intracellular Delivery System

DL/PEG vesicles changed their structures and coincidently released contents

promptly. Their transition pH is around 6.5, which is near to endosomal pH of cells. Therefore, intracellular delivery of proteins using DL/PEG vesicles was finally examined. Rh-PE (0.6 mol%) and FITC-OVA containing DL/PEG vesicles and EYPC/PEG liposomes were added to DC2.4 cells and 4 h later cells were observed by CLSM. Figure 6-7 shows cellular distribution of carriers and their contents. In the case of EYPC/PEG liposome, the fluorescence of FITC-OVA was punctate within the DC2.4 cells and overlapped with Rh-fluorescence (lipid). On the other hand, in the case of DL/PEG vesicles, FITC-OVA were diffused within cytosol and nuclear of DC2.4 cells. These results indicate DL/PEG vesicles may generate the vesicle-micelle transition responding to endosomal pH and disrupt or solubilize the endosomal membrane by formation of mixed micelles with endosomal membranes, resulting in the release contents into cytosol.

6. 4. Conclusion

In this study, pH-sensitive lipid-based unique intracellular delivery system was established. DSC, optical density analysis, DLS and TEM measurements revealed that the inclusion of PEG-lipid in DL molecular assemblies promoted the DL's unique structural transition responding to pH. Results showed that molecular assemblies of DL/PEG formed stable vesicles at neutral pH and aggregated vesicles at alkaline pH and micelles at acidic pH. Critical transition pH from vesicles to micelles was around 6.5, resulting from the change of hydrophilic-hydrophobic balance by the protonation of tertiary amines in head group of DL. Below this pH, vesicles promptly changed to micelles and this change coincidently caused accurate drug release from carriers. In addition, DL/PEG vesicles could deliver their contents into the cytosol of immune cell lines by their unique structural transition. Consequently, DL/PEG vesicles are promising protein carriers for immune cells, which are useful for cancer immunotherapy and their unique structural transition mechanisms provide the novel strategy to develop the newly delivery systems.

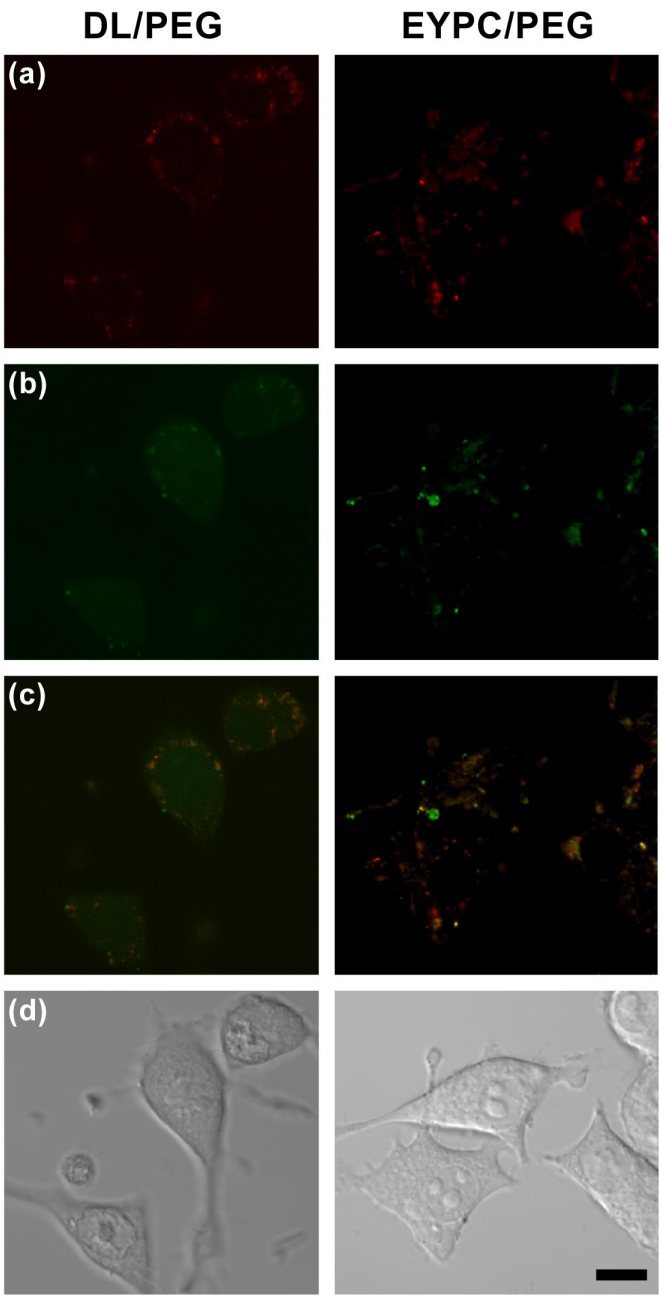

Figure 6-7. CLSM images of DC2.4 cells treated with FITC-OVA-loaded DL/PEG and EYPC/PEG. DC2.4 cells were incubated in the presence of 60 nM lipids for 4 h at 37 °C without serum. The intracellular localization of lipids (a) and OVA (b) was determined by a CLSM. (c) Superimposed pictures for Rh and FITC-fluorescence. (d) Differential interference contrast pictures for DC2.4 cells.

6. 5. References

[1] S. Mukherjee et al., *Physiol. Rev.* 1997, **77**, 759–803.

[2] D. Liu and L. Huang, *Biochim. Biophys. Acta* 1990, **1022**, 348–354.

[3] H. Ellens et al., *Biochemistry* 1984, **23**, 1532–1538.

[4] K. Seki and D. A. Tirrell, *Macromolecules*, 1984, **17**, 1692–1698.

[5] M. Maeda et al., *J. Am. Chem. Soc.* 1988, **110**, 7455–7459.

[6] M. Fujiwara et al., *J. Colloid Interface Sci.* 1997, **185**, 210–216.

[7] N. Murthy et al., *J. Controlled Release* 1999, **61**, 137–143.

[8] K. Kono et al., *Biochim. Biophys. Acta* 1994, **1193**, 1–9.

[9] N. Sakaguchi et al., *Bioconjugate Chem*., 2008, **19**, 1040-1048.

[10] T. Takahashi et al., *Bioconjug. Chem.* 2003, **14**, 764–773.

[11] T. Takahashi et al., *Bioconjug. Chem.* 2005, **16**, 1160–1165.

[12] T. Takahashi et al., *Bioconjug. Chem.* 2007, **18**, 1163–1169.

[13] T. Takahashi et al., *Bioconjug. Chem.* 2007, **18**, 1349–1354.

[14] T. Takahashi et al., *Res. Chemical Intermediates*, 2009, **35**, 1005-1014.

[15] T. Douura et al., *J. Controlled Release* submitted.

[16] Z. Shen et al., *J. Immunol.* 1997, **158**, 2723-2730.

Chapter 7

Preparation and characterization of complexes of liposomes with gold nanoparticles

7. 1. Introduction

Gold nanoparticles (Au NPs) have attracted much attention recently because of their interesting shape-dependent and size-dependent physical and chemical properties, which are different from those of bulk gold and gold atoms [1,2]. Especially, Au NPs strongly absorb light in the visible region of the spectrum, due to the surface plasmon resonance (SPR) [3], and convert the absorbed light to heat [4]. Recently, Au NPs were considered to be useful for photothermal therapy as well as for imaging in the biomedical field [5–8]. However, Au NPs generally aggregate and lose their unique photo-properties under physiological conditions due to the shielding of the repulsion at the surface. Therefore, it is desirable to develop a proper modification of Au NPs for biological applications. It is also important to target Au NPs to the affected tissues for biomedical applications. The direct complexation of biocompatible or bioactive molecules to Au NPs can improve the stability of the particle and the targeting ability. It has been reported that the surface modification of Au NPs can be achieved using materials such as poly(ethylene glycol) (PEG), proteins and nucleotides [1,2,5–13].

Drug carriers can also be useful for the preservation and delivery of Au NPs, since Au NPs are generally considered as a kind of drug. Drug carriers are also of great benefit for the delivery of other functional molecules in addition to Au NPs. For example, a carrier loaded with both Au NPs and drug molecules can act as a diagnostic and therapeutic multimodality agent [14]. The author previously reported that dendrimers comprising PEG chains are useful candidates for carrying Au NPs. Here, the Au NPs loaded in the PEG-attached dendrimer were stably dispersed and exhibited typical photothermal properties

[15]. Liposomes, which were classically studied and subsequently approved for use as a drug carrier, are composed of phospholipids having a hydrophobic tail and a hydrophilic head to construct vesicular structures. Many kinds of molecules can be encapsulated in liposomes: that is, hydrophilic molecules can be encapsulated in the inner phase of liposomes, and hydrophobic molecules can be encapsulated in the bilayer of the lipid membrane. In addition, liposomes can be modified with many molecules at the surface [16].

There are three types of complexes of Au NPs with liposomes, as shown in Fig. 7-1. The first is a liposome containing Au NPs in the inner phase. The second contains Au NPs bound to the lipid membrane, while the third is a liposome modified with Au NPs at the surface. The first complex, which has already been prepared by reducing Au ions in the liposome, is used to investigate the in vivo distribution of liposomes [17]. Similarly, the second type of complex is also known, and is prepared by mixing lipid and Au NPs possessing hydrophobic surfaces [18–20]. In this study, the author prepared the complex of Au NPs with liposomes by the third method via physical absorption. This kind of complex has not been reported as yet, although the phospholipid-coated Au NPs are known [21]. Consequently, this third method provides the benefit that the complex comprising certain bioactive molecules such as drugs, can be easily prepared by using liposomes containing them through simple mixing. In this study, the author examined the time-dependent SPR to demonstrate the stability of the complexes under physiological conditions. In addition, the author also performed transmittance electron microscopy (TEM) and dynamic light scattering (DLS) studies, and analyzed the release of encapsulated molecules from the liposome to in an attempt to ascertain their morphology.

7. 2. Materials and Methods

7. 2. 1. Materials

Egg yolk phosphatidylcholine (EYPC) was kindly provided by NOF Corp. (Tokyo,

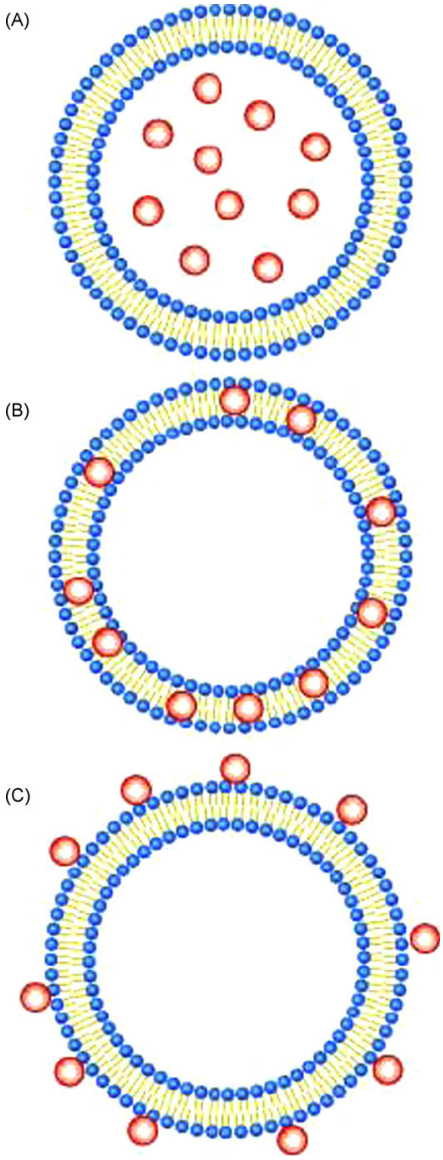

Figure 7-1. A schematic image of the complexes formed between liposomes and Au NPs. (A) A liposome encapsulating Au NPs, (B) a liposome loaded with Au NPs in the membrane, and (C) a liposome modified with Au NPs at the surface.

Japan). Distearyldimethylammonium bromide (DDAB) and distearoyl-*sn*-glycero-3-phosphoethanolamine-*N*-[methyl(polyethyleneglycol)-2000] (PEG-PE) were obtained by Tokyo Chemical Industry Co. Ltd. (Tokyo, Japan) and Avanti Polar Lipids Inc. (Alabaster, AL), respectively. Calcein, HAuCl4, and trisodium citrate were purchased from Sigma (St. Louis, MO), Wako Pure Chemical Industries Ltd. (Osaka, Japan), and Kishida Chemical (Osaka, Japan), respectively.

7. 2. 2. Liposome Preparation

The liposomes were prepared as previously reported [22]. A chloroform solution of EYPC (5.0 mg, 6.25 μmol) was prepared, and then the solvent removed by evaporation. The obtained thin lipid membrane was further dried under vacuum for at least 2 h, and then dispersed in 0.5 mL of an aqueous calcein solution (63 mM, pH 7.4) or phosphate-buffered saline (PBS, 20 mM Na_2HPO_3–NaH_2PO_3, 150 mM NaCl, pH 7) with sonication for 3 min. The liposome suspensions were freeze-thawed four times. The obtained liposome suspension was extruded through a polycarbonate membrane with a pore diameter of 50, 100, 200 or 400 nm. The free calcein was removed by gel permeation chromatography on a Sepharose 4B column using PBS. A PEG-PE-containing liposome with diameter of 200 nm was also prepared, which was composed of 5 mol% of PEG-PE (0.31 μmol) and 95 mol% of EYPC (5.94 μmol), as the above. A DDAB-containing liposome (10 mol% DDAB (0.625 μmol) and 90 mol% EYPC (5.625 μmol)) was also prepared by sonication for more than 10 min after the incubation of the suspension at 4 ◦C for 1 day. The lipid concentrations were estimated by Test Wako (Wako Pure Chemical Industries Ltd.) according to the manufacturer's instructions.

7. 2. 3. Preparation of the Complex of Liposomes with Au NPs

Au NPs of diameter 13 nm were prepared by reducing Au ions with citric acid according to a previous report [23]. The complexes were prepared by adding the Au NP dispersion to the liposome suspension in PBS at different ratios and stirred with a vortex.

7. 2. 4. Characterization

UV–vis absorption spectra ranging from 400 to 800 nm were measured using a Jasco Model V-560 spectrophotometer (Jasco Inc., Japan) at 25 ◦C [15]. TEM analysis was performed as follows [24]. A small drop of Au NP samples was placed on a collodion-coated

grid and drawn off with filter paper. A drop of 2% (w/v) phosphotungstic acid was applied to the grid, drawn off with filter paper, and the stained sample was allowed to dry. The grid was viewed under an electron microscope (JEOL Ltd., JEM-2000FEX II). DLS analysis was performed in the vesicle mode of Nicomp ZLS380 (Nicomp) at room temperature using EYPC suspension around 0.01 mM.

7. 2. 5. Calcein Release from Liposomes

The calcein release measurements were performed according to the method previously reported [25], with some modification. An aliquot of dispersion of calcein-loaded liposomes was added into 3 mL of PBS containing 0.5 mM ethylenediaminetetraacetic acid (EDTA) (final concentration of the lipids, 0.2 μM), and the fluorescence intensity of the solution was monitored using a spectrofluorometer (Jasco Inc., FP-6500) before and after the addition of Au NPs to the liposome suspension at the EYPC/Au ratio of 1/10. The excitation and monitoring wavelengths were 480 and 515 nm, respectively.

7. 3. Results and Discussion

7. 3. 1. Preparation and Surface Plasmon Resonance of the Complexes of Gold Nanoparticles with Liposomes

Au NPs reduced using citric acids are small with a narrow distribution, and are stably dispersed due to the repulsion of the anion surface in citric acid solution [26]. The author prepared Au NPs according to a previous report [23], and then mixed them with EYPC liposomes (200 nm in diameter) at different ratios in PBS. The author examined the time course of the SPR, a characteristic property of Au NPs. The SPR absorption around 523 nm corresponding to the Au NPs almost disappeared under physiological conditions (Fig. 7-2A). This is caused by the aggregation due to the shielding of the electrostatic repulsion [1,2]. In contrast, the complexes of Au NPs with EYPC liposomes retained the SPR feature, which is

dependent on the ratio. Although the SPR signal of the complexes formed with EYPC/Au ratios of 1/10 and 1/1 decreased (rapidly and slowly, respectively), the SPR signal for the complex having a 10/1 ratio remained after 1 day. This showed that the Au NPs in the presence of liposomes were stably dispersed under isotonic condition. This indicated that the EYPC liposomes contributed to the stability of the Au NPs by preventing their aggregation, suggesting complex formation.

The author also prepared the complexes of Au NPs with EYPC liposomes with various diameters, 50, 100 and 400 nm, in addition to 200 nm. The particle concentrations of these liposomes were dependent on the particle sizes. Lipid molecules of 2.2×10^4, 8.8×10^4, 3.5×10^5 and 1.4×10^6 are composed of EYPC liposomes having diameters of 50, 100, 200 and 400 nm, respectively, as determined from the following calculation.

$$N = 4\pi r^2 \times 2/A \qquad (1)$$

where N, r, and A refer to the number of lipids, the radius of the liposomes, and the section area of the EYPC head group, which has a value of 0.717 nm^2 [16]. The author prepared the complexes of Au NPs with EYPC liposomes with various diameters at different ratios. As shown in Fig. 7-2C and the left panels of Fig. 7-3, the stability and intensity of the SPR signal of the complexes at EYPC/Au = 1/1 was almost unaffected by the size of these liposomes. As shown in Fig. 7-2D and the right panels of Fig. 7-3, the stability of the SPR signal of the complexes at EYPC/Au = 10/1 was almost unchanged by the size of these liposomes, although the intensity of the complexes with larger diameters was higher due to the turbidity of the liposome suspension. These might suggest that the complex formation was not attributed to the particle concentration, but to the surface area of the liposome. Since the surface area of Au NPs (13 nm in diameter) is calculated as 5.3×10^2 nm^2, the lipid number to cover with the Au NPs is calculated as 7.4×10^2 molecules per Au NP. On the other hand, the Au NP is composed of 6.8×10^4 gold atoms, as determined from the following calculation.

$$U = (2/3)\pi(D/a)^3 \qquad (2)$$

where *U*, *D*, and *a* refer to the number of Au atoms, the diameter of the Au NPs, and the edge of a unit cell, which has a value of 0.40786 nm [27]. From these calculations, the amount of lipid in the complex at the EYPC/Au ratio of 1/10 (6.8×10^3 EYPC molecules/6.8×10^4 Au atoms) is estimated to be in about a 10-fold excess in order to cover with Au NPs (7.4×10^2 molecules). Therefore, a large excess of liposomes was necessary to stabilize Au NPs sufficiently under isotonic condition.

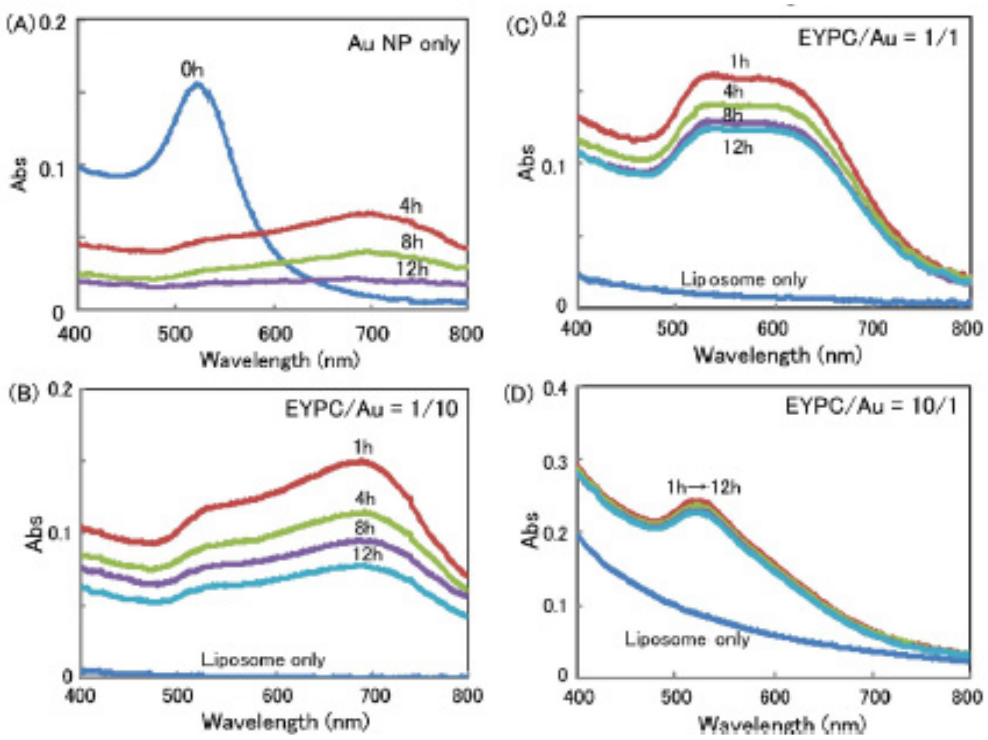

Figure 7-2. Time-dependent UV–vis spectra of the complex of EYPC liposomes (200 nm in diameter) with Au NPs at different ratios in PBS (20 mM Na_2HPO_3–NaH_2PO_3, 150 mM NaCl, pH 7). The time-dependent UV–vis spectra of Au NPs only are shown as a control (A). The mole ratio of EYPC to Au is 1/10 (B), 1/1 (C) and 10/1 (D). [Au] = 45.5 μM.

7. 3. 2. Morphology of the Complexes of Gold Nanoparticles with Liposomes

The author investigated the morphology of the complexes of liposomes with Au NPs. Using calcein-loaded liposomes, the author first analyzed the collapse behavior of liposomes by adding Au NPs. Although the fluorescence of the calcein loaded in the liposomes was essentially quenched, an intense florescence was observed after their release from the liposome. The fluorescence intensity (%) of calcein is shown in Fig. 7-4. The fluorescence

intensity of calcein after the addition of Au NPs at the EYPC/Au ratio of 1/10 was the same as that in the intact liposome, suggesting that essentially no calcein was released by adding Au NPs. The percentage of fluorescence intensity of calcein in the complexes was almost unchanged after 24 h. As mentioned before, Fig. 7-2 indicates that the SPR of these complexes gradually decreased. These indicate that the Au NPs in the complexes at the EYPC/Au ratio of 1/10 aggregated without the collapse of liposomes. This suggests that the liposomal membrane remained intact after the interaction with Au NPs. The author characterized the complexes of liposomes with Au NPs using TEM. Fig. 7-5 shows the TEM

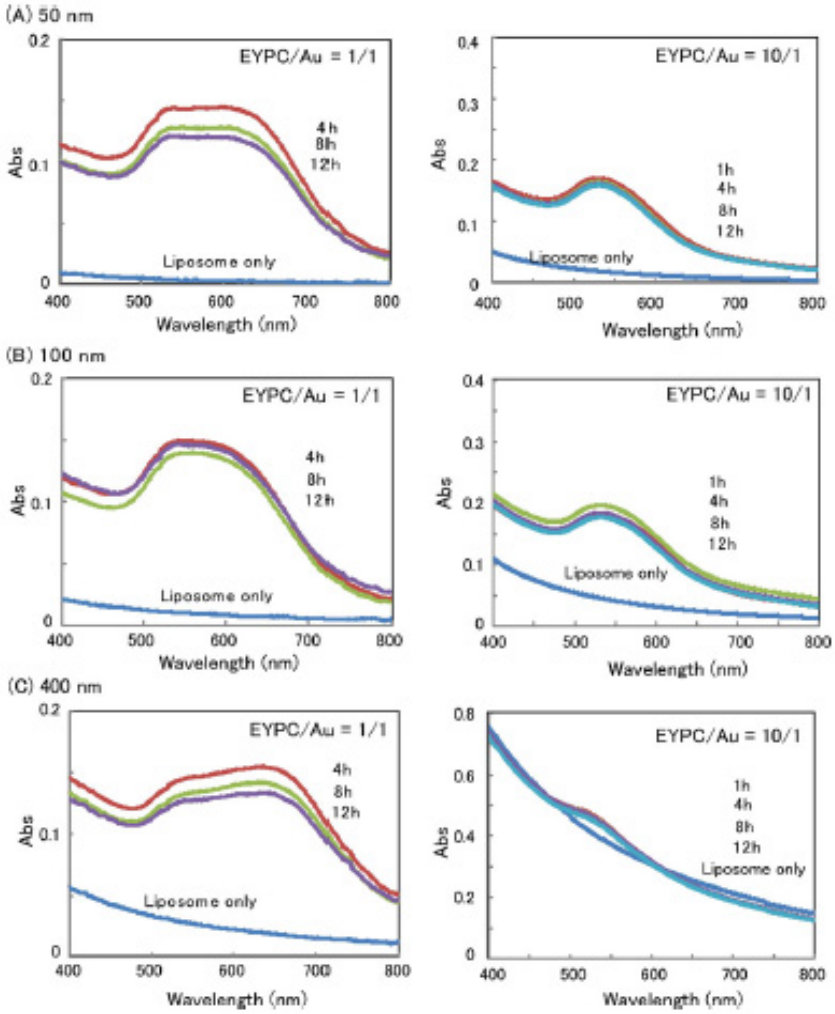

Figure 7-3. Time-dependent UV–vis spectra of the complex of various EYPC liposomes with Au NPs at the EYPC/Au ratio of 1/1 (left) and 10/1 (right). The diameter of the EYPC liposomes is 50 nm (A), 100 nm (B), and 400 nm (C). The experimental condition was the same as Fig. 7-2.

images of Au NPs and their complexes with EYPC/Au ratios of 1/10 and 10/1. Large aggregates were observed in the TEM image for the sample comprising only Au NPs and for the sample comprising the complex with a small amount of EYPC liposomes. In the complex at the EYPC/Au ratio of 10/1, on the other hand, there are no large aggregates of Au NPs. These are consistent with the SPR analysis. In the TEM image of the complex at the EYPC/Au ratio of 10/1, many Au NPs were observed at the boundary surface within the liposomal assembly. This indicates that the Au NPs complexed with the liposomes. The liposomal aggregation might be an artificial production brought about by the TEM sample preparation, because DLS analysis indicated that the size of the complexes was almost the same as the intact liposome (Fig. 7-6). As described before, Fig. 7-2 shows that the Au NPs were dispersed stably in the presence of the liposomes, and Fig. 7-4 shows that the liposomes were still intact after the addition of Au NPs. In addition, it is reported that the head group of phosphatidylcholine was associated with the Au NPs via physical absorption [21]. Taken together, the author suggests that the liposomes were physically associated with the Au NPs at the surface without disturbing the membrane, by which the Au NPs were stably dispersed

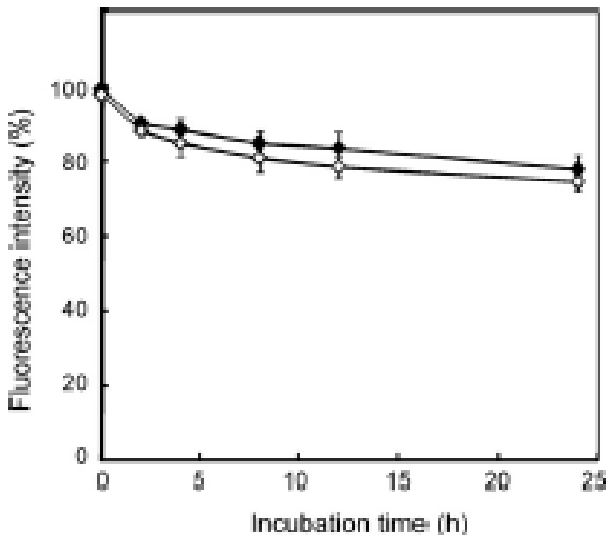

Figure 7-4. The time-dependent fluorescence intensity (%) of calcein in the liposomes with (open symbols) and without (closed symbols) of Au NPs is shown. The fluorescence intensity after the addition of Triton X-100 (final concentration 0.03%) is defined as 100%.

under isotonic condition.

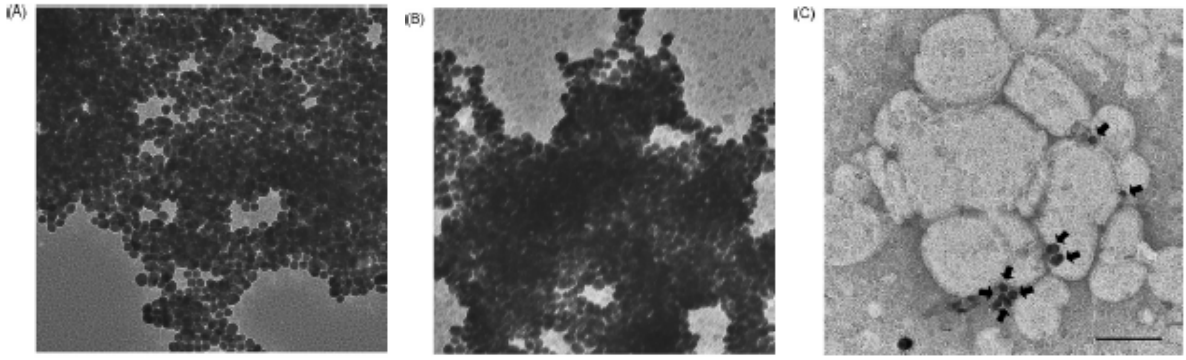

Figure 7-5. TEM images of the complexes of EYPC liposomes with Au NPs at the EYPC/Au ratio of 0/10 (A), 1/10 (B) and 10/1 (C) in PBS after the 6 h-incubation. Arrows indicate the Au NPs. Bar: 100 nm.

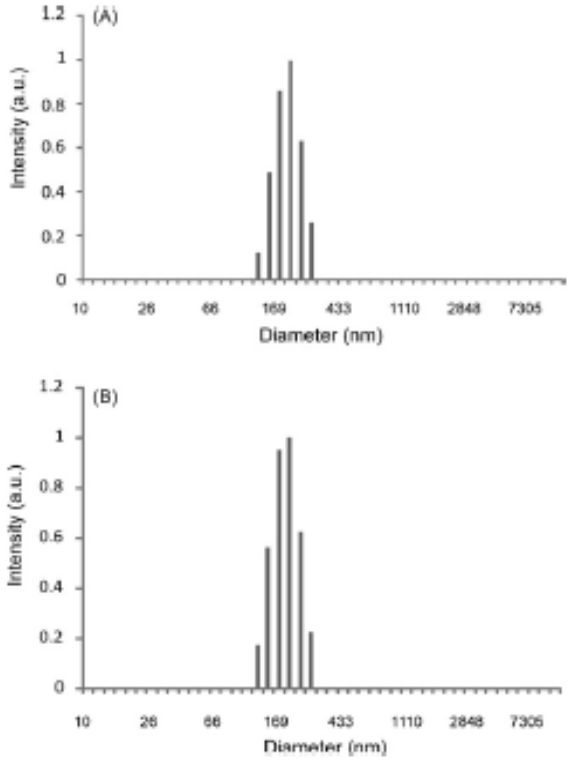

Figure 7-6. Intensity-weighted distributions of the intact liposomes (A) and the complexes of liposomes with Au NPs at the EYPC/Au ratio of 10/1 (B) in PBS after the 6 h-incubation by DLS.

7. 3. 3. Preparation of the Complexes of Gold Nanoparticles with Various Liposomes

Finally, the author prepared various complexes of Au NPs with various different liposomes, DDAB-bearing liposomes and PEG-bearing liposomes as a cationic and

biocompatible liposome. Cationic liposomes are widely used as a vector for transfection, since they can interact with anionic DNA [28,29]. PEG-bearing liposomes are widely used as a drug carrier due to their biocompatibility and prolonged blood circulation [30]. Fig. 7-7 shows the time-dependent SPR absorption spectra of the complexes of DDAB- or PEG-bearing liposomes. These liposomes also inhibited the decrease of the SPR signal of the Au NPs. In addition, the stability of the SPR signal for these liposomes was similar to the EYPC liposomes. These complexes were analyzed by TEM and DLS, as also shown in Fig. 7-7. The diameters of these complexes, estimated by DLS, were almost the same as these intact liposomes, which is similar to EYPC liposomes (Fig. 7-6). These complexes were also characterized by TEM. The Au NPs were observed at the surface of these liposomes. These suggest that these liposomes might form complexes with Au NPs in a similar manner to EYPC liposomes. The dispersed liposomes were observed in these TEM images, unlike the EYPC liposomes. This may be caused by the repulsion induced by the hydrodynamic effect of PEG and the cationic charges of DDAB. It is anticipated that these complexes can act as gene and drug carriers with diagnostic function.

7. 4. Conclusion

The author prepared the complex of liposomes with Au NPs by simply mixing dispersions of liposomes and Au NPs. The liposomes improve the stability of the Au NP dispersion under isotonic condition, in which the stability was found to be dependent on the liposome/Au NPs ratio. Here, the Au NPs interacted with intact liposomes to obtain the stable complex, which indicates that these complexes could be made from liposomes encapsulating small molecules such as drug molecules. In addition, these complexes could be formed by using cationic liposomes and PEG-modified liposomes as well as EYPC liposomes, making them ideal candidates for use as drug and gene delivery. We propose that this kind of complex will find useful application as a nanomedicine with diagnostic and therapeutic ability.

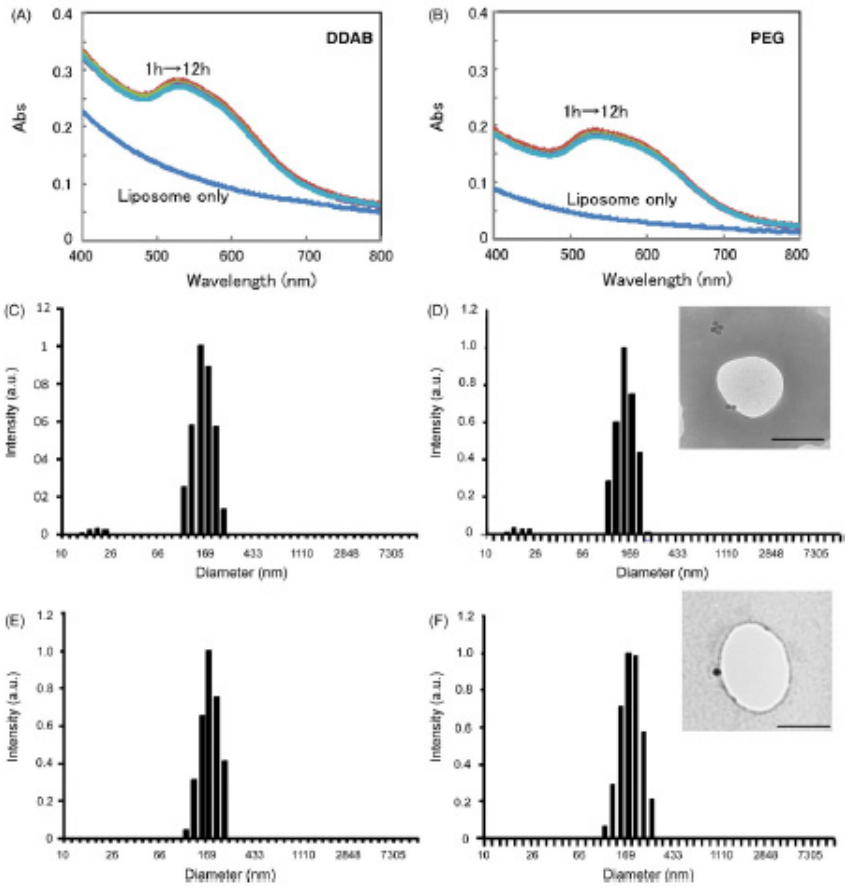

Figure 7-7. The complex formation of DDAB- (A, C, and D) or PEG-(B, E, and F) bearing liposomes. (A and B) Time-dependent UV–vis spectra of the complex of various liposomes with Au NPs at the lipid/Au ratio of 10/1. The experimental condition was the same as Fig. 7-2. (C–F) Intensity-weighted distributions of the intact liposomes (C and E) and the complexes (D and F) of various liposomes with Au NPs at the lipid/Au ratio of 10/1. The TEM images of the complexes are inserted in the panels of (D and F). Bar: 100 nm. The experimental conditions were the same as Figs. 7-5C and 7-6.

7. 5. References

1. C. Burda et al., *Chem. Rev.* 2005, **105**, 1025-1102.

2. M.C. Daniel and D. Astruc, *Chem. Rev.* 2004, **104**, 293-346.

3. S. Link and M.A. El-Sayed, *J. Phys. Chem. B* 1999, **103**, 8410-8426.

4. S. Link and M.A. El-Sayed, *Int. Rev. Phys. Chem.* 2000, **19**, 409-453.

5. P.K. Jain et al., *Nanotoday* 2007, **2**, 18-29.

6. A.O. Govorov, H.H. Richardson, *Nanotoday* 2007, **2**, 30-38.

7. D. Pissuwan et al., *Trends Biotech.* 2006, **24**, 62-67.

8. D. Kim et al., *J. Am. Chem. Soc.* 2007, **129**, 7661-7665.

9. W.P.Wuelfing et al., *J. Am. Chem. Soc.* 1998, **120**, 12696-12697.

10. B.D. Chithrani and W.C.W. Chan, *Nano Lett.* 2007, **7**, 1542-1550.

11. K. Sokolov et al., *Cancer Res.* 2003, **63**, 1999-2004.

12. C.C. Chen et al., *J. Am. Chem. Soc.* 2006, **128**, 3709-3715.

13. N.L. Rosi et al., *Science* 2006, **312**, 1027-1030.

14. W.T. Al-Jamal and K. Kostarelos, *Nanomed.* 2007, **2**, 85-98.

15. Y. Haba et al., *Langmuir* 2007, **23**, 5243-5246.

16. D.D. Lasic, *Liposomes, from Physics to Applications, Elsevier, Amsterdam,* 1993.

17. K. Hong et al., *Biochim. Biophys. Acta* 1983, **732**, 320-323.

18. X. Li et al., *Langmuir* 2004, **20**, 3734-3739.

19. S.-H. Park et al., *Colloids Surf. B* 2006, **48**, 112-118.

20. L. Paasonen et al., *J. Control. Release* 2007, **122**, 86-93.

21. H. Zhu et al., *Collioids Surf. A* 2005, **257–258**, 411-414.

22. K. Kono et al., *Biochim. Biophys. Acta* 1999, **1416**, 239-250.

23. K.C. Grabar et al., *Anal. Chem.* 1995, **67**, 735-743.

24. H. Hayashi et al., *Bioconjugate Chem.* 1998, **9**, 382-389.

25. K. Kono et al., *J. Control. Release* 1994, **30**, 69-75.

26. G. Frens, *Nature Phys. Sci.* 1973, **241**, 20-22.

27. B.D. Chithrani et al., *Nano Lett.* 2006, **6**, 662-668.

28. L.Wasungu and D. Hoekstra, *J. Control. Release* 2006, **116**, 255-264.

29. T. Niidome and L. Huang, *Gene Ther.* 2002, **9**, 1647-1652.

30. R.B. Greenwald et al., *Crit. Rev. Ther. Drug Carrier Syst.* 2000, **17**, 101-161.

Chapter 8

General Conclusion

This thesis described the demonstration of generating novel stimuli-sensitive drug delivery systems for efficient delivery of bioactive molecules. The author demonstrated that the conjugation of functional materials with liposomes produced ideal functional liposomes. The author prepared pH- and photo-sensitive liposomes by conjugating pH-sensitive polymers, pH-sensitive lipid and photo-sensitive metal nanoparticles. The author also evaluated and optimized their functions as intracellular delivery systems of model drugs, proteins, genes. Then, the highly potent of intracellular delivery system based on the pH-sensitive polymer-modified liposome was prepared, which can achieve efficient gene and protein delivery by their excellent perfomances. This promising carrier would ensure advanced medical technology such as gene therapy, immunotherapy and regenerative tharapy. The results and findings in this work are summarized as follow.

Chapter 2 demonstrated the cytoplasmic delivery of antigenic proteins to immune cells and the induction of antigen-specific immune responses using pH-sensitive fusogenic liposomes. The author revealed the correlation between membrane fusion ability of liposomes and the ability of induced cellular immune responses. Higher fusogenic liposomes delivered their contents into immune cell's cytosol and induced antigen-specific cellular immunity more efficiently. In addition, induced immune responses were comparable to the widely used immunoactivation reagents. pH-Sensitive fusogenic liposomes and their relevant liposomes might be promising antigen carriers for establishment of cancer immunotherapy and mucosal vaccination.

In **Chapter 3**, the author synthesized novel pH-sensitive poly(glycidol) derivatives with a three-dimensional backbone structure, MGlu-HPG as highly pH-sensitive fusogenic

polymers. MGlu-HPG exihibited high hydrophobicity and strong interaction to liposomal membrane with increasing molecular weight. These prpoperties were higher than the counterpart polymers with a linear backbone structure. Modification of liposomes with MGlu-HPG produced highly pH-sensitive liposomes that undergo content release at mildly acidic pH and deliver their contents efficiently into the cytosol of immune cells by strong membrane fusion ability. Therefore, they might have potential usefulness for the delivery of antigenic proteins.

Chapter 4 described the achievement of efficient transfection of DCs by hybrid complexes of lipoplex and pH-sensitive polymer-modified liposomes. First the author revealed that irrespective of possession of ligands, the complexes were taken up efficiently by DCs, probably because carboxylate anions of the polymers on the complexes were recognized by scavenger receptors of the cells. In addition, the hybrid complexes with higher fusion ability, MGluPG complexes exhibited more efficient transfection of DCs. Their levels of transgene production were higher than some commercially available transfection reagents. Because these complexes might introduce high concentration of intracellular antigen in DCs, induction of efficient presentation of epitope and strong immune response may be expected.

In **Chapter 5**, the author synthesized various pH-sensitive polyampholytic polymers comprised of varying molar ratios of DEAEMA and AA and modified the EYPC liposome surface with these polymers. The correlation between their charge states and the ability to induce drug release was assessed. The critical pH for the drug release from these polymer-liposome conjugates tested in buffer solutions ranged from pH 4 to 10 decreased with increasing DEAEMA content in the polymers, resulting from the increase in hydrophobicity of the polymer. This study contributes to the knowledge that pH-responsive polyampholytes are a class of polymers that can be used to modify the surface of liposomes. The results from this work are of significance as the information derived is expected to be useful for the future synthesis of pH-responsive polymer-liposome comjugates with desired

conditions in mind.

Chapter 6 described the construction of pH-sensitive lipid-based unique intracellular delivery system. Poly(amidoamine)-dendron-bearing lipid (DL) was used as a pH-sensitive amphiphilic molecule. DSC, optical density analysis, DLS and TEM measurements revealed that the inclusion of PEG-lipid in DL molecular assemblies promoted the DL's unique structural transition responding to pH. Results showed that molecular assemblies of DL/PEG formed stable vesicles at neutral pH and aggregated vesicles at alkaline pH and micelles at acidic pH. Critical transition pH from vesicles to micelles was around 6.5, resulting from the change of hydrophilic-hydrophobic balance by the protonation of tertiary amines in head group of DL. Below this pH, vesicles promptly changed to micelles and this change coincidently caused accurate drug release from carriers. In addition, DL/PEG vesicles could deliver their contents into the cytosol of immune cell lines by their unique structural transition. Consequently, DL/PEG vesicles are promising protein carriers for immune cells, which are useful for cancer immunotherapy and their unique structural transition mechanisms provide the novel strategy to develop the newly delivery systems.

Chapter 7 described the preparation of the complex comprising of liposomes and Au NPs. The stability of the Au NP dispersion under isotonic condition was found to be dependent on the liposome/Au NPs ratio. In addition, release, DLS and TEM analysis revealed that the Au NPs interacted with intact liposomes, which indicates that these complexes could be made from liposomes encapsulating small molecules such as drug molecules. These complexes could be also formed by using cationic liposomes and PEG-modified liposomes as well as EYPC liposomes, making them ideal candidates for use as drug and gene delivery. The author proposes that this kind of complex will find useful application as a nanomedicine with diagnostic and therapeutic ability.

The author demonstrated the preparation of the promising drug delivery systems

pertaining desirable properties for intracellular delivery system such as high uptake, high membrane fusion/disrupting activity, and extremely high ability to induce the specific immune responses. Theses results obtained in this thesis would form the basis for constructing novel drug delivery system and conducting successful advanced medical therapy.

Acknowledgements

This thesis research was carried out at Osaka Prefecture University from 2005 to 2010.

The author would like to express his sincere gratitude to Professor Kenji Kono for his kind guidance, invaluable discussion, and encouragement throughout this study.

The author wishes to express his sincere acknowledge Professor Masamitsu Shirai and Professor Tsutomu Nagaoka for their useful advices and reviewing this thesis.

The author is sincerely grateful to Associate Professor Shinobu Watarai of Osaka Prefecture University for his helpful advice, valuable discussion, technical supports and continuous encouragement in carrying out this work.

The author expresses his sincere appreciation to Associate Professor Atsushi Harada and Tenure-Track Lecturer Chie Kojima of Osaka Prefecture University for their helpful advice, valuable discussion, and continuous encouragement in carrying out this work.

The author expresses his grateful acknowledge to Senior Lecturer Loo-Teck Ng of University of Western Sydney for her cooperation, valuable discussion and continuous encouragement in the present research.

The author would like to thank his senior member of Kono laboratory, Dr. Yasuhiro Haba, Dr. Toshinari Takahashi, Dr. Akihumi Kawamura and Dr. Naoki Sakaguchi. The author also would like to thank Mr. Yusuke Hirano and Ms. Megumi Yamada for their cooperation in the present research.

The author wishes to thank all people he met through his study. Especially, he wishes to thank the members of Kono Laboratory.

Finally, the author wishes to express his deep gratitude to his parents, Takeshi Yuba, and Chiaki Yuba, for their support and sincere encouragement.

February 2010

Eiji Yuba

Department of Applied Chemistry

Graduate School of Engineering

Osaka Prefecture University

List of Publications

1. "pH-Sensitive Fusogenic Polymer-Modified Liposomes as a Carrier of Antigenic Proteins for Activation of Cellular Immunity."
   E. Yuba, C. Kojima, A. Harada, Tana, S. Watarai, K. Kono,
   Biomaterials, Vol. 31, pp. 943-951 (2010). (Chapter 2)

2. "Carboxylated Hyperbranched Poly(glycidol)s for Preparation of pH-Sensitive Liposomes."
   E. Yuba, A. Harada, Y. Sakanishi, K. Kono,
   J. Controlled Release, in press. (Chapter 3)

3. "Gene Delivery to Dendritic Cells Mediated by Complexes of Lipoplexes and pH-Sensitive Fusogenic Polymer-Modified Liposomes."
   E. Yuba, C. Kojima, N. Sakaguchi, A. Harada, K. Koiwai, K. Kono,
   J. Controlled Release, Vol. 130, pp. 77-83 (2008). (Chapter 4)

4. "Modification of Liposome Surface with pH-Responsive Polyampholytes for the Controlled-Release of Drugs."
   L. T. Ng, E. Yuba, K. Kono,
   Research on Chemical Intermediates, Vol. 35, pp. 1015-1025 (2009). (Chapter 5)

5. "pH-Sensitive Vesicles That Undergo Transition to Micelles for Intracellular Delivery"
   M. Yamada, E. Yuba, T. Douura, C. Kojima, A. Harada, K. Kono,
   J. Controlled Release, submitted. (Chapter 6)

6. "Preparation and Characterization of Complexes of Liposomes with Gold Nanoparticles."
   C. Kojima, Y. Hirano, E. Yuba, A. Harada, K. Kono,
   Colloids and Surfaces B: Biointerfaces, Vol. 66, pp. 246-252 (2008). (Chapter 7)